An Experimental Investigation of Paraffin Wax Deposition in a Batch Oscillatory Baffled Column

Lukman Ismail

Thesis submitted for the degree of Doctor of Philosophy
To Heriot-Watt University, Edinburgh UK.
On the completion of research in the
Centre for Oscillatory Baffled Reactor Application (COBRA)
Department of Mechanical and Chemical Engineering
School of Engineering and Physical Sciences

July 2007

ABSTRACT

Problems related to crystallisation and deposition of paraffin waxes on oil pipelines during production and transportation of crude oil caused huge operational and financial losses to petroleum industry. This study is focused on the fundamental understanding of the mechanisms of wax deposition and investigates the effect of several major parameters on such deposition in a batch oscillatory baffled column (OBC). The OBC is a relatively new mixing technology and offers more uniform mixing and particle suspension than traditional reactors. It is the intention of this work to characterise the effect of oscillatory mixing on the wax deposition process perhaps as an alternative way for mitigation of wax deposition problems. Experiments have been carried out to examine the effects of OBC's operational parameters, wax-oil volume, paraffin wax content, carbon number of the solvents, baffles materials and structure on the wax deposition. Analyses conducted to evaluate and characterise the wax deposition are: the percentage of wax deposition (δ, wt.%); the Avrami exponent (n) which corresponds to the type of wax crystals; and the half time of deposition ($t_{1/2}$) which is associated with the rate of deposition. On the study of the effect of OBC's parameters, it was found that increasing the oscillation frequency and amplitude reduced the overall deposition; baffles oscillation altered the type of wax crystal formed from needle type to clustered plate-like shapes; and accelerated the rates of deposition. On the effect of wax-oil volume, it was observed that increasing the volume reduced the deposition, increased n values and $t_{1/2}$ hence reduced the deposition rates. The study on the effect of paraffin wax content revealed that increasing the wax content increased the deposition, reduced n values and caused higher crystallisation rates. On the effect of solvent carbon numbers, it was found that the higher the carbon numbers, the more the deposition,

lower n and $t_{1/2}$. Lastly on the study of baffles materials and structure, it can be deduced that using different baffle materials had no significant impact on the deposition in the OBC. In summary, oscillatory baffled flow can be an effective means of mitigation of wax deposition problems. This work may also lead to a screening test for wax deposition inhibitors. Since the deposition of viscous materials is common to other sectors of the process industries, the results of this study will provide essential information for understanding and perhaps later implementation of the OBC technology in the related fields.

Acknowledgements

I would like to express my utmost gratitude to my primary supervisor, Professor Xiong-Wei Ni for his continuous support, motivation and patience throughout the course of this work. The experience gained from his guidance truly invaluable in my pursuit to become a successful researcher. My thanks also go to my second supervisor Dr. Robin E. Westacott for his assistance and advice. Gratitudes to the support staff of Chemical Engineering Department especially Ronald and Marian Millar, Richard Kinsella, Aftab Aziz and Malcolm McWilliams. I am thankful to the colleagues who were very supportive; Dr. Andrew W. Fitch, An Ting Liao, Ricardo Caldeira, Panagiotis and many more.

My appreciation also goes to the Malaysian friends in Edinburgh for their support and help especially Fauzi Ariffin, Maimunah Sapri, Dr. Hisham Hamid, Ustaz Nik Roskiman Samad and family, Nasri Sulaiman, Badrulhisham, Dr. Fadzil Hassan, Zulhakimi, Thariq, Sulaiman, Hazem Eslah, Amir, Fazri, Sanif, Azmil, Wafi, Afiq, Azam, Hanim, Anis Suhaila, Jefrizal and many, many more from the members of Edinburgh Malaysian Students Association. Thank you for being there through thick and thin. Acknowledgment also goes to Universiti Teknologi PETRONAS for the sponsorship of the PhD programme. My beloved wife, Suriani Ghazali, my sons, Tariq Ishraf, Muhammad Iqbal Hakimi and Amjad Lutfi, without whom I can never survive and to whom this work is dedicated. Dedications also to my family back home in Malaysia, my mother and father, Rukiah Mat Husain and Ismail Awang; parents in laws, Ghazali Omar and Marziah Umar; thank you for the prayers.

ACADEMIC REGISTRY
Research Thesis Submission

Name:	LUKMAN ISMAIL		
School/PGI:	EPS / Chemical Eng.		
Version: *(i.e. First, Resubmission, Final)*	Final	Degree Sought:	PhD

Declaration

In accordance with the appropriate regulations I hereby submit my thesis and I declare that:

1) the thesis embodies the results of my own work and has been composed by myself
2) where appropriate, I have made acknowledgement of the work of others and have made reference to work carried out in collaboration with other persons
3) the thesis is the correct version of the thesis for submission*.
4) my thesis for the award referred to, deposited in the Heriot-Watt University Library, should be made available for loan or photocopying, subject to such conditions as the Librarian may require
5) I understand that as a student of the University I am required to abide by the Regulations of the University and to conform to its discipline.

* *Please note that it is the responsibility of the candidate to ensure that the correct version of the thesis is submitted.*

Signature of Candidate:	[signature]	Date:	3/7/07

Submission

Submitted By *(name in capitals)*:	NIK HAMIDI NIK MUSTAPHA
Signature of Individual Submitting:	[signature]
Date Submitted:	6/7/2007.

For Completion in Academic Registry

Received in the Academic Registry by *(name in capitals)*:	VAL MURDOCH		
Method of Submission *(Handed in to Academic Registry; posted through internal/external mail)*:	By hand		
Signature:	Valerie A Murdoch	Date:	6/7/07

Table of Contents

Nomenclature

Symbol	Definition [SI unit]
D_{bo}	Orifice size [m]
Dc	Diameter of the column [m]
f	Oscillation frequency, Hz
γ	Solid suspension correlation $\left(\gamma = \left[1 - \exp\left(-R\frac{V_m}{V_s}\right)\right]\right)$
H_b	Baffle spacing [m]
K	Growth rate [min^{-n}]
n	The Avrami exponent [-]
Re_o	Oscillatory Reynolds number $\left(\mathrm{Re}_o = \frac{\omega x_o \rho_L D_c}{\mu}\right)$ [-]
St	Strouhal number $\left(St = \frac{D_c}{4\pi x_o}\right)$ [-]
T	Temperature [°C]
t	Time [s]
$t_{1/2}$	The half time of deposition, $t_{1/2} = \left(\frac{\ln 2}{K}\right)^{1/n}$ [min]
T_b	Thickness of the plate [m]
Vm	The maximum oscillation velocity (m/s)
V_t	Volume or volume fraction of crystallisation [-]
X	Degree of crystallisation [-]
x	Displacement [m]
x_o	Oscillation amplitude (centre to peak) [m]
k_La	Volumetric mass transfer coefficient (k_La)

Greek Letters

Symbol	Definition [SI unit]
α	Baffle free area $\left(\alpha = \left(\frac{D_{bo}}{D_c}\right)^2\right)$ [-]
β	Baffle spacing $\left(\beta = \frac{H_b}{D_c}\right)$ [-]
δ	Deposition [wt. %]
δ_0	Initial deposit in liquid [wt. %]
δ_∞	The maximum or asymptotic deposition [wt. %]
δ_r	Relative deposition [wt. %]
δ_t	The total deposition at time t [wt. %]
μ	Viscosity of the fluid [kg m^{-1} s^{-1}]
ρ_L	Density of Fluid [kg m^{-3}]
ω	Angular frequency (=$2\pi f$) [s^{-1}]

Abbreviations

ID	Internal diameter
MPLI	Multipurpose Lab Interface
OBC	Oscillatory baffled column
OBR	Oscillatory baffled reactor
OD	Outside diameter
OFR	Oscillatory flow reactor
PSP	Pulsed sieve packed column
PSPC	Pulsed sieve-plate column
PTFE	Polytetrafluoroethylene
PVDF	Polyvinylidene difluoride
RPC	Reciprocating plate column
RPM	Revolution per minute
RTD	Residence time distribution
SS	Stainless steel
STR	Stirred tank reactor
WAT	Wax appearance temperature

List of Figures

List of Tables

List of Publications and Presentations

Journal Papers

1. Ismail, L., Westacott, R.E. and Ni, X. (2006). On the Characterisation of Wax Deposition in an Oscillatory Baffled Device. *J Chem Technol Biotechnol.* **81**, 1905-1914.
2. Ismail, L., Westacott, R.E. and Ni, X. (2007). On the Effect of Wax Content on Paraffin Wax Deposition in a Batch Oscillatory Baffled Tube Apparatus. *Chem Eng J.* (2007). doi:10.1016/j.cej.2007.04.018.

Journal Papers in Preparation

1. Ismail, L., Westacott, R.E. and Ni, X. Wax Deposition in a Batch Oscillatory Column: On the Effect of Oscillatory Parameters.
2. Ismail, L., Ni, X. and Westacott, R.E. Effect of Solvent Carbon Numbers on the Wax Deposition in an Oscillatory Baffled Column.

Proceedings

1. Ismail, L., Westacott, R.E. and Ni, X. (2006). Paraffin Wax Deposition in a Batch Oscillatory Baffled Column. Proceedings of the Malaysian Research Group International Conference 2006, University of Salford UK, 19-21 June 2006.

Conference Presentations

1. Ismail, L., Ni, X. & Westacott, R.E. (2003). Laboratorial Studies of Paraffin Wax Deposition – A Review. *Edinburgh Malaysian Students Research Forum*, Edinburgh University, Edinburgh, 25 Oct. 2003.
2. Ismail, L., Ni, X. & Westacott, R.E. (2004a). Wax Deposition Inhibition Utilising Oscillatory Flow. *7th Scottish Fluid Mechanics Meeting*, University of Strathclyde, Glasgow, 19 May 2004.
3. Ismail, L., Ni, X & Westacott, R.E. (2004b). Mitigating Wax Deposition Through Oscillatory Flow: Experimental Study Using Batch Oscillatory Baffled Column. *Postgraduate Seminar Day*, HWU, Edinburgh, UK, 2 June 2004.
4. Ismail, L., Ni, X & Westacott, R.E. (2004c). On the Deposition of Paraffin Wax in a Batch Oscillatory Baffled Column. *10th Meeting of the Process Intensification Network*, Heriot-Watt University, Edinburgh, 3rd June 2004.

CHAPTER 1

INTRODUCTION

1.1 Motivation for the study

It has been the aspiration of chemical engineers and scientists to identify and study the problems endured in the chemical industries and find ways to solve or mitigate the problems. Deposition of paraffin wax is one of the major problems facing the petroleum industries, with the main implication being wax blockage in oil and gas pipelines especially during offshore production, leading to severe financial consequences. Oil enters the pipeline at 60-70 °C and because the ocean water is much colder (4 °C in deep waters) the oil is cooled causing heavy hydrocarbons to precipitate out as the oil flows through the pipeline. The precipitated wax deposits on the pipe inner wall, forming a solid layer that narrows the flow passage and eventually reduces the flow rates (Ribeiro *et al.*, 1997). Traditional methods of management, prevention and remediation have been established over many years. These involve mechanical means such as pigging; thermal treatment such as circulation of warm liquid; and chemical treatment such as addition of solvent and/ or dispersant (Creek *et al.*, 1999).

Removal of wax from wells and pipelines accounts for significant operating costs, *e.g.* the direct cost of using deep sea divers to cut and remove paraffin blockage in a pipeline of 40 000 ft. in length and 6 in. in diameter is about $6 million, while the production loss during downtime is approximately $40 million. In some extreme cases such as the Lasmo field, UK., the entire field was abandoned with the cost of over $100 million because of recurrences of paraffin blockage (Nguyen *et al.*, 2001). Flow

blockage with viscous and waxy fluids is also a major issue for food industries, *e.g.* milk production (Changani *et al.*, (1997)), and food oil/fat processing (Fernandez-Torres *et al.*, 2001).

In this work a batch oscillatory baffled column (OBC) is used as the model system to investigate possible means for mitigation of wax deposition; while paraffin wax is used as the model material. The OBC is a relatively new mixing technology and offers more uniform and efficient mixing, and better particle suspension than traditional devices. Although the OBC technology has been applied to a wide range of chemical reactions and organic synthesis, this work was the first in studying wax deposition. While the majority of the research works on wax deposition have focused on chemical treatment using wax inhibitors, there is a strong need to understand the effect of fluid mechanic conditions and mixing on wax deposition; there has been lack of this type of research. It is the intention of the study to understand the behaviours of the waxy fluids and the deposition process in the novel environment; to evaluate the mechanism and kinetics that govern such a process; and to establish the effect of oscillatory mixing on the wax deposition process.

1.2 The objectives of the project

The overall aim of the project is to investigate and understand the mechanism of paraffin wax deposition in a batch oscillatory baffled column (OBC), and specific objectives of the project are:

i. To design and set up a batch oscillatory baffled column for the wax deposition study;
ii. To examine the effects of OBC's operational parameters, namely the oscillation amplitude and frequency on the deposition;
iii. To investigate the effects of the wax and oil mixture volume used in the column on the deposition;
iv. To explore the effects of the paraffin wax content on the deposition;
v. To examine the effects of carbon numbers of the solvents on the deposition;
vi. To study the effect of baffle materials and structure on the deposition.

1.3 Structure of the thesis

This thesis is divided into five chapters and its structure is as follows. Following the introduction, Chapter 2 presents a review of background information relevant to oscillatory baffled column (OBC) and paraffin wax deposition. The design and set up of the OBC, as well as the experimental procedures are described in Chapter 3. In Chapter 4, results will be presented and followed by appropriate discussions. Chapter 5 presents the conclusions drawn out for this study together with recommendations for future work. In addition several data calculations and graphs are given in the Appendices.

CHAPTER 2

LITERATURE REVIEW

This chapter reviews the background literature that is relevant to Oscillatory Baffled Column/Reactor (OBC/OBR) development and paraffin wax deposition, and is divided into two main sections. Section 2.1 introduces background information including operating and geometric principles, governing dimensionless numbers and the relevant research and development for the OBC/OBR. Section 2.2 covers the background studies of paraffin wax deposition which includes the characterisation of paraffin wax, crystallisation, wax structure, factors that affect paraffin wax deposition and several laboratory studies.

2.1 The Oscillatory Baffled Column

2.1.1 Background

The principle of oscillatory flow mixing was first introduced by van Dijck (1935) who proposed the pulsed sieve plate (PSP) column as a device for liquid-liquid extraction. The PSP was used in the nuclear industry in the 1940s and 1950s to enhance solvent extraction (Long, 1967). Oscillation of the fluids in PSP was achieved through hydraulic pulsation using a piston or pneumatic movement (Figure 2.1(a)) with typical frequencies of 1 to 2 Hz, and amplitudes 0.5–2.0 cm. The pulsation enhanced multi-phase mixing and led to better mass transfer performance compared to conventional, steady-flow counter-current columns (Karr, 1959). Similar advantages also showed in reciprocating plate column (RPC) used for the extraction of penicillin from fermentation broths (Karr,

1959) (Figure 2.1(b)). The baffle plates were mounted on a single or several vertical shafts and the movement was achieved by using an electrical motor. The plates were perforated with many holes of about 14 mm in diameter. The open area of 50 to 60% resulted in lesser flow restriction than that of the pulsed plate or packed columns and this reduced fouling risks (Karr, 1959). The RPC has been used in many extraction applications and manufactured in industrial sizes up to 1.7 m diameter (Godfrey and Slater, 1994). Higher frequencies up to 3 Hz and longer amplitudes up to 2.5 cm were utilised compared to the PSP due to lower plate constriction. These studies in PSP and RPC involved baffled plates with multiple holes. Research into mixing enhancement using a single hole orifice baffle began in the late 1980s at Cambridge (Brunold *et al.*, 1989), and have blossomed ever since. Table 2.1 summarises the chronological developments of the oscillatory flows in baffled columns.

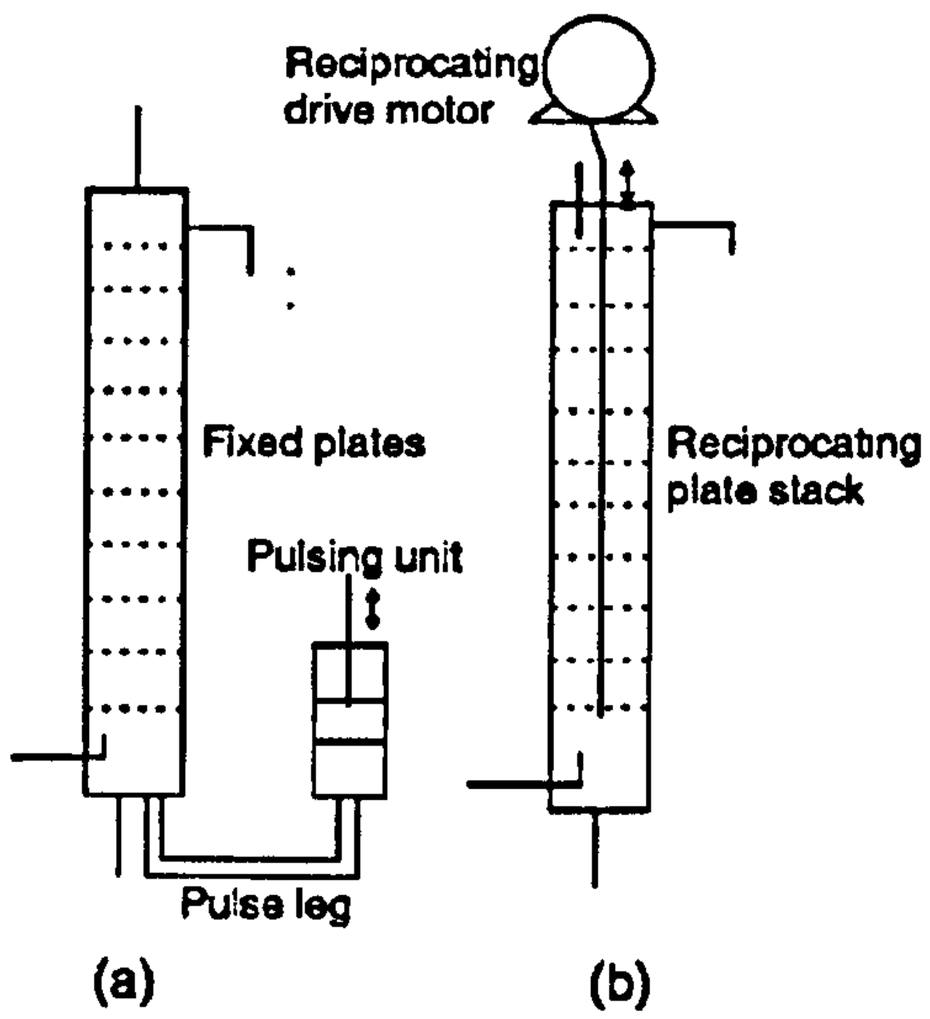

Figure 2.1 Schematic diagram of pulsed plate columns (a) and reciprocating plate columns (b) (Karr, 1959)

Table 2.1 Chronological summary of the development of oscillatory flow technology (Ni *et al.*, 2003, 2004; Ismail *et al.*, 2006, 2007)

First development	Process	Equipment	Typical references
1950s 1960s	Solvent extraction	Pulsed packed columns Pulsed plate columns Reciprocating plate columns	Review chapters in Lo *et al.* (1983) and Godfrey and Slater (1994)
1970s	Gas–liquid mass transfer	Pulsed plate columns	Baird and Garstang (1972)
		Furrowed channel oxygenator	Bellhouse *et al.*, (1973)
1980s	Mixing and dispersion	Baffled tubes	Dickens *et al.*, (1989)
1990s	Heat transfer enhancement	OBR	Mackley *et al.*, (1990), Mackley and Stonestreet (1995)
	Gas liquid mass transfer	OBC	Ni *et al.* (1995a, 1997), Ni and Gao (1996), Gao *et al.* (1998)
	Solid–liquid contacting	Pulsed packed column	Mak *et al.* (1991)
	Chemical reaction	Baffled tube reactors	Ni and Mackley (1993)
	Bio-processing	Baffled tube column	Ni *et al.* (1995b)
	Membrane separation	Pulsed baffled cell	Finnegan and Howell (1989) Coleman and Mitchell (1991)
	Filtration	Pulsed filtration cell	Mackley and Sherman (1992, 1993)
	Bulk mixing and mass transfer	Vortex generation in large tanks	Latto (1992), Baird *et al.* (1992)
2000	Flocculation	OBR	Ni *et al.* (1998, 2001a)
	Saponification reactor	OBC	Harvey and Stonestreet (2001)
	Suspension polymerisation	OBR	Ni *et al.* (1998, 1999, 2000a, 2001b)
	Phase transfer catalysis	OBR	Wilson *et al.* (2001a, 2001b)
	Fermentation	OBR	Gaidhani *et al.* (2002)
	Crystallisation	OBC	Ni *et al.* (2004)
	Wax deposition	OBC	Ismail *et al.* (2006, 2007)

2.1.2 Mechanism and principle

The production of discrete cyclic vortices in the bulk fluid is the basic mechanism for mixing enhancement in the OBC. Vortices are created when either the fluids or the baffles are oscillated. Due to the periodical reversing fluid motion interacting with the baffles, this provides efficient and uniform mixing in the zones between successive baffles. These baffles' fractional open cross-sectional area is usually 20–30%, to minimise frictional losses and maximise the mixing effect. The typical spacing between the baffles is in the range of 1–2 times the tube diameter (Ni *et al.*, 2003).

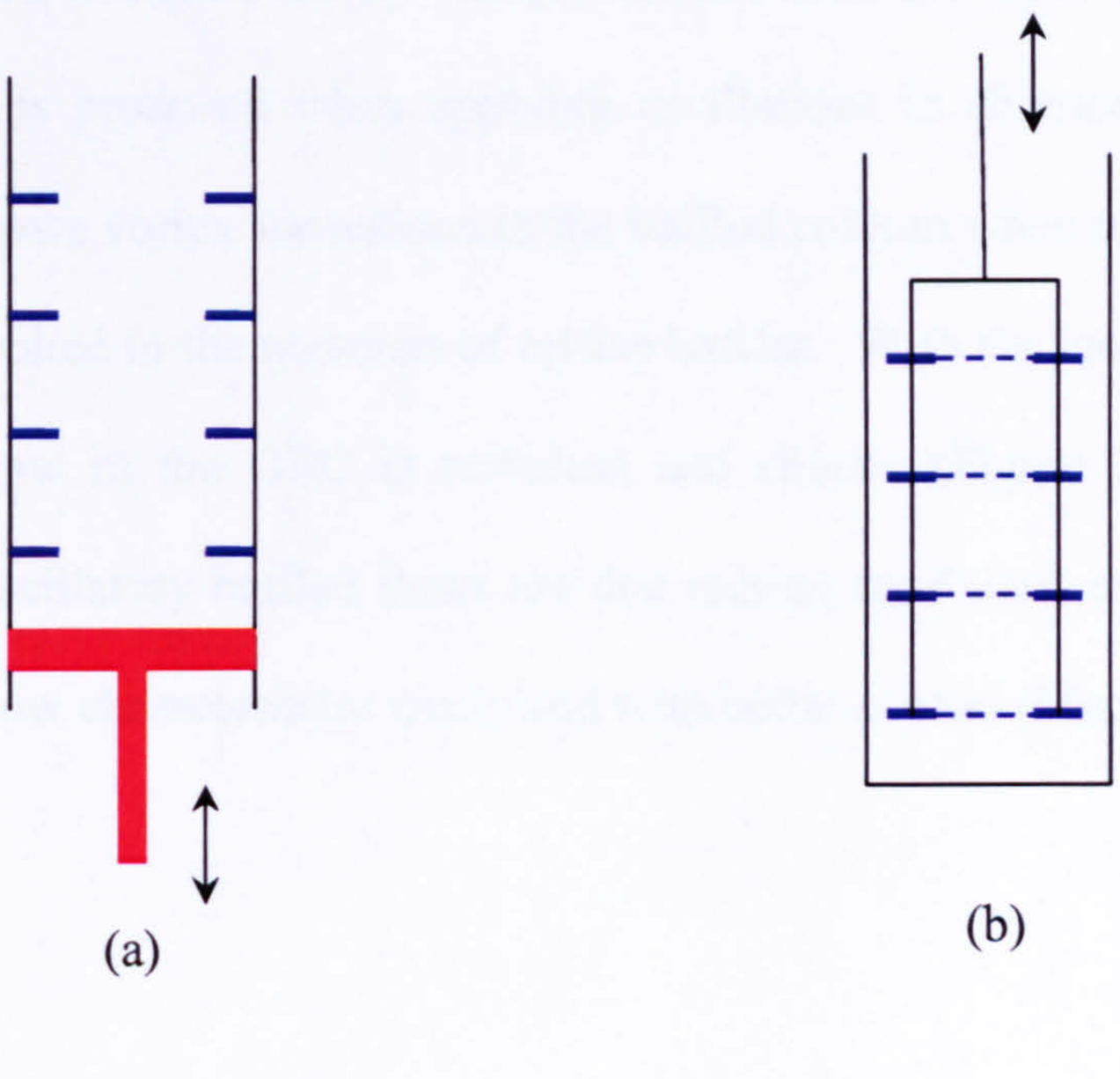

Figure 2.2 Basic configurations of oscillatory baffled column

There are essentially two basic configurations of an OBC in terms of oscillation mechanisms: by oscillating the fluid at the bottom as shown in Figure 2.2(a) and by oscillating the baffles from the top (Figure 2.2(b)). The latter set up has an advantage in the scale up study as well as in applications that require larger amplitudes of oscillation

(Ni *et al.*, 1998). Oscillation of the fluid can be achieved by means of a diaphragm (Mackay *et al.*, 1991), using bellows at the base of the column (Mackley *et al.*, 1993) which are normally made of steel, or plastic material such as PTFE which has a very low friction coefficient and high strength (Zhao and Liu, 2004); and also using a piston at either one or both ends. A single piston assembly was reported by Howes and Mackley (1990) while a double piston design was used by Mackley *et al.* (1990) for a heat transfer study, and also by Masngut *et al* (2006) in the study on the fermentation of palm oil mill effluent.

Typical flow patterns in a column where the fluid is subjected to an oscillatory motion are shown in Figure 2.3(a) – 2.3(c). From Figure 2.3(a), it can be seen that no eddy or vortex is produced when applying oscillations in absence of baffle inserts. Figure 2.3(b) shows vortex formations in the baffled column when moderate oscillation intensity was applied in the presence of orifice baffles. With the increase of oscillation intensity, the flow in the OBC is turbulent and chaotic (Figure 2.3(c)). The major advantages of oscillatory baffled flows are that mixing conditions can be tailored from plug to mixed flow characteristics easily and with better control (Mackley and Ni, 1991).

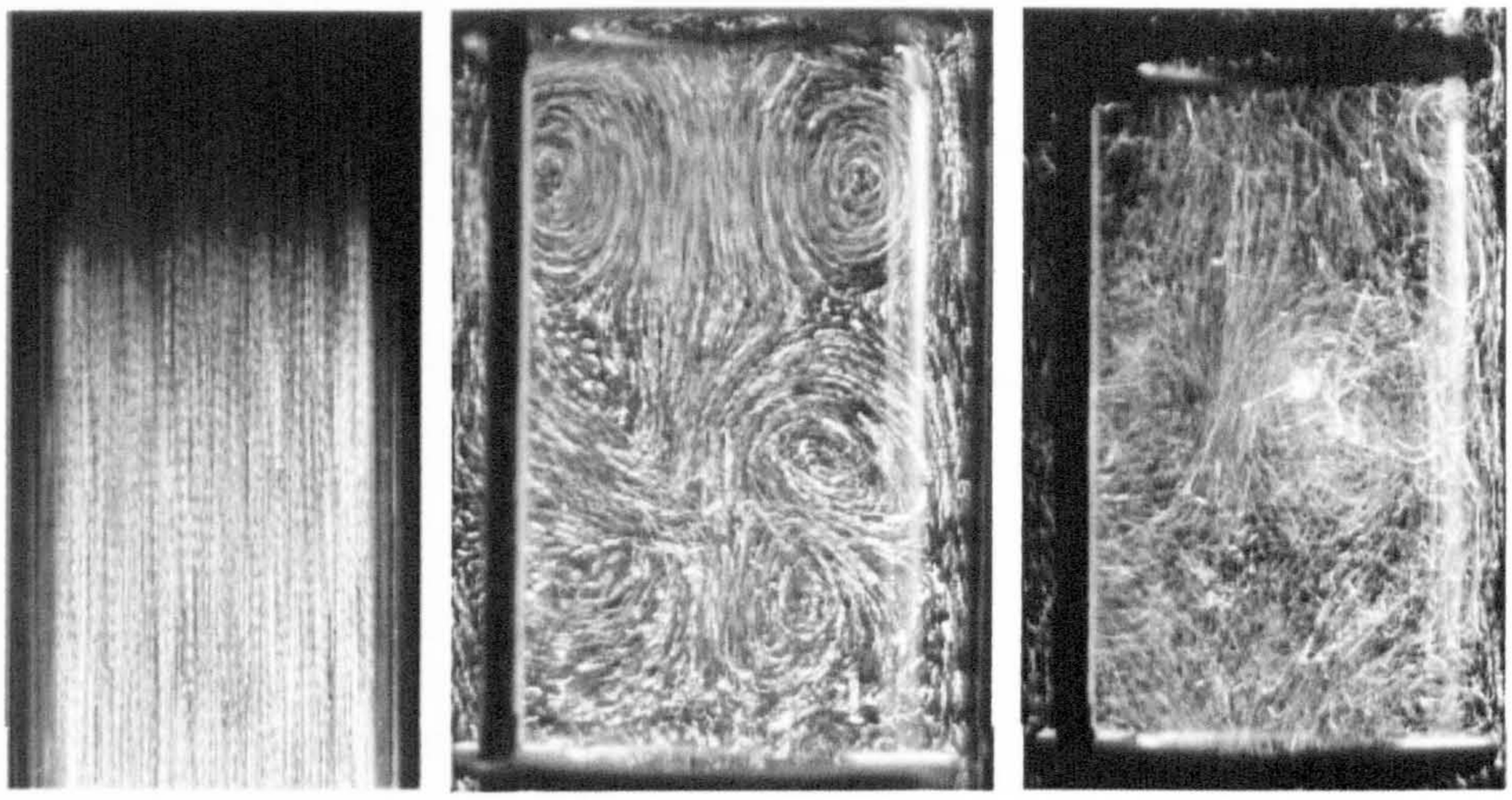

(a) (b) (c)

Figure 2.3 (a) Visualization of flow in a smooth walled column, (b) and (c) visualization of flow in an oscillatory baffled column (Ni *et al.*, 2003)

Figure 2.4 explains the development of eddies in an OBC over one oscillation cycle. At the start of the upstroke (Figure 2.4a), vortices begin to form adjacent to the downstream edge of the baffles, taking the fluid element near the wall with them and become fully developed at the point of maximum oscillatory velocity (Figure 2.4b). As the flow decelerates, the vortices are swept into the bulk of the baffled cell (Figure 2.4c) and reach the centre of the cell at the point of flow reversal (Figure 2.4d), *i.e.* the radial motions of eddies. As the downstroke begins, these vortices are pushed into the centre while new vortices are formed on the opposite edge of the baffle (Figure 2.4e). The cycle repeats itself in the opposite direction of flow. As a result of these activities, the radial velocities are of similar order to the axial ones.

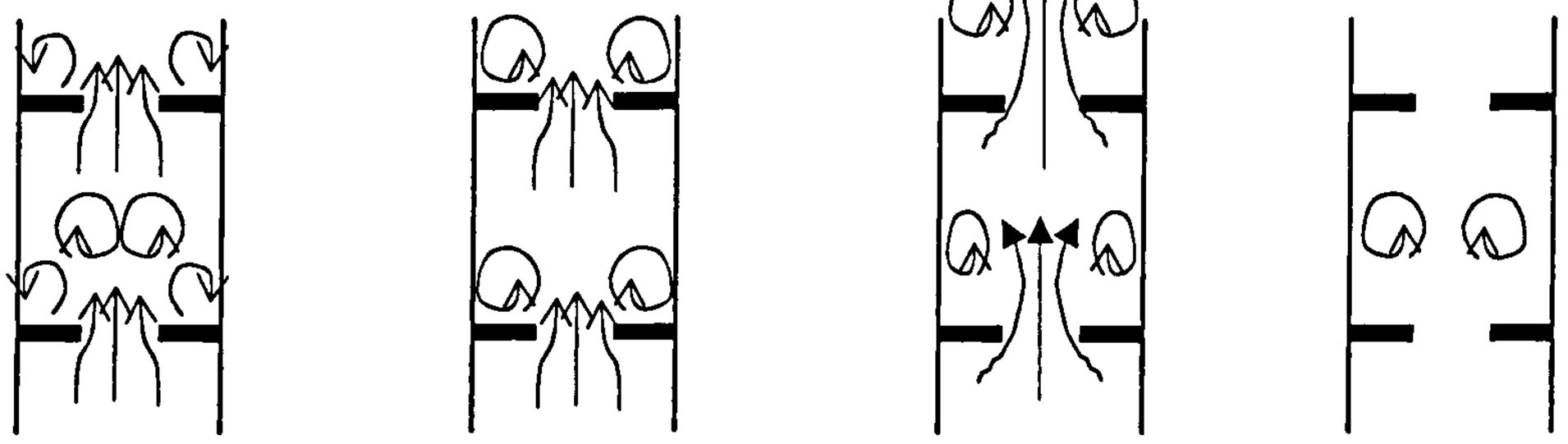

Figure 2.4 Schematic representation of eddy motion within a baffled column (Ni and Mackley, 1993)

There are two dimensionless groups that control the fluid mechanic of fluid in an OBC: the oscillatory Reynolds number (Re_o) and the Strouhal number (St), defined as:

$$\mathrm{Re}_o = \frac{\omega x_o \rho_L D_c}{\mu} \tag{2.4}$$

$$St = \frac{D_c}{4\pi x_o} \tag{2.5}$$

where ρ_L is the fluid density (kg m^{-3}), μ the fluid viscosity (kg m^{-1} s^{-1}) and D_c the column diameter (m). The oscillatory Reynolds number is related to the oscillation intensity, with its peak velocity as the model velocity. Strouhal number is a ratio of column diameter to stroke length which measures the effective eddy propagation (Howes, 1988).

2.1.3 Geometry of the OBC

The OBC mixing intensity and flow pattern inside the column are governed by the operational variables as well as the geometry of the OBC. Therefore, an appropriate geometric configuration must be investigated so that the performance of the column can be optimised. Several studies to establish the optimal OBC configuration have been performed and mainly focused on the characteristics of the baffles and the oscillation unit. The orientation of the column depends on the type of application, as well as on the mode of operation. For continuous type of operations, the OBC can either be vertical or horizontal (Mackley and Ni, 1991), while for batch operations it is usually in the upright position (Ni and Mackley, 1993). Orifice baffles can be characterised by the orifice size (D_{bo}), the thickness of the plate (T_b) and the baffle spacing (H_b), as shown in Figure 2.5.

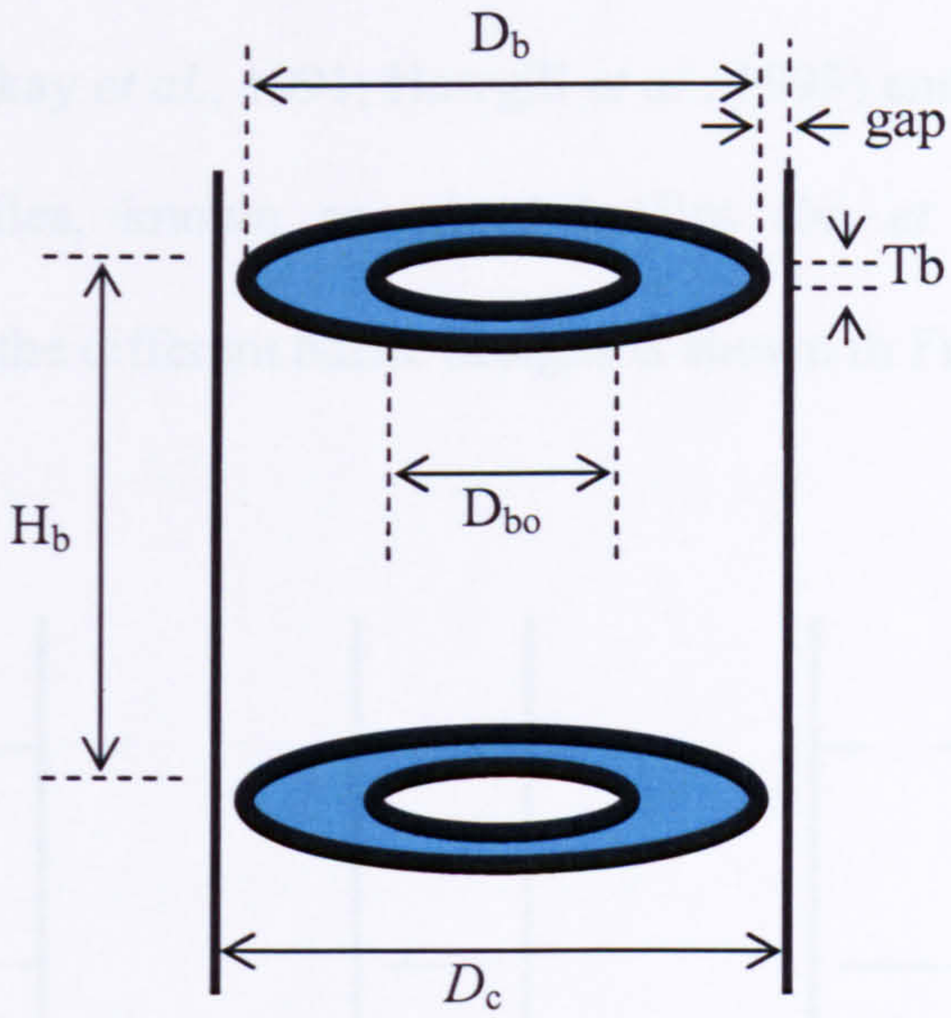

Figure 2.5 Schematic diagram of orifice baffles (Oliveira, 2003)

The orifice diameter influences the size of eddies generated by the oscillation, and is usually expressed in terms of the baffle free area (α), which is defined as the ratio of the orifice area to the column cross-sectional area:

$$\alpha = \left(\frac{D_{bo}}{D_c} \right)^2 \tag{2.6}$$

The baffle spacing is the distance between two consecutive baffles and determines the space available for eddies to expand and propagate within the baffled cell. It can be expressed in dimensionless form as:

$$\beta = \frac{H_b}{D_c} \tag{2.7}$$

In addition to orifice baffles (Dickens, 1989; Mackley and Ni, 1993), a number of different baffle designs have been considered, including helical (Hewgill *et al.*, 1993), central disc (Mackay *et al.*, 1991; Hewgill *et al.*, 1993) and a combination of orifice and central disc baffles, known as mixed baffles (Ni *et al.*, 1995b). A schematic representation of the different baffle designs is shown in Figure 2.6.

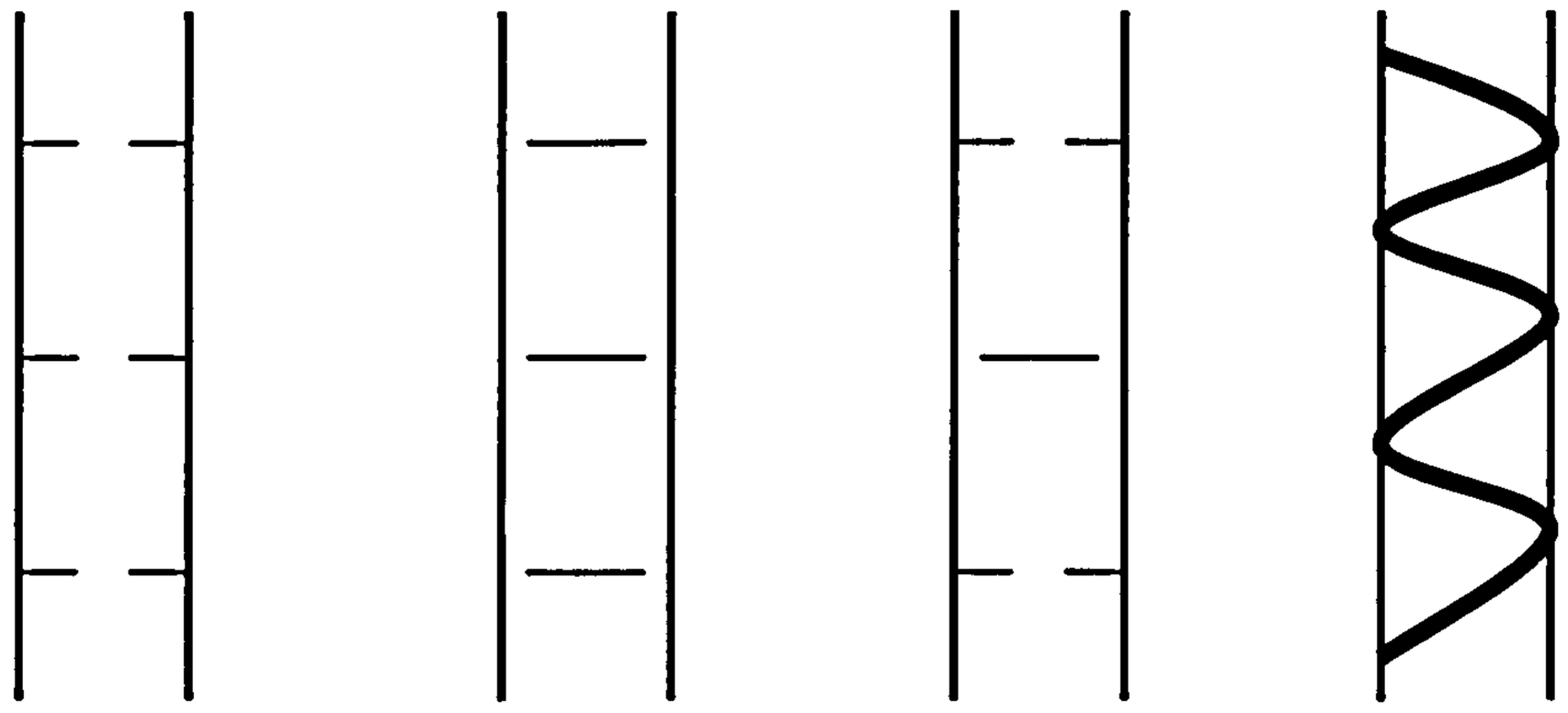

Figure 2.6 Diagram of an OBC containing different types of baffles (Hewgill *et al.*, 1993)

Central disc baffles led to poor results for mixing intensity, but produced high shear rates at the wall, which suggest that they may be useful for cross-flow filtration (Mackay *et al.*, 1991). In a study of filtration, it was verified that central disc baffles resulted in a better performance than orifice baffles. This effect was attributed to more efficient cake erosion caused by the central disc, rather than to any improvement in the mixing properties (Mackley and Sherman, 1993). Helical baffles were shown to provide better overall mixing than central disc, but worse than orifice baffles (Hewgill *et al.*, 1993). Orifice baffles that are not fitted closed to the wall, *i.e.* "loose-fit" orifice

baffles, were also examined. It was shown that the existence of the gap between the baffle and the wall increased the mixing time, *i.e.* the time at which a state of uniform mixing was achieved (Ni and Stevenson, 1999). Orifice baffles designed to give a "push-fit" seal were proven to be the most efficient in terms of mixing/dispersion (Mackay *et al.*, 1991; Zhang *et al.*, 1996) and mass transfer (Hewgill *et al.*, 1993; Ni *et al.*, 1995b) and are therefore the most commonly used.

Baffle free areas from 11% to 51% have been tested in OBCs. Based on flow visualisation and mixing time evaluations, a baffle free area of 0.20-0.32 and a baffle thickness of 2-3 mm were identified as optimum values (Ni *et al.*, 1998). It is important to identify the optimum distance between baffles, since the vortex interaction is insufficient when the spacing is too large, and there is not enough room for the vortices to develop if the spacing is too small. Spacing of 1.5 times the column diameter was found to be the optimal since it provided a good compromise between the two extremes described above (Brunold *et al.*, 1989). However other studies on a range of baffle spacings from 0.9 to 2.5 times the column diameter suggested that a value of $\beta = 1.8$ was optimal (Ni and Gao, 1996a; 1996b; Ni *et al.*, 1998). A possible reason for the difference was the coupled effect of the baffle spacing and oscillation amplitude (Ni *et al.*, 2000a). In this thesis study, a baffle free area of 30% and baffle spacing of 1.6 are used. The following sections present summaries of typical advantages of oscillatory flows in various process operations.

2.1.4 Heat transfer characteristics

It was reported that heat transfer can be enhanced by oscillating the fluid. The heat transfer coefficient (Nusselt number) for laminar flow in oscillated condition possessed similar values as in a smooth tube when the fluid flow is turbulent (Mackley and Stonestreet, 1995). This is an important factor for considering the OBC in the application of wax deposition, however, one likely consequence of applying fluid oscillation is that, with heat transfer enhancement, the cooling rates would be increased, leading to an increase in crystallisation and finally the deposition rates.

2.1.5 Mass transfer characteristics

Considerable work has been carried out to examine the effect of oscillatory flows on gas-liquid mass transfer. The earliest attempt was by Bellhouse *et al.* (1973) who studied the transport of oxygen into blood, where the liquid and the gas were separated by a gas permeable membrane. They reported that liquid oscillation enhanced the oxygenation process. Ni and Gao (1996) compared the mass transfer coefficients between OBC and STR for air and water and reported much higher mass transfer coefficients for OBCs. Oliveira and Ni (2001) suggested that the improvement was due to the breakage and coalescence of bubbles and the much longer bubble residence times as well as the larger gas hold-ups. The effect of having different baffle designs on gas-liquid mass transfer was also investigated (Baird and Rama Rao, 2002). It was found that mass transfer in OBCs was comparable to the STR but with lower shear rate, which is crucial to bio-process applications (Ni *et al.*, 1995c, 2000b). The example was in the

production of pullulan biopolymer, where the production of the biomass in the OBC was found to be almost doubled compared to that in an STR, for the same production time and operational conditions. This was thought due to enhanced mass transfer and low shear rates of oscillatory fluid flow (Gaidhani *et al.*, 2002).

2.1.6 Dealing with solids

Oscillatory flow also has advantages because solid particles can be suspended either in a vertical or horizontal column. The solid-liquid suspension can be controlled either uniformly throughout the column/reactor or separately according to the particles sizes (Mackley *et al.*, 1993). In a study of flocculation, Ni *et al.* (2001a) used bentonite and the bacteria *Alcaligenes eutrophus* as the model systems, and their results indicated that a similar degree of flocculation was obtained in the OBC, but at much lower shear rates than traditional stirred tank devices. This implies that more uniform mixing is achieved in OBCs at much lower power density.

Crystallisation was another example of solid handling in OBCs. Crystallisation of paracetamol was attempted in an OBC and the crystals produced were found to be more uniform in shape and less defective compared to the crystals produced using a stirred tank crystalliser (STC) (Ni *et al.*, 2003). Ni *et al.* (2004) also studied the crystallisation of L-glutamic acid in an OBC and observed smaller and more consistent metastable zone width (MSZW) in the OBC compared to that in the stirred tank crystalliser (STC), indicating that crystallisation in the OBC was better controlled than that in an STC. As the mechanism of wax deposition is crystallisation-based, the advantages presented here would be of great benefit to this thesis study.

2.1.7 Reactions

Many chemical processes involve liquid-liquid phases where the reactant is dispersed in the form of droplets. Controlling the droplet size and morphology is very important to ensure uniform reaction and product. This is achievable using either batch or continuous oscillatory flows by controlling the oscillation intensity, and producing droplets with narrow size distribution as well as higher repeatability and predictability. Examples of this type of reaction carried out in OBCs are suspension polymerisation of methylmethacrylate and styrene; and inverse phase suspension polymerisation of acrylamide (Ni *et al.*, 1998, 1999, 2000a, 2002; Stevens, 1996; Zhang, 1998; Bennett, 2001; Pereira, 2002, Nelson, 2001). It was observed that high quality polymer beads were produced with similar molecular weights and narrow size distributions.

Problems endured in the conventional batch processes are the low efficiency and large volume of solvent usage which also presents safety risks. One reaction carried out to exhibit the advantage of OBR was the production of sterols by saponification of steryl esters (Harvey *et al.*, 2001). The main problems in batch production of this compound were the large volume of solvent (ethanol) and the long reaction time. Migrating the batch process to a conventional continuous tubular reactor would be unfeasible due to high length-to-diameter ratio caused by the high net flow velocity required to achieve high Reynolds numbers for good mixing and plug flow. However, using OBR, this problem can be avoided as the mixing is controlled by oscillations rather than the net flow, hence the length-to-diameter ratio is smaller. This is related to process intensification.

Another example of a reaction carried out in OBR was the multi-phase photochemical reaction where catalyst-coated particles were suspended in the liquid phase by fluid oscillation, and contacted with gas bubbles passing through the column. The catalyst was activated by ultraviolet light from an axially positioned cylindrical lamp. Separation of the solids from the liquid occurred at the top of the reactor where the effect of oscillatory flow was minimal (Fabiyi and Skelton, 1999). Fabiyi and Skelton (2000) applied the concept in the oxidation of contaminants in wastewater using titanium dioxide as the catalyst and found that photon utilisation efficiency was higher compared to the conventional photo-reactors and less fouling was also observed.

2.1.8 Plug flow characteristics and scale up perspective

Mixing under plug flow conditions could be achieved even when the bulk fluid flow is laminar as opposed to the conventional plug flow reactor where mixing can only be accomplished if the net flow is in a turbulent state. This leads to better residence time distribution and more complete reaction (Dickens *et al.*, 1988; Mackley and Ni, 1991, 1993). These advantages provide process enhancements especially for reactions that require long residence time such as in pharmaceutical and biochemical operations (Ni, 1995; Stonestreet and van der Veeken, 1999).

Smith (2000) demonstrated that scale-up of OBRs is easily achieved by linear geometric scaling and the axial dispersion was shown to be comparable regardless of the scale, provided that geometric and dynamic similarities are maintained. Lee *et al* (2001) reported that similar performance was observed in the protein refolding reaction

for both laboratory and large scale OBR. The performance after scaling-up using air-water mass transfer coefficient as the indicator was also studied. It was found that mass transfer coefficients increased linearly with the scale for a given oscillation intensity (Ni and Gao, 1996). By comparing the polymerisation of methylmethacrylate in a small reactor of 0.05 m diameter OBR with that of 0.38 m diameter, the size distribution of the polymer beads was found to be identical (Ni et al., 1998, 1999; Nelson, 2001). It suggests that scale-up and design of OBRs has now been well understood, and full-scale continuous OBRs have been developed for a number of applications. In this thesis work, only a batch OBC is used.

2.2 Paraffin Wax Deposition

Problems associated with wax deposition cause huge economic losses to the petroleum industry worldwide through the cost of chemicals, reduced production, well shut-in, less utilisation of capacity, choking of the flowlines, equipment failure, extra horse-power requirement and increased manpower attention. The problem is more serious for deepwater oilfields as pipeline blockage could occur in the cold subsea conditions (Matzain *et al.*, 2001). Understanding of such problems is vital to oilfield operators in their search for technical and economic solutions. Figure 2.7 shows the cross section of a pipeline blocked due to wax deposition.

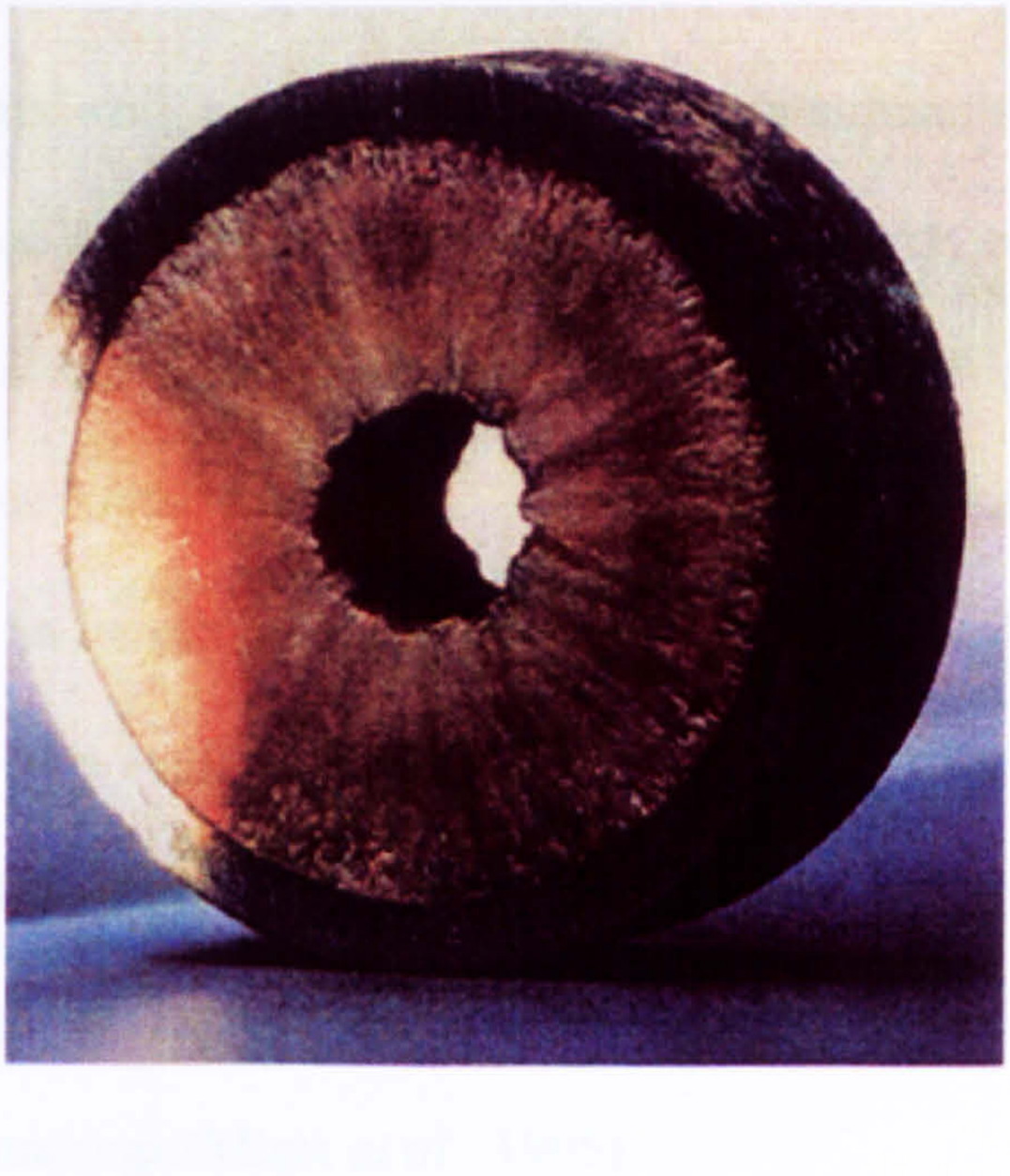

Figure 2.7 Photo of cross section of a pipeline blocked with wax deposit (Singh *et al.*, 2001)

2.2.1 Characterisation of paraffin wax

The four main classes of compounds found in wax deposits are aliphatic hydrocarbons, aromatic hydrocarbons, naphthenes, resins and asphaltenes (Gruse and Stevens, 1960). The major constituents of macrocrystalline waxes are n-paraffins that usually form needle-shaped crystals while the microcrystalline waxes are mainly branched-chain paraffins. It has been suggested that macrocrystalline waxes are the major causes of paraffin problems in production and transportation, whereas microcrystalline waxes are the major contributor to sludge problems in vessels and tanks (Jorda, 1966; Shock *et al.*, 1955).

In one study on the analysis of oilwell equipment deposits, it was reported that the main components were paraffins with 52% content and less than 5% resins; and the balance consisted of crude oil, water and mechanical contaminants (Misra *et al.*, 1995). Paraffin wax molecules are straight-chain alkanes. Compounds of this type containing more than 20 carbon atoms pose a risk through wax deposition problems (Holder and Winkler, 1965). Waxes containing up to C_{80} paraffin compounds have been reported by Woo *et al.* (1984). In an investigation of whether certain crude oils could have the risks of wax deposition, it was suggested that several indicators can be examined, *i.e.* the concentration of paraffin waxes; the carbon number distribution; the concentration of other compounds such as asphaltenes and aromatics; and the temperatures of the oilfields and the surroundings (Misra *et al.*, 1995).

2.2.2 Crystallisation of paraffin waxes

Temperature changes affect the solubility of paraffin waxes and reducing the oil temperature will promote wax crystallisation. Paraffin waxes usually remain dissolved in the crude oil under reservoir conditions until the equilibrium states are disturbed, through the changes in temperature and pressure. Paraffin may also crystallise and precipitate due to changes in the composition resulting from the loss of volatile light ends with smaller carbon numbers. Hydrocarbons with small carbon numbers usually act as solvents for the paraffin waxes (Holder and Winkler, 1965). Similar observations were reported by Weingarten and Euchner (1988); indicating that wax crystallisation increased when the pressure was reduced.

The high temperatures and pressures in the underground reservoir usually cause many light components of the crude oil (*e.g.* methane, ethane, N_2, CO_2) to be in supercritical states (Carnahan. 1989). Therefore the heavy ends of the crude remain dissolved until the well starts flowing, when the pressure will be released causing the solvating power of the supercritical fluids to be decreased. This again will promote paraffin wax crystallisation (Fernandez-Lozano and Rodriguez, 1984). Other components in the crude oils such as tars and asphaltenes also affect the solubility of paraffin waxes in such a way that the solubility increases as the content of tars and asphaltenes increases. This is due to the colloidal state of the components that prevent crystallisation through suppression of the crystal growth as well as interlocking of the wax crystals (Misra *et al.*, 1995).

2.2.3 Structure of wax deposits

Several studies have been conducted to identify the possible structure of wax deposits. Fernandez-Lozano and Rodriguez (1984) suggested a micellar structure of wax crystals in the deposits. It has been established that under the most favourable conditions, the waxes form an orthorhombic lattice. But changes in conditions could lead to a mixture of orthorhombic and hexagonal forms (Srivastava *et al.*, 1992). The orthorhombic crystals have been seen forming star-like shapes or plate-like layers with better interlocking behaviour. The wax crystals can interlock or trap the solvents and star or plate-like formations were reported to have very good interlocking tendencies (Knox, 1962). The interlocking can be increased by rapid cooling, the presence impurities and additives, which would lead to softer wax gel (Knox, 1962, 1966). Pauly *et al.* (2004) observed some non-uniform plate-like structures with large crystals size as shown in Figure 2.8.

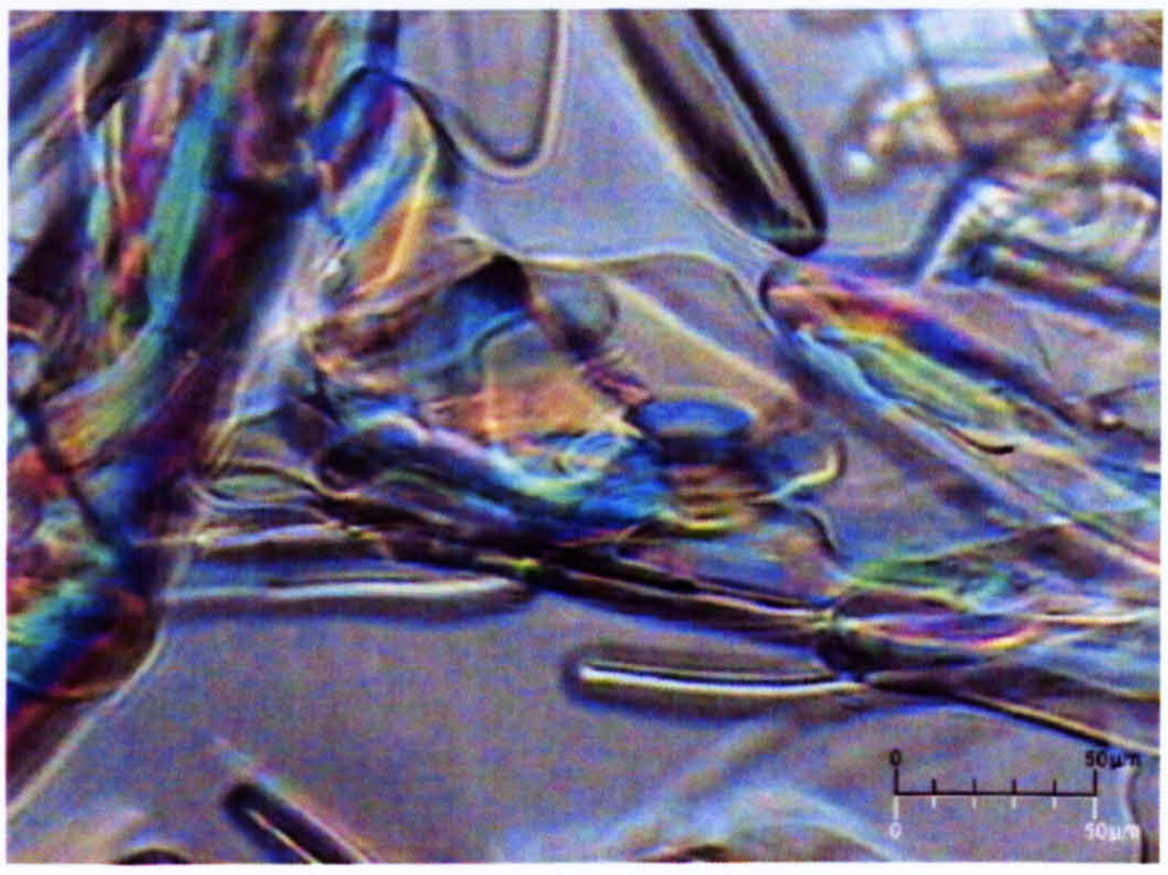

Figure 2.8 Microscopy photo of liquid-solid equilibrium for the C_{10}+(C_{24}-C_{25}-C_{26}) system (Pauly *et al.*, 2004)

Kane *et al.* (2003) produced photographs showing the structure of the solvent-precipitated paraffins of crude oil in Figure 2.9, which clearly exhibits the platelet structure with stratified lamellas parallel to each other. The picture shows independent blocks with a shape resembling 'pine cones' and also unevenness from the top to the bottom of the 'pine cones'. The basic structure of the blocks is platelet-like where the orientation is different from one block to the other, but similar within an individual block.

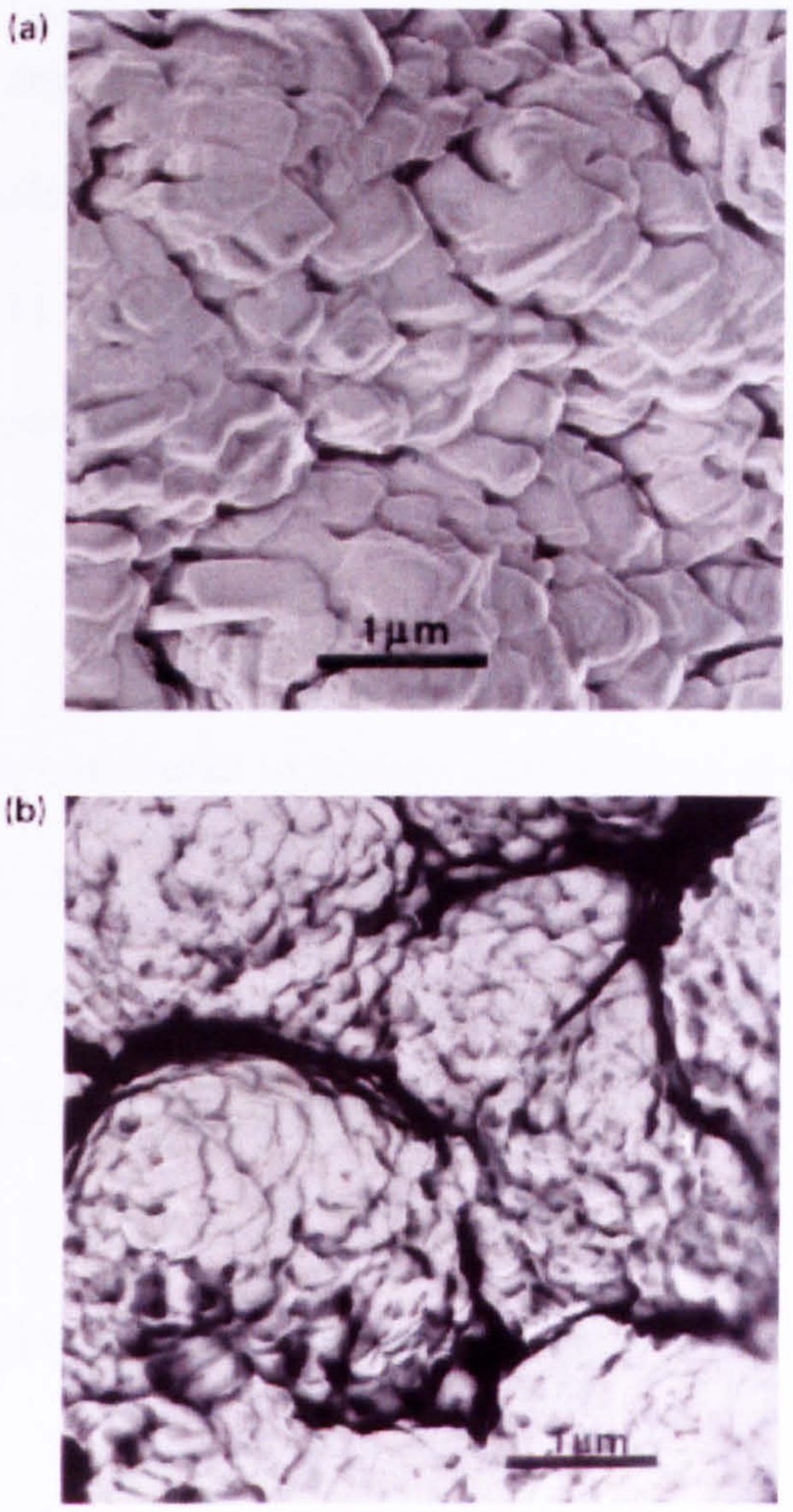

Figure 2.9 (a) Platelet structure of solvent precipitated paraffins, (b) the pine cone structure of solvent precipitated paraffins (Kane *et al.*, 2003)

Figure 2.10 shows the wax crystal network formed under no shear, low shear and high shear conditions (Venkatesan *et al.*, 2005). They suggested that "each gel crystal was roughly "pennyshaped," *i.e.*, a thin platelet having, generally, an elliptical cross-section or could be characterised as oblate spheroids (resulting in the elliptical cross-section)". In the study, an elliptical cross-sectioned cylinder (thin platelet) was assumed as the shape of each individual wax crystal due to the difficulty in determination of crystal extension in the depth dimension.

Mauricio *et al.* (2003) conducted a laboratory experiment that was designed to observe the motion of wax crystals subjected to an imposed temperature gradient. A special sample holder was built to adapt to a motorised optical microscope, with digital image acquisition. Figure 2.11 shows image sequences in which the evolution of the crystallisation front and the growth of wax crystals are clearly visible, mostly in needles and plate-like shapes.

Studies have also been conducted to observe the effect of anti-wax agents on the structures of wax deposits. Figure 2.12 shows the optical micrographs of the precipitation of C_{23} wax with and without anti-wax agent (Hutter *et al.*, 2004). In the absence of anti-wax agent, the growth front consisted of overlapping flat plates which grew simultaneously (Figure 2.12(a)). With the addition of anti-wax agent the crystal growths are in the form of highly branched networks (Figure 2.12(b)).

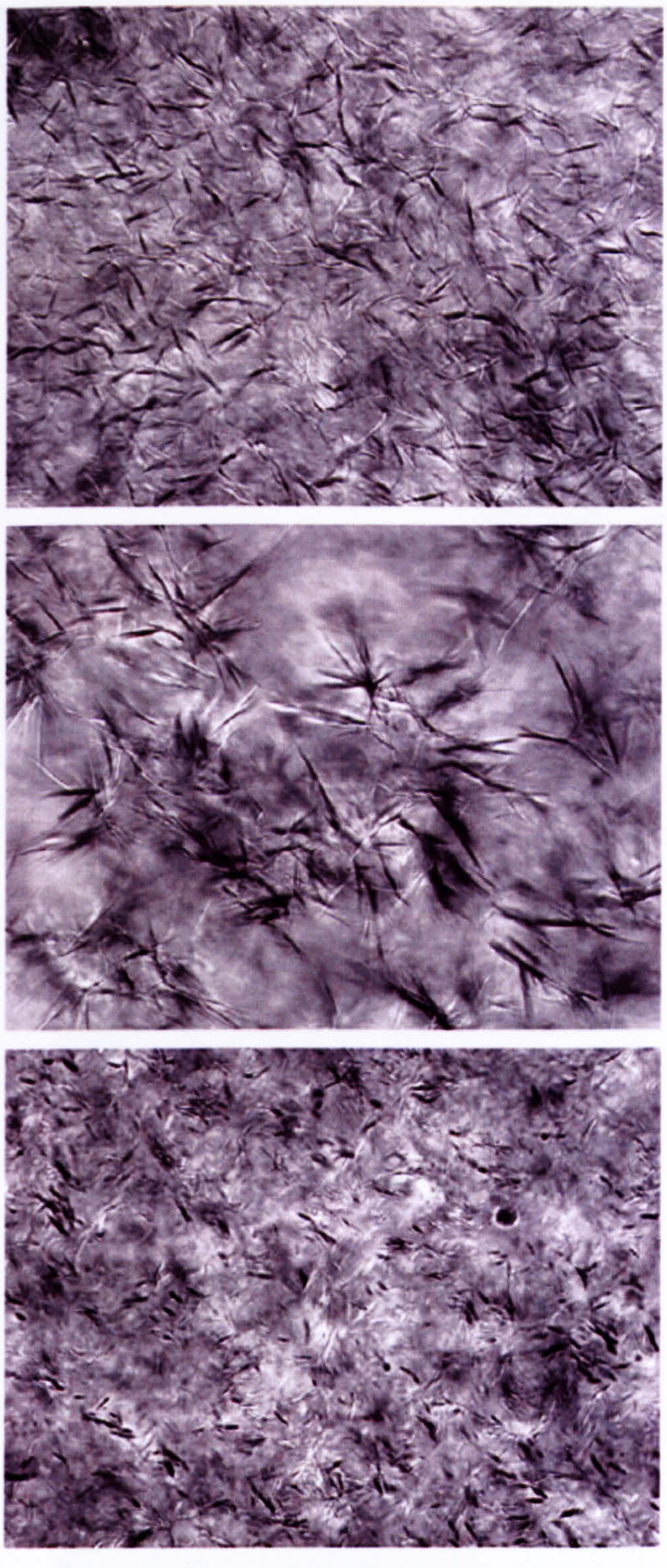

Figure 2.10 Wax crystal formed under no shear conditions (top), low shear conditions (middle) and high shear conditions (bottom) (Venkatesan *et al.*, 2005)

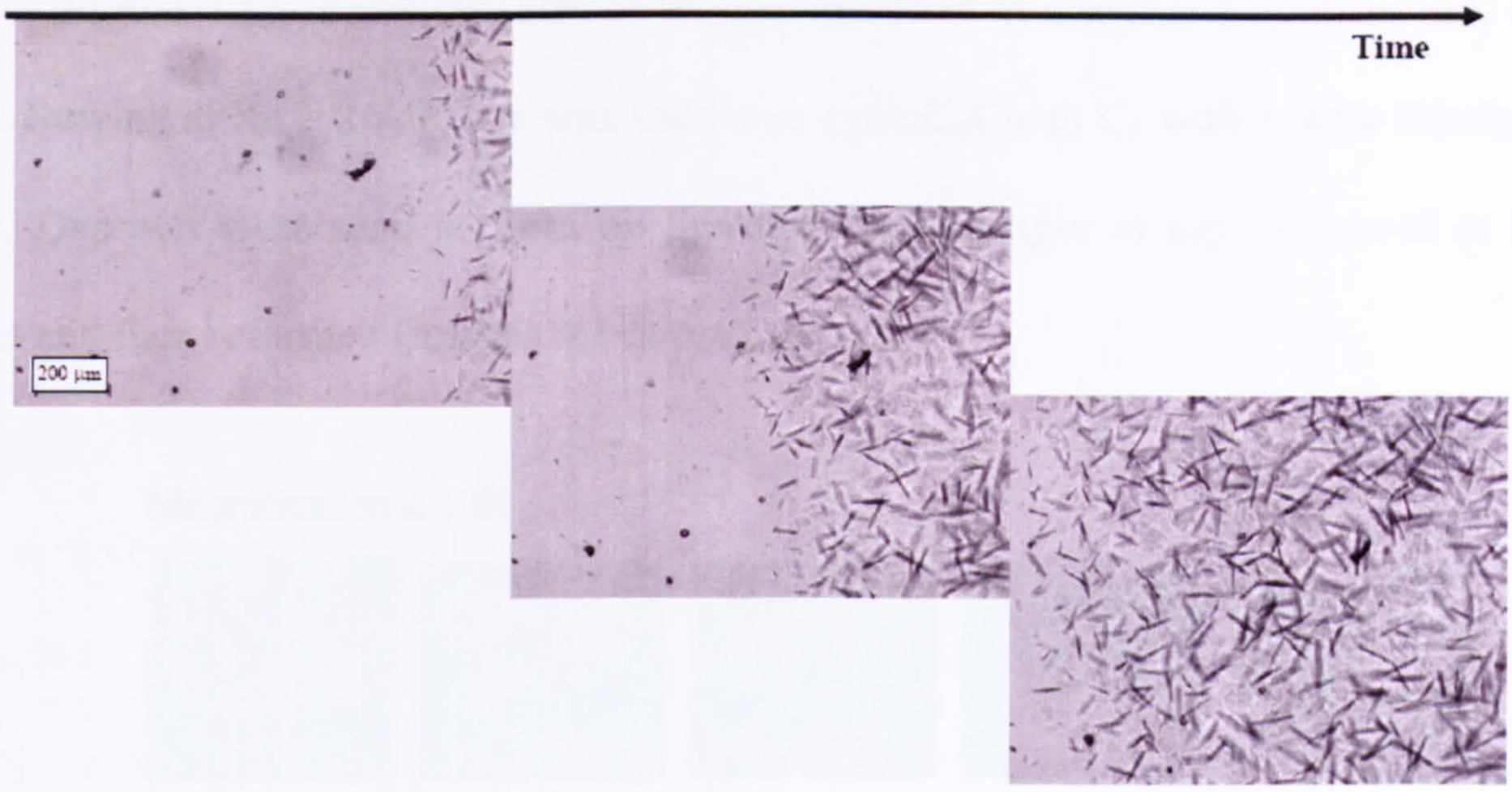

Figure 2.11 A time sequence of wax crystallisation front with the cold wall at the right side of the images (Mauricio *et al.*, 2003)

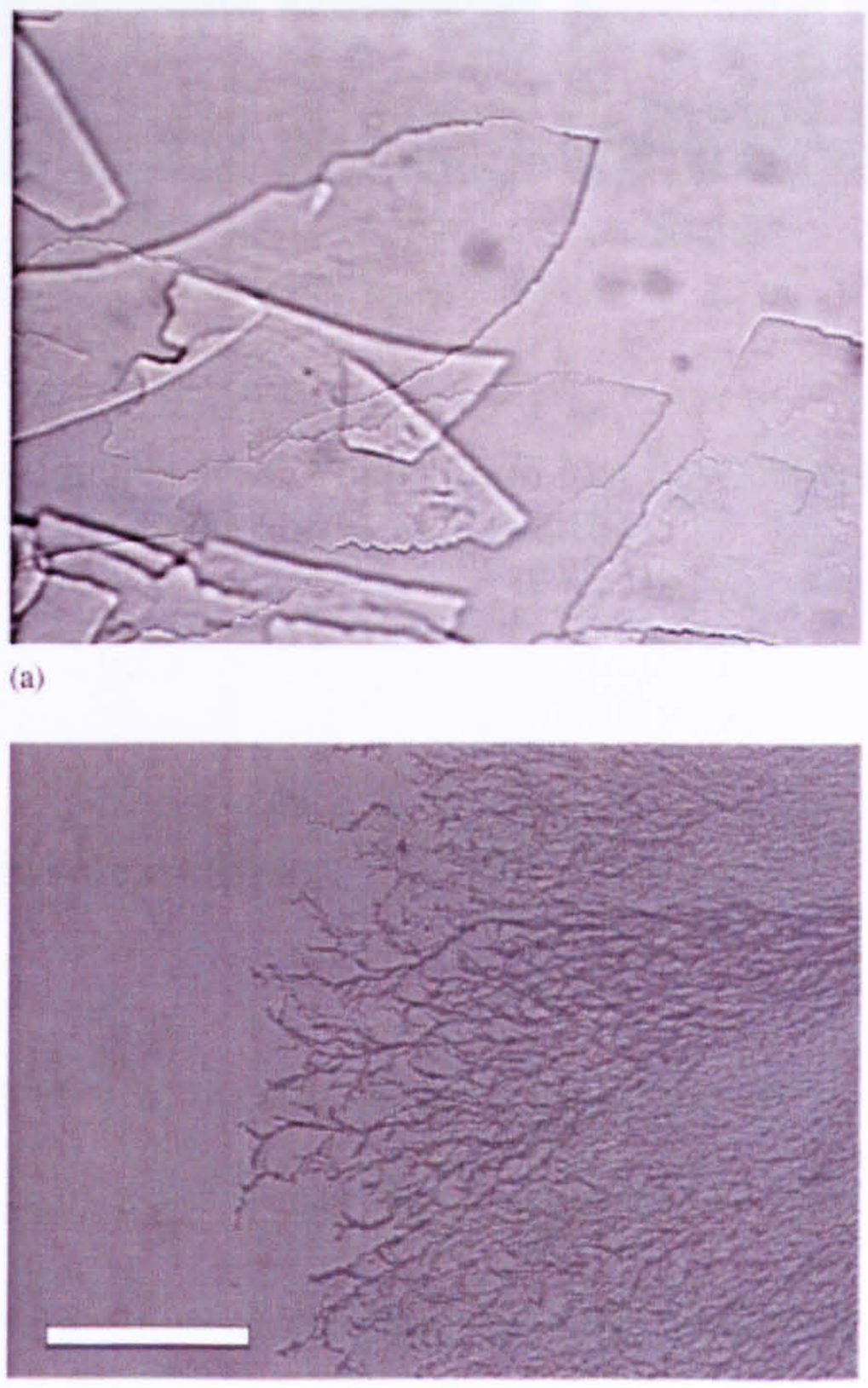

Figure 2.12 Optical micrographs of C_{23} precipitates. (a) Precipitates formed from a solution without anti wax agent. (b) Precipitates formed from a solution with anti wax agent. The scale bar spans 100 μm and applies to both images (Hutter *et al.*, 2004)

Figure 2.13 shows two sets of images recorded in a square and clean tube with fluid flowing at Re = 2400. The wax used was cycloC_6C_{19} in C_8 with a mole fraction of 0.06. Deposits were seen to form on the tube wall (images at top), removed at later times and then reformed (images at bottom).

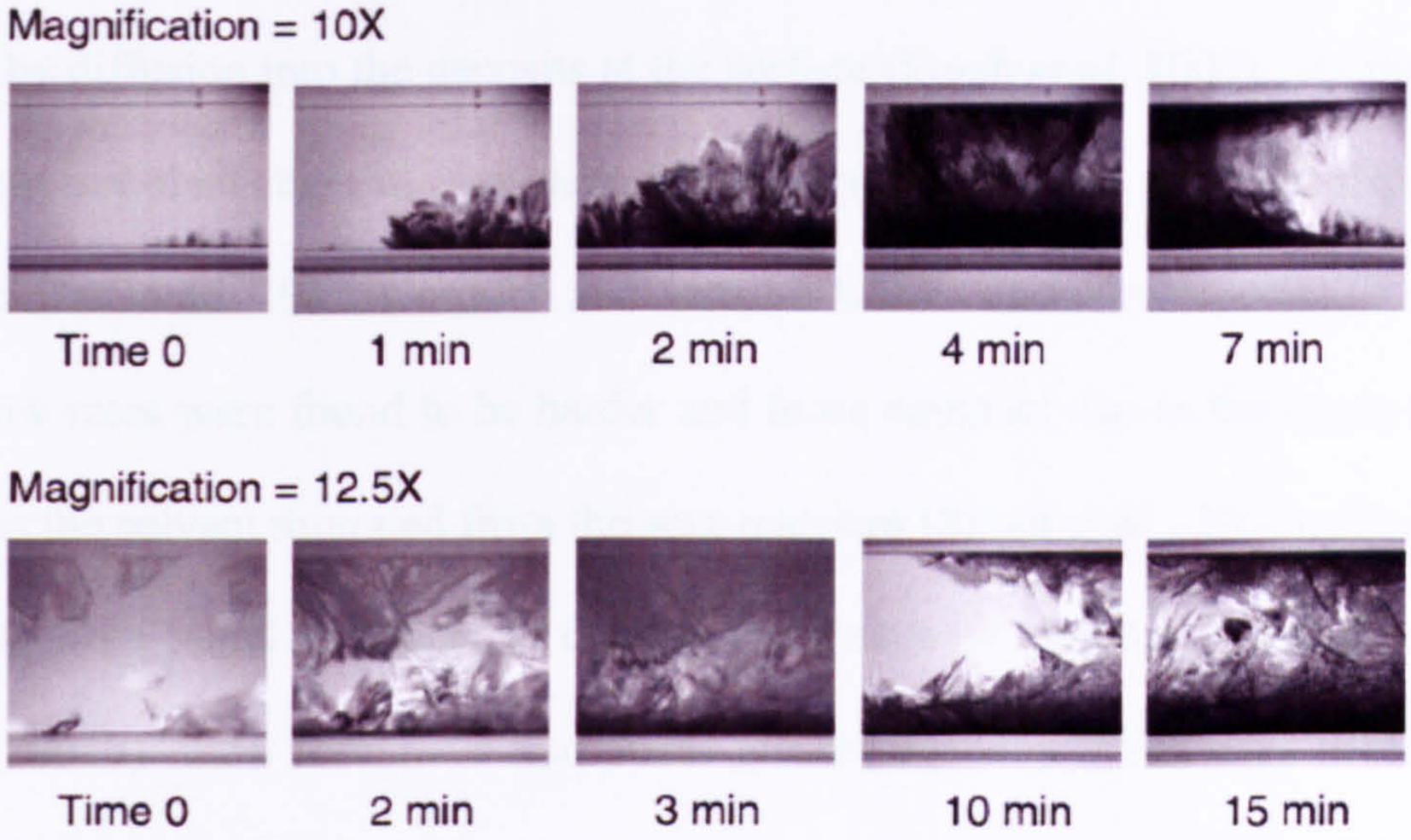

Figure 2.13 Images of wax deposition in a flow condition (Cordoba and Schall, 2001b)

2.2.5 Factors affecting wax deposition

The mechanism and extent of wax deposition have been studied by many researchers (Nguyen *et al.*, 2001; Thanh *et al.*, 1999; Imai, *et al.*, 2001; Ribeiro *et al.*, 1997; Hennessy *et al.*, 1999) using a range of different methods (Pedersen, 1995; de Boer *et al.*, 1995; Monger-McClure *et al.*, 1999). Three major factors influencing deposition are flow rate, temperature differential and cooling rate, and surface properties (Bott and Gudmundsson, 1977a).

a) Flow rate

It was shown that in laminar flow, wax deposition increases with flow rate (Creek *et al*, 1999; Cordoba and Schall, 2001b) due to availability of more wax particles to be transported by diffusion into the deposits at the surface (Singh *et al*, 2001). As the flow increases into turbulent regions, wax deposition decreases because of shear dispersion (Hartley and Bin Jadid, 1989; Cordoba and Schall 2001b). The wax deposits produced at higher flow rates were found to be harder and more compact due to the aging of the deposition as the solvent migrated from the wax matrices (Singh *et al.*, 2001). The aged wax deposits were found to adhere to the pipe wall even in turbulent flows (Cordoba and Schall, 2001b). Low flow rates also posed greater wax deposition risks because of the longer residence time of the oil in the tubing that permits more heat loss and leads to wax precipitation and deposition (Weingarten and Euchner, 1988).

b) Temperature differential and cooling rate

The temperature differential between the bulk solution and cold surface is one of the vital factors for wax deposition. It is a well known fact that wax deposition increases with an increase in this temperature difference (Cole and Jessen, 1960; Towler and Rebbapragada, 2004; Wardbaugh and Boger, 1991). The difference between the wax appearance temperature (WAT) and the temperature at the cold surface is more likely to affect the deposition than that between the bulk fluid and the cold surface. Wax

deposition only occurs when the surface temperature is below both the solution temperature and the solution WAT (Patton and Cassad, 1970).

Different cooling rates can affect wax crystallisation in such a way that higher rates of cooling induce smaller crystal size but in larger numbers, whereas at lower rates of cooling the crystallisation process is more uniform leading to more packed crystal lattices (Bott and Gundmundsson, 1977a). It was shown that wax deposits produced at high rate of cooling had weaker structures due to the trapping of the solvent/oil (Bott and Gundmundsson, 1977b).

c) Surface properties

It is a well known fact that wax crystals adhere to the pipe surface during deposition, thus surface properties can be important factors in the wax deposition mechanism in pipelines. Several studies have been conducted on the effect of the presence of films or lining on the pipe's metal surface on wax deposition. Parks (1960) demonstrated that treating the pipe metal surface with certain adsorbed films reduced the adherence of paraffin to that surface. Zhang *et al* (2002) studied the effect of internal coatings on wax deposition, where it was found that coating with polymer increased the efficiency of deposition prevention. Wettability of the pipe surface could be affected by the nature of the absorbed compounds (Zisman, 1963). In the study by Li *et al.* (1997) it was clearly demonstrated that the water wetting property of glass can be utilised to avoid wax deposition on the walls of a pipeline with an inner glass layer. The water film formed

between the oil and the glass lining prevented the wax being deposited on the wall of the tube, thus the amount of wax deposition on the wall was reduced (Li *et al.*, 1997).

2.2.6 Laboratory studies on paraffin deposition

Paraffin deposition has been studied in laboratories under conditions resembling those in the oilfields. Current theories on the mechanism of deposition have evolved from both field observations and laboratory tests. One example was the study conducted by Hennessy *et al* (1999) in which the effect of the bulk and surface kinetics on the overall nucleation process was examined. Model oil comprising 5% wax, 90% decane, 5% toluene and an inhibitor was pumped through a test rig (Figure 2.14) and the differential pressure (ΔP) was monitored across a stainless steel pipe (5 m length and 2.16 mm ID). The temperature of the mixture was lowered using a water bath. The temperatures at the initial ΔP increased were determined for the wax and two inhibitors.

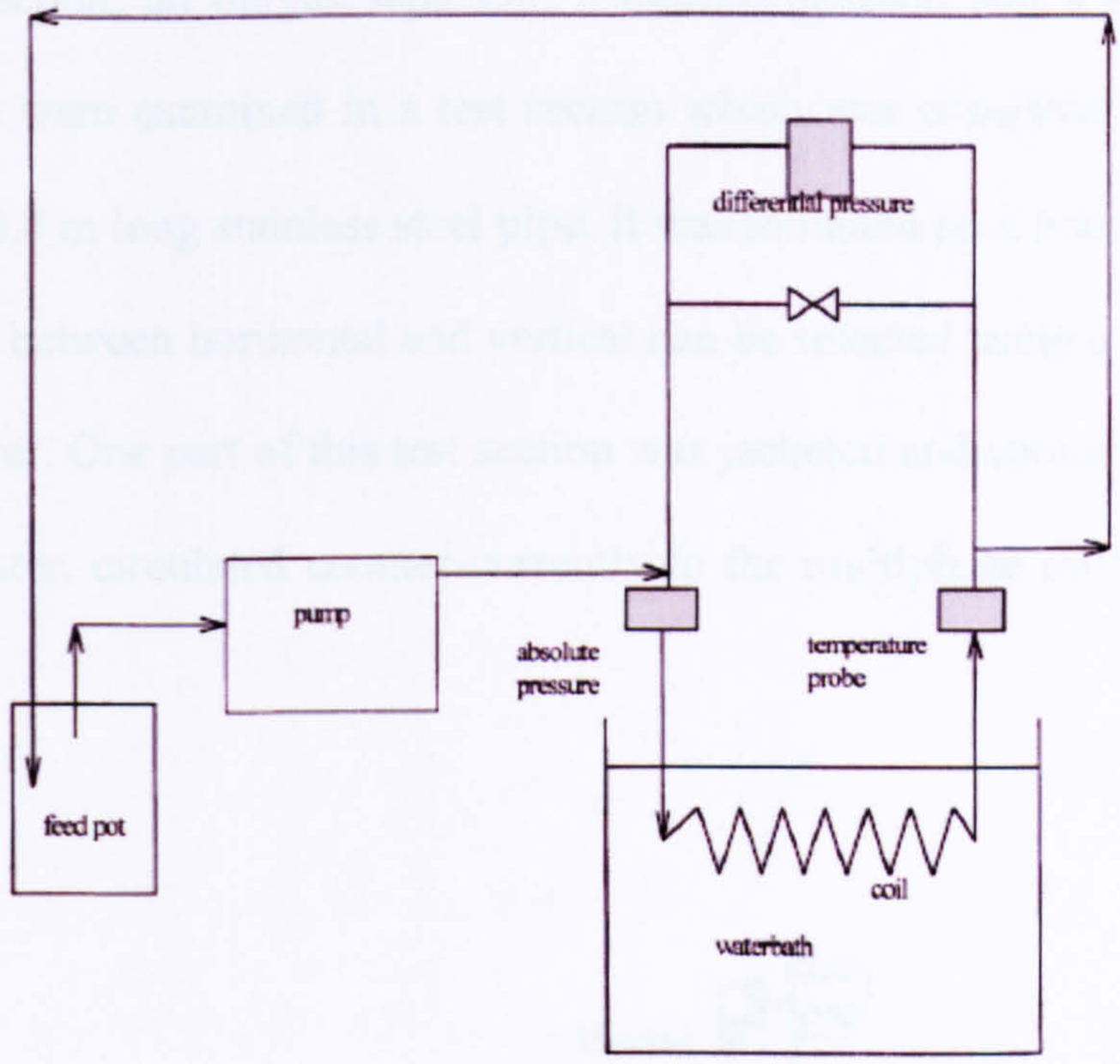

Figure 2.14 Schematic representation of the tube blocking apparatus used for the surface nucleation measurements (Hennessy *et al.*, 1999)

It was found that bulk nucleation occurred either in the absence or presence of both wax deposition inhibitors. The meta-stable zone width (MSZW) was found to be increased when the inhibitors were added and the kinetics of inhibition between the two additives was also different. The temperature at which blockage occurred was lowered and fractional crystallisation was observed in the bulk phase (Hennessy *et al.*, 1999).

Matzain *et al.* (2002) carried out experiments to investigate paraffin deposition during multiphase flow. The experimental facility used (Figure 2.15) was designed for conducting paraffin deposition tests for a two-phase mixture of natural gas and crude oil flowing in horizontal, near-horizontal and vertical pipes. The test facility consisted of an oil system, a gas system, a multiphase system with an oil/gas temperature trimming

section, a test section, an oil/gas separator, a chilling system, and a heating system. Wax depositions were examined in a test section which was consisted of a U-shaped, 52.5-mm I.D., 48.8 m long stainless steel pipe. It was mounted on a boom such that any inclination angle between horizontal and vertical can be selected using a hydraulic hoist attached to a tower. One part of this test section was jacketed and cooled with a mixture of glycol and water, circulated counter-currently to the multiphase mixture flowing in the inner pipe.

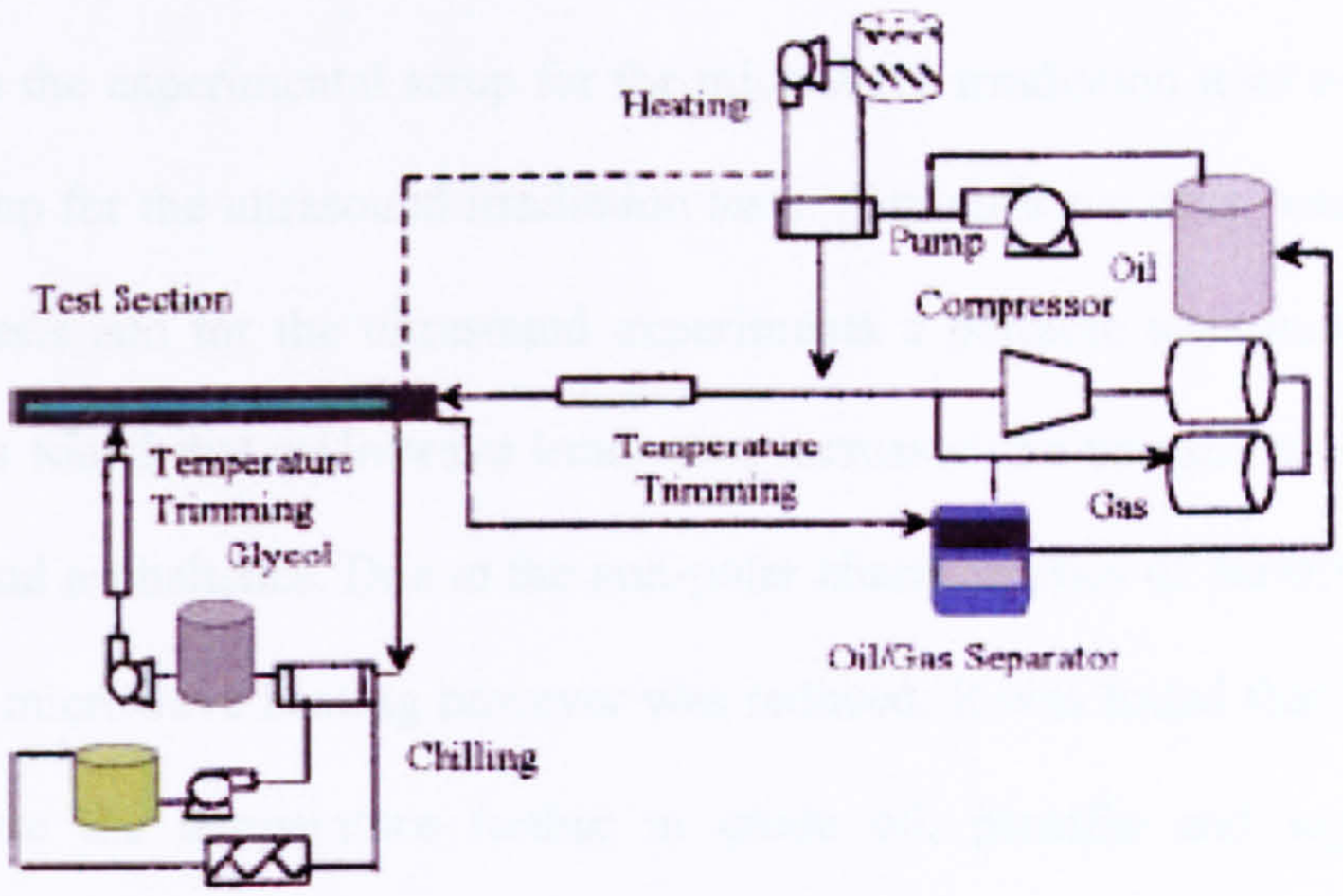

Figure 2.15 Test facility for wax deposition in a multi phase system (Matzain *et al.*, 2002)

In the two phase fluids study, it was found that wax deposition was affected by the flow pattern and velocities. The deposition occurred along the pipe wall and higher fluid flow produced thinner and harder deposits. Compared to the tests conducted in a single phase with laminar flow, it was observed that the trend of wax deposition was similar to that of the two phases when low velocity was applied. Likewise, the trend at

high velocities of two phase systems is similar to the trend when turbulent flow is applied to single phase fluids. In horizontal and near horizontal intermittent flow tests, thinner and harder deposits were observed at the bottom of the pipe. Thicker and harder deposits were produced in slow annular flows velocities, whereas in stratified flow tests, no wax deposition was observed along the upper portion of the pipe (Matzain et al., 2002).

Laboratory study was also conducted to investigate the use of microwave and ultrasound as ways to mitigate wax deposition (Bjorndalen and Islam, 2004). Figure 2.16(a) illustrates the experimental setup for the microwave irradiation tests and Figure 2.16(b) is the setup for the ultrasound irradiation tests. A microwave oven was used for the microwave tests and for the ultrasound experiments a portable ultrasound system was used. It was found that microwave irradiation increased the temperature of crude oil, paraffin oil and asphaltenes. Due to the non-polar characteristics of paraffin oil, the efficiency of the microwave heating however was reduced. It was found that bentonite helped to increase the temperature further in crude oil, paraffin and asphaltenes, whereas gypsum showed little effect. The effect of asphaltenes content in the crude was also investigated that at higher concentration, microwave irradiation reduced the mixture viscosity due to the re-orientation of molecules as well as the breakdown of asphaltenes particles. In the ultrasound experiments, it was found that the paraffin viscosity was reduced initially but over time ultrasound irradiation increased the viscosity. In terms of particles suspension, it was observed that microwave irradiation keeps particles in suspension when the irradiation time is greater than 20 s while, ultrasound irradiation also suspends particles after 20 s but to a lesser degree (Bjorndalen and Islam, 2004).

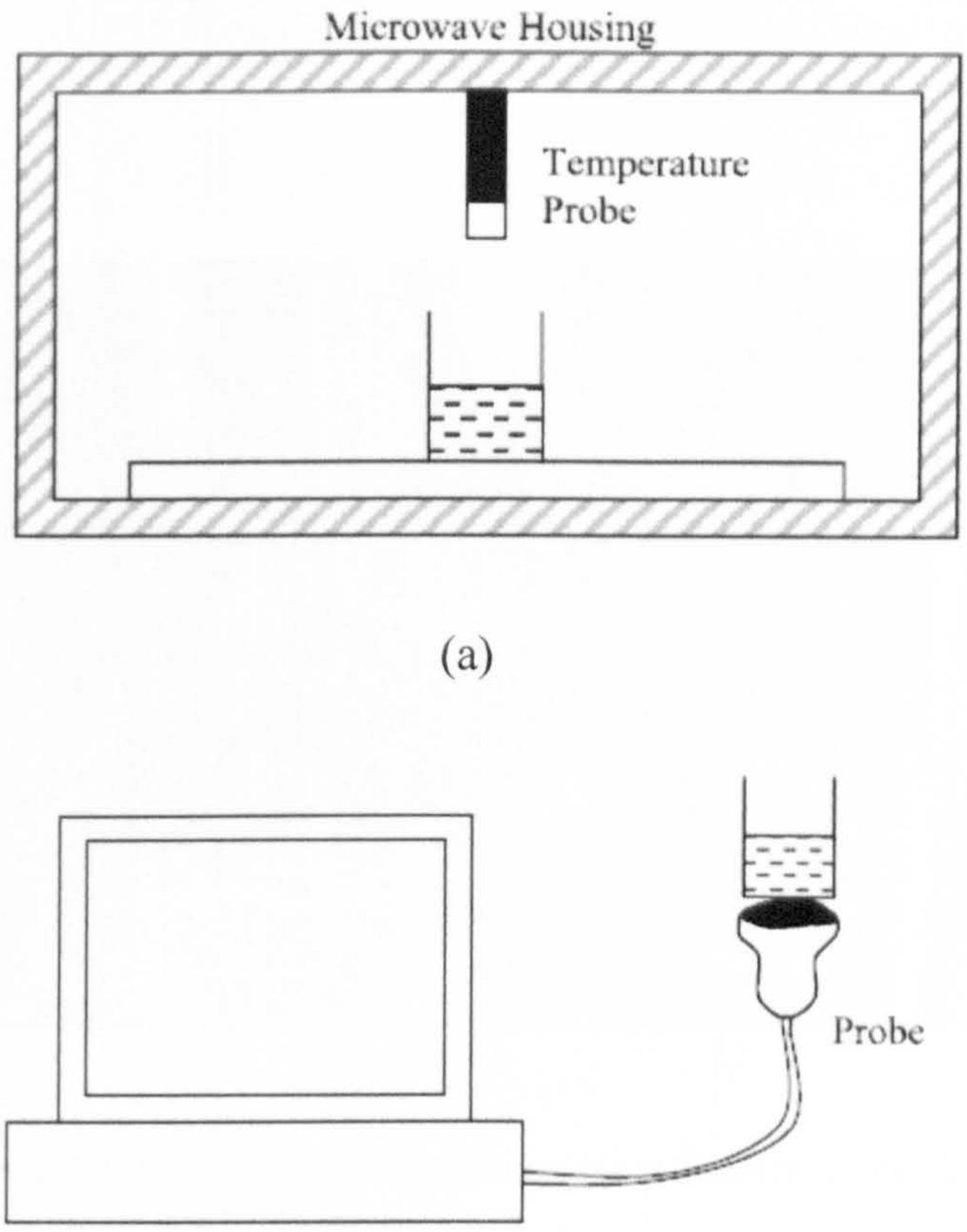

Figure 2.16 Experimental set up for the microwave and ultrasound irradiation tests (Bjorndalen and Islam, 2004)

In a study using the cold finger apparatus aimed to learn about paraffin deposit formation in two types of Brazilian crude oils, the petroleum samples were heated to several different temperatures in a heating bath in contact with the cold fingers kept at lower temperatures (Figure 2.17) (dos Santos *et al.*, 2004). The heating bath temperature was initially set to a temperature of 90 °C and then reduced to temperatures of 60, 50 and 40 °C. The cooling bath that supplied cold water to the cold fingers was set at 7, 3

and -1 °C. Figure 2.17 shows the apparatus after the experiment with a typical paraffin deposition.

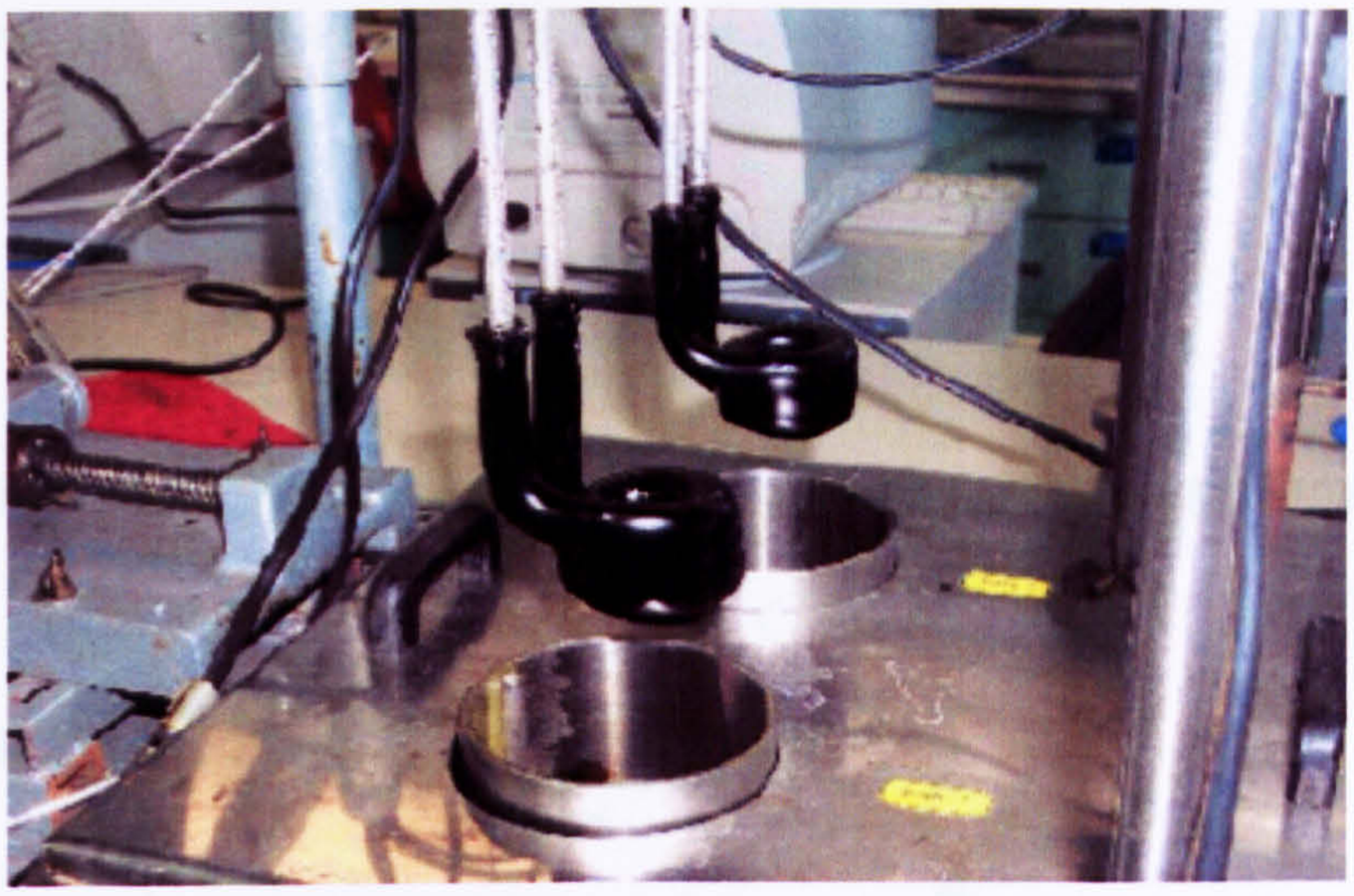

Figure 2.17 Cold finger apparatus (dos Santos *et al.*, 2004)

The aim of this study was to evaluate the critical time of deposition as well as the critical temperature difference between the hot crude oil and the cold sub-sea temperature. Measurements of the thickness of the deposits, deposition rates and the degree of sub-cooling were taken. The deposition rates were found to be influenced by the temperature difference as well as the crystals nucleation kinetics and growth on the cold finger surface. They proposed two mechanisms of deposition *i.e.* "(i) if the critical temperature is attained at the surface, nucleation will occur at the pipe wall and deposits will be formed; (ii) if the temperature difference between the pipe wall and the petroleum bulk is less than the critical temperature difference, nucleation will occur at the petroleum bulk and no deposition will occur at the pipe wall" (dos Santos *et al.*, 2004).

Towler and Rebbapragada (2004) used a laboratory-scale flow system to simulate the deposition of paraffin in the oil wells. A schematic diagram of the system is shown in Figure 2.18. The equipment consisted of two concentric tubes with a facility to measure the pressure drop between the ends of the inner tube which was called the test section.

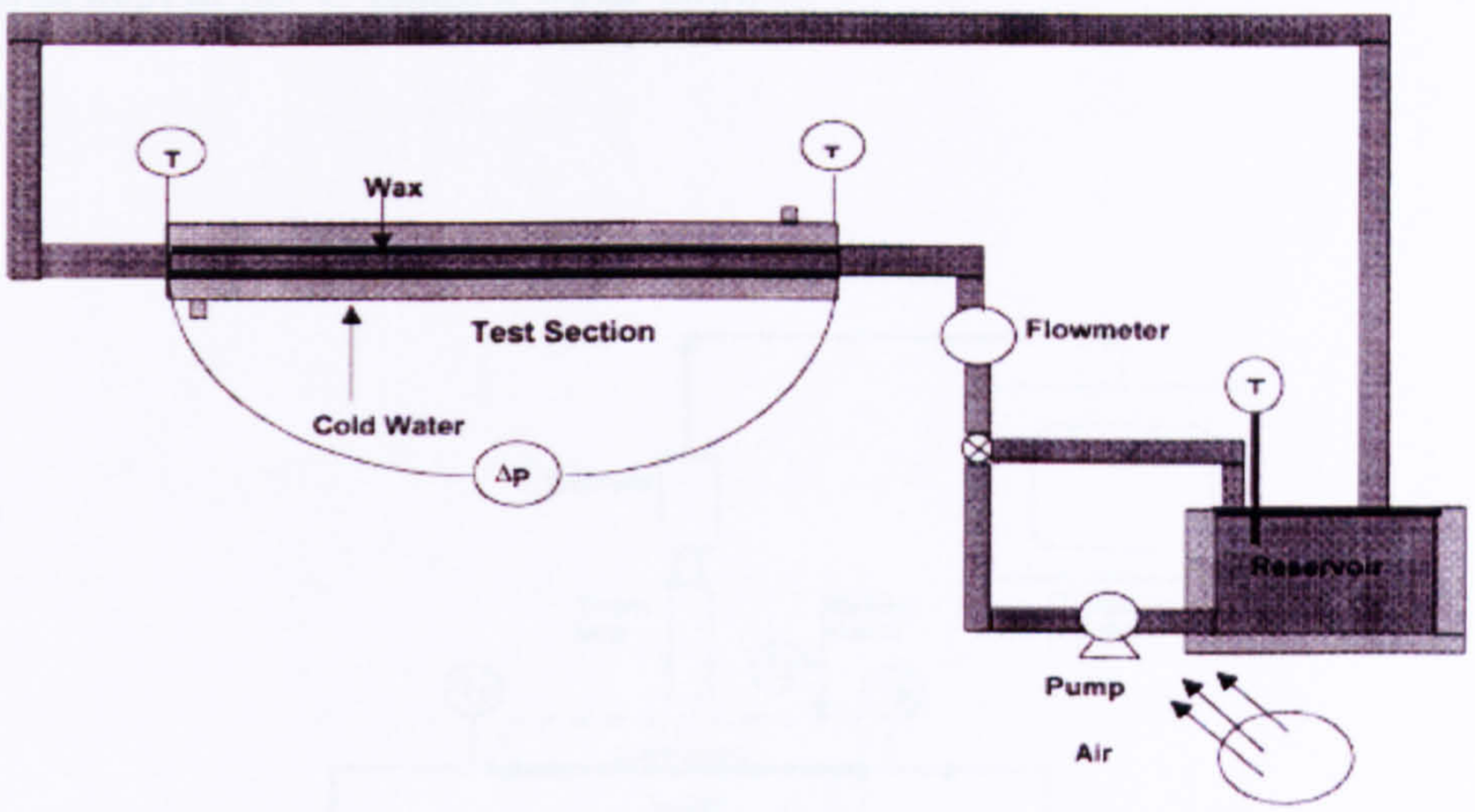

Figure 2.18 Paraffin deposition flow system (Towler and Rebbapragada, 2004)

It was observed that the paraffin deposited at a faster rate initially and then grew more slowly to some maximum. For two commercial chemical wax inhibitors tested (only revealed as Solvent A and B), the results indicated that one gave up to a 35% reduction in the amount of wax deposited and the other solvent was ineffective in inhibiting wax deposition. It was also determined that this solvent was not effective in removing wax once it had already deposited. Lastly, the crude appears to become waxier and more viscous with time after it has been exposed to air.

Cordoba and Schall (2001a) designed a flow system to study the deposition of paraffin wax (nonadecylcyclohexane) in octane (Figure 2.21). The length of the test section was 25.4 cm, made of glass tubing and jacketed with an acrylic cylinder. The coolant temperature was kept at 0 °C and temperature data were continuously recorded by the thermocouples located at the entrance and the exit of the pipe; at the entrance and the exit of the cooling jackets, as well as at the reservoir. The temperature of the reservoir was kept at 30 °C using a water bath.

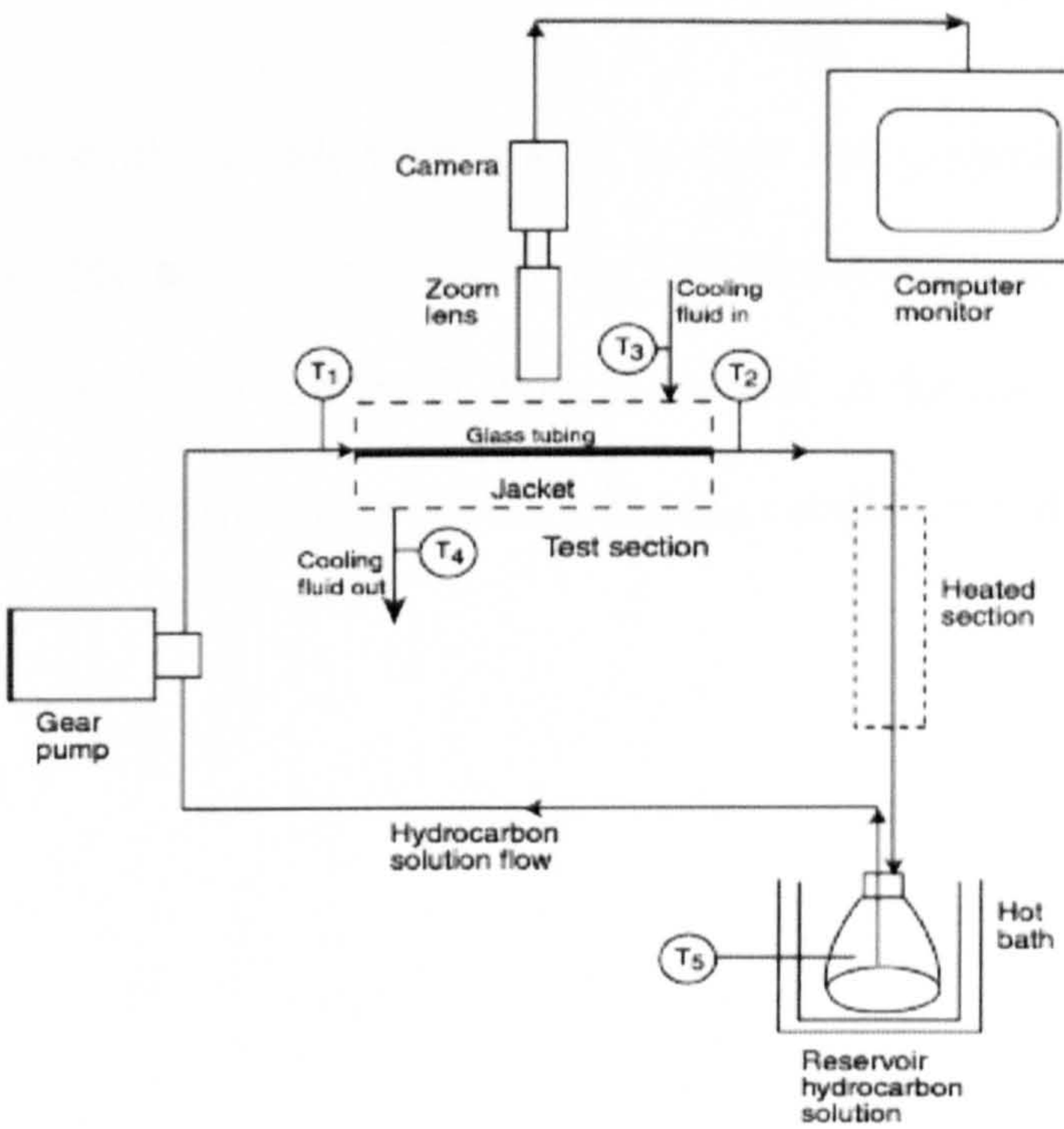

Figure 2.19 Schematic of the flow loop system used to measure and visualised wax deposition (Cordoba and Schall, 2001a)

A heat transfer method was used to measure the wax thickness formed from the flowing binary system of hydrocarbons. It was found that the thickness of the wax deposits increased steadily with time and reached an asymptotic value. It was shown that the results obtained with the heat transfer method were comparable to those obtained using gravimetric measurements. It was suggested that the heat transfer method can be a reliable alternative way to measure wax deposition (Cordoba and Schall, 2001a). In another study using the same test rig (Cordoba and Schall, 2001b), it was observed that solvent content in the deposited nonadecylcyclohexane decreased over time, consistent with the deposit aging phenomenon reported by Singh *et al.*(2000, 2001).

From the relevant literature review, it is clear that considerable research have been conducted in the area of oscillatory baffled reactor as well as wax deposition individually. The novelty of this thesis work is the link of the two areas, establishing a viable technology of mitigating wax deposition using oscillatory baffled flow.

CHAPTER 3

EXPERIMENTAL SET-UP AND PROCEDURES

This chapter presents the design, construction and operation of the oscillatory baffled column (OBC) as well as the measurement and calibration protocols; experimental and the analytical procedures.

3.1 Oscillatory Baffled Column

The schematic diagram of the batch OBC used in this study is shown in Figure 3.1 and a photo of the assembly is shown in Figure 3.2. The OBC was made of a jacketed glass column (Figure 3.3) of 25 mm in internal diameter, 50 mm in external diameter and 130 mm in height, a total liquid capacity of 64 ml and a working fluid capacity of 60 ml.

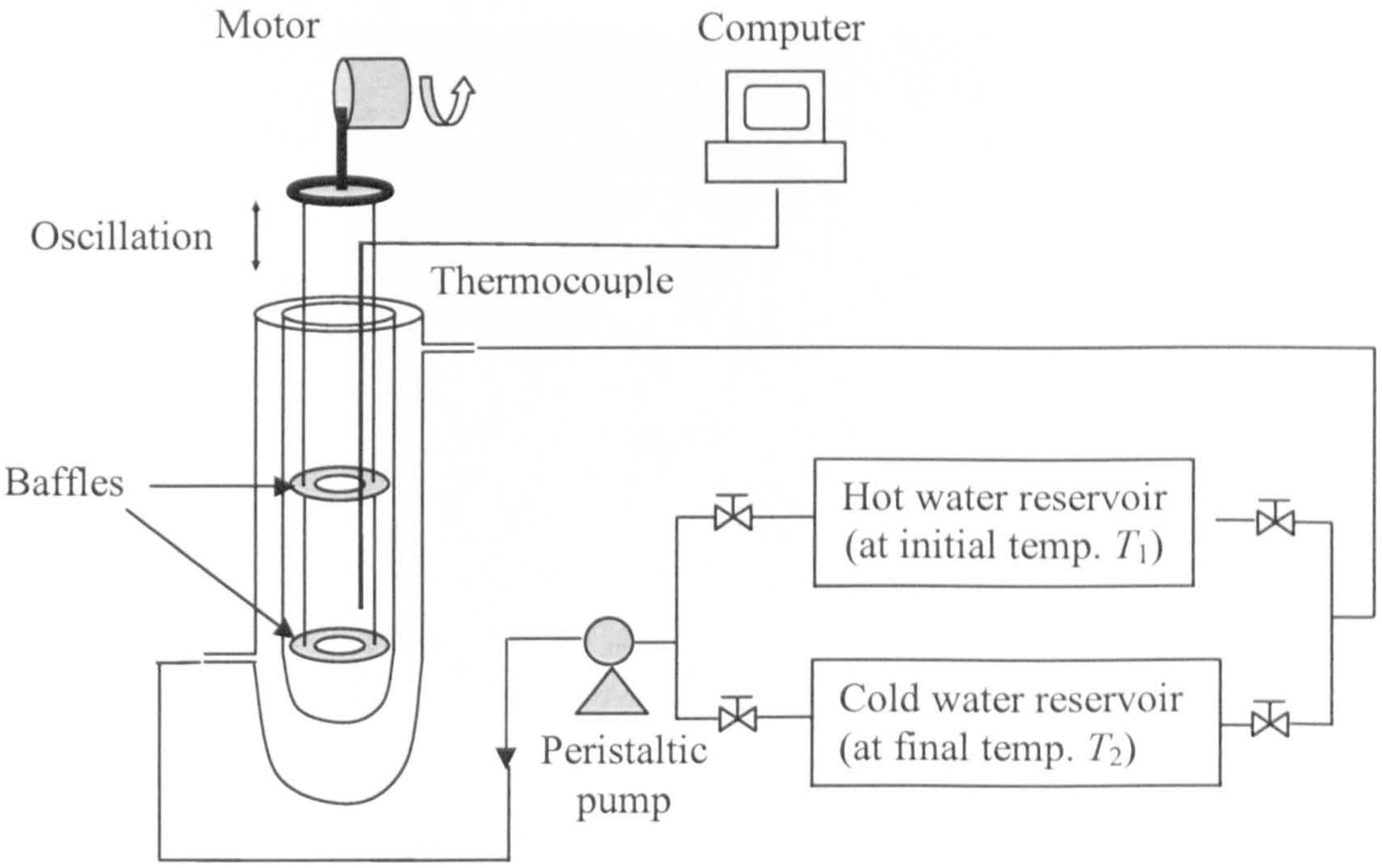

Figure 3.1 Schematic diagram of oscillatory baffled column

Figure 3.2 Photograph of the experimental set up

Figure 3.3 Photograph of the jacketed column

A *K*-type thermocouple is located within and connected to a computer via Multipurpose Lab Interface (MPLI) supplied by Vernier Software Inc., USA to record temperature profiles inside the column. A set of two stainless steel baffles of 3 mm thickness were used in this study and designed to fit closely to the wall of the column. The baffles are spaced 35 mm apart and supported by two 1.2 mm diameter stainless steel rods. The orifice diameter was 14 mm, creating a baffle free area of 30%. The baffle set was connected to the shaft of a piston through a supporting plate and driven by an electrical motor. Oscillation frequencies in the range of 0.1 to 6 Hz were controlled using a digital speed controller. Oscillation amplitudes of 2.5 to 15 mm (centre-to-peak) were generated by adjusting the preset distance between the linkage and the flying arm.

A peristaltic pump (Watson Marlow 505S) was used to circulate the heating and cooling water from the two water baths. The maximum operational speed of the pump was 220 rpm. Both water baths were temperature controlled and the hot water bath was kept at the desired initial temperature throughout the experiment. As for the cold water bath, cooling is achieved by circulating refrigerant (water + ethylene glycol) through a brass cooling coil of tubing from a refrigerator (Julabo F200). The cold bath temperature was kept at the desired final temperature throughout the experiment. The flow rate of the cooling water was controlled by adjusting the peristaltic pump speed (rpm). Prior to the start of an experiment, the computer, the water baths and the refrigerator were switched on. The hot and cold temperatures in the water baths were preset and all the tubes were then attached.

3.2 Preparation of wax and oil mixture stock

Stocks of wax and oil mixture solutions were prepared with a given paraffin wax and oil mixture ratio (*e.g.* 10, 20, 40 and 60 wt.% of paraffin content). Paraffin wax was purchased from Sigma-Aldrich Chemical, UK, and was in the form of solid chunks (Figure 3.4) which were scraped into powdery form using a knife. The melting point of the wax was 52-58 °C. Diesel oil was used as the model oil and was purchased from The National Pump Station, Balerno, Edinburgh.

Figure 3.4 Photograph of paraffin wax chunks

All experiments used the same stock of oil to ensure consistent composition in the material. A known amount of the powdered wax was weighed in a conical flask and diesel oil was added to make up the desired percentage of wax solution. The stock solution was kept at room temperature to be used for the experiments. Prior to experiments, the stock slurry solution was heated using a magnetic stirrer to dissolve the

solid wax and was then measured to a certain volume using a measuring cylinder before pouring it into the column.

3.3 Calibration of the peristaltic pump

The peristaltic pump was calibrated for its flow rate by measuring the volume delivered against time. The correlation graph is shown in Figure 3.5 below.

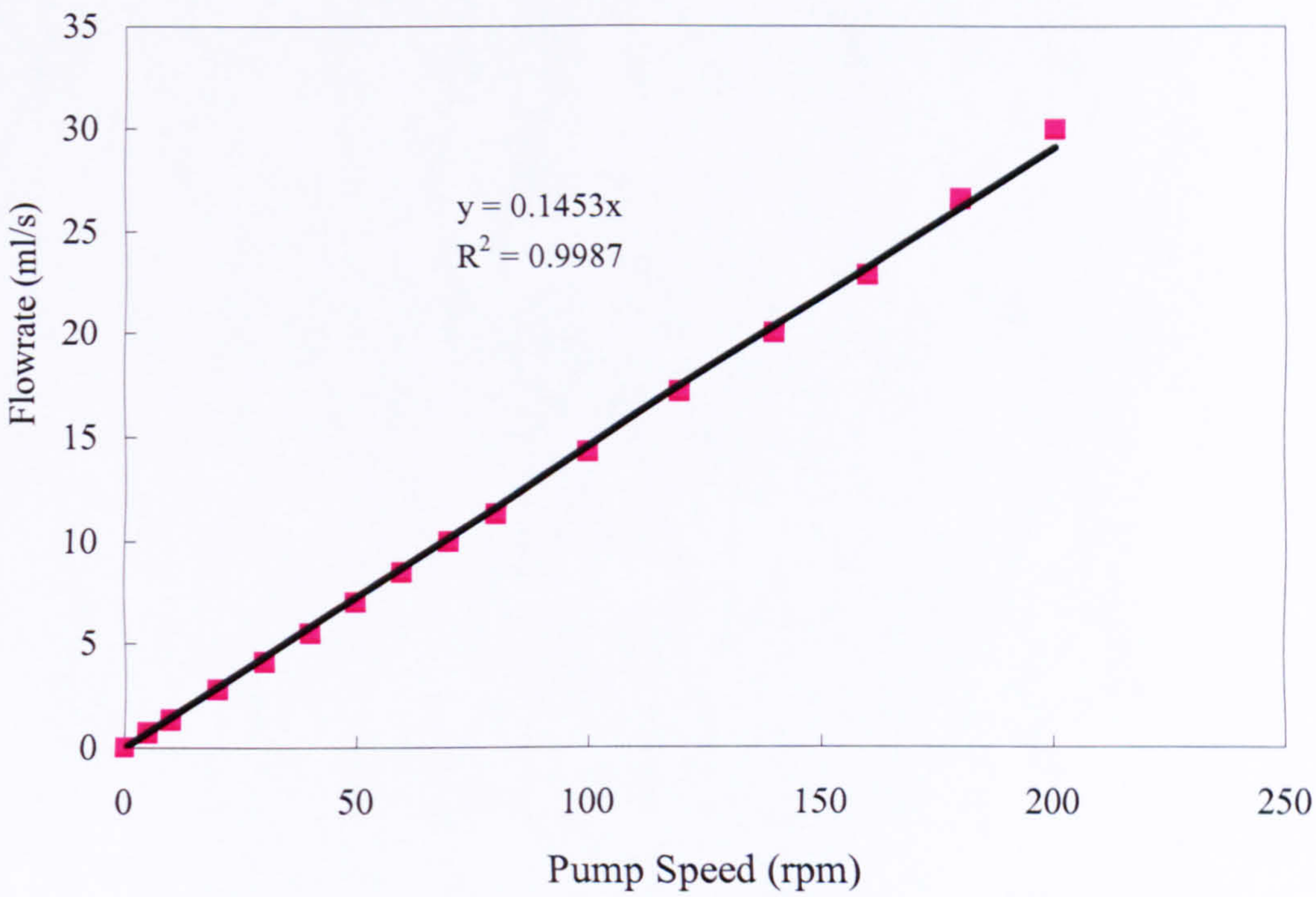

Figure 3.5 Calibration curve for cooling water flow rate (ml/s) and peristaltic pump speed (rpm).

The correlation between the pump speed and the flow rate is $y = 0.1453x$ where y is the flow rate (ml/s) and x is the pump speed (rpm). The linear regression coefficient obtained (R^2) is 0.9987, which signifies a reliable linear correlation of both parameters.

3.4 Measurement of the deposition

The gravimetric method was chosen to quantify the amount deposition. At the end of each experiment, the column was dismantled from its supporting platform, the baffles taken out and the column was put upside down. The non-deposited liquid of wax and oil mixture was drained out of the column through gravity to a beaker and then weighed. The deposited wax inside the column is then quantified by weighing the whole column minus the weight of empty column (298.45 g). The same procedure was used to measure the weight of the deposited wax on the baffles. The wax deposit was then calculated as a weight percentage of the total wax and oil mixture solution used as shown below:

$$\text{Deposit, } \delta = \frac{\text{weight of deposit on both the column and the baffles}}{\text{the total weight of wax and oil solution}} \times 100\% \qquad (3.1)$$

Experiments were repeated at least three times and error bars are included in the results presentation to indicate data repeatability.

3.5 Calibration of the oscillator

The oscillator (*i.e.* the flying arm) that connected to the baffles was required to be calibrated for its frequency due to the gearing system in the motor. The frequency of the oscillator was measured using a digital optical counter. The graph of the counter frequency against the motor frequency was then plotted and the correlation was

obtained from the trend line. The calibration curve of the counter frequency against the motor frequency is plotted in Figure 3.6. From the trend line, the regression linear equation obtained is $y = 0.1076x$ with R^2 value of 0.9994. The equation was used to convert the motor frequencies into the true frequency values of the oscillator.

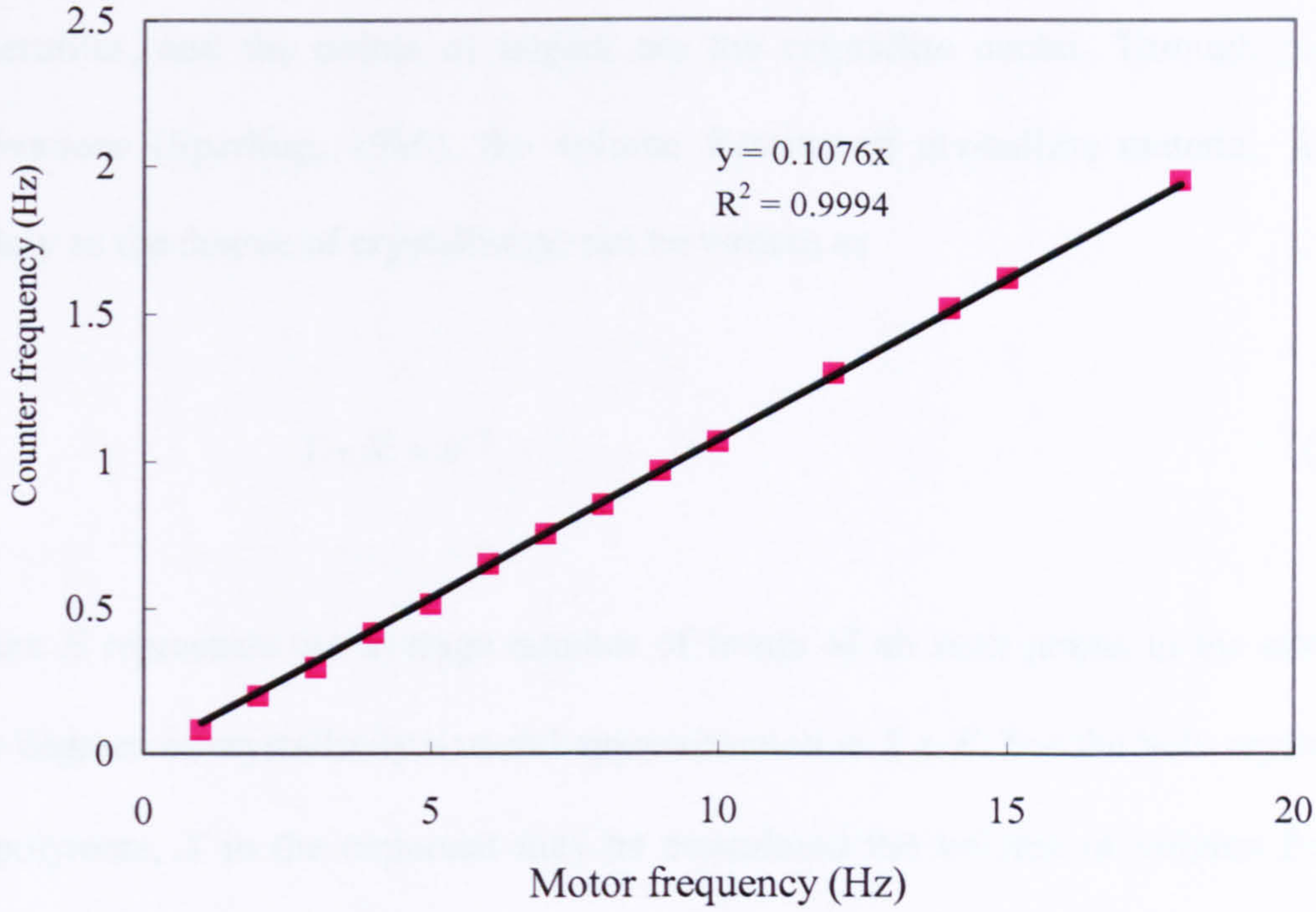

Figure 3.6 Calibration curve for the frequency of the oscillation motor and the flying arm

3.6 Kinetic analysis

The mechanism of paraffin wax deposition is largely based on nucleation and crystallisation processes where oil is entrapped between crystals leading to gel formation; and can be treated as bulk crystallisation (Singh *et al.* 2000). The Avrami phase transition equation is a well-known principle in describing such crystallisation kinetics. The original derivations by Avrami (1939) have been simplified by Evans

(1945) and included in polymer context by Meares (1965) and Hay (1971). The basic principle can be illustrated by imagining raindrops falling in a puddle. The raindrops produce expanding circles of waves which intersect and cover the whole surface. The drops may fall sporadically or all at once. In either case, they must strike the puddle surface at random points. The expanding circles of waves are the growth front of the spherulites, and the points of impact are the crystallite nuclei. Through probability derivations (Sperling, 1986), the volume fraction of crystalline material, X, known widely as the degree of crystallinity, can be written as

$$1 - X = e^{-E} \tag{3.2}$$

where E represents the average number of fronts of all such points in the system. For low degrees of crystallinity a useful approximation is $X \approx E$. For the bulk crystallisation of polymers, X in the exponent may be considered the volume or volume fraction of crystalline materials, V_t, *i.e.*

$$1 - X = e^{-V_t} \tag{3.3}$$

This has widely been accepted and is commonly used to describe crystallisation (Caze *et al.*, 1997; Connor *et al.*, 1997; Lu *et al.*, 1998; Bhattacharyya *et al.*, 2003; Campos *et al.*, 2003; Chen *et al.*, 2003; Luo *et al.*, 2004; Litwinenko *et al.*, 2004; Li *et al.*, 2005; Pal and Nandi, 2005; Pereira and Rocco, 2005; Huang *et al.*, 2005; Wang and Vlassak, 2006). For either instantaneous or sporadic nucleation, equation (3.3) can be written as

$$1 - X = e^{-Kt^n} \tag{3.4}$$

where K represents the growth rate, and n is the Avrami exponent, which depends not only on the structure of the crystal, but also on the nature of nucleation (Avrami, 1940). The Avrami exponent, n, is the phenomenological index of crystallisation, which can be used to distinguish between different mechanisms of crystallisation (Campos *et al.*, 2003). For example, when $n = 1$ it corresponds to rod-like growth from instantaneous nuclei; whereas $n = 3$ or 4 refers to spherulitic growth from either sporadic or instantaneous nucleation (Sharples, 1966). For polymer and organics systems, an n value of 2 or 3 indicates two or three dimensional nucleation of the crystal nucleus. However, fractional values of n also exist due to secondary crystallisation, *e.g.* lower n values (<1) are caused by linear crystal growth (Pal and Nandi, 2005). For ethylene/methacrylate blends, the Avrami exponent ranged from 2.75 to 6.42 (Pereira and Rocco, 2005). The Avrami exponent is strongly affected by crystallisation temperature, in crystallisation of milk fat, the n values ranged from 0.5 to almost 5. At lower temperature (5 °C) the milk fat crystallised in the form of granules, whereas at higher temperature (25 °C) they crystallised in the form of spherulites (Campos *et al.*, 2003). In a study of the kinetics of 5α-cholestan-3B-yl N-(2-naphthyl)carbamate/n-alkane organogel by Huang *et al.* (2005), the gelation process involved one-dimensional growth and 'instantaneous nucleation' with the self-assembled fibrous network. However the size and appearance changed abruptly from spherulitic to rod-like as the temperature of crystallisation was increased. Using both n and K as the diagnostic tool of crystallisation mechanism, Hay (1971) derived a model for spheres, discs and rods, representing three-, two- and one-dimensional forms of growth, which are summarised in Table 3.1.

Table 3.1 The Avrami parameters for crystallisation of polymers (Hay, 1971)

Crystallisation mechanism		*n*	Growth form
Spheres	Sporadic	4	3 dimensions
	Instantaneous	3	3 dimensions
Discs[a]	Sporadic	3	2 dimensions
	Instantaneous	2	2 dimensions
Rods[b]	Sporadic	2	1 dimension
	Instantaneous	1	1 dimension

[a] Constant thickness; [b] Constant radius

In this study, wax deposition has been investigated in the novel reactor system, and the degree of crystallinity is measured by the relative deposition, δ_r, defined as the mass fractions of the depositions on both the wall and the baffles of the OBC divided by the initial mass of the wax and oil mixture liquid, *i.e.*

$$\delta_r = \frac{\delta_t - \delta_0}{\delta_\infty - \delta_0} \tag{3.5}$$

where δ_t is the total deposition at time t (g), δ_∞ the maximum or asymptotic deposition obtained from the deposition curves when the asymptotic condition or quasi-steady state

has been achieved (g); δ_0 the initial mass of the wax content in liquid (g). Replacing X by δ_t and taking log twice in equation (3.4) it becomes,

$$\text{Log}[-\ln(1-\delta_t)] = \text{Log}\,K + n\text{Log}(t) \tag{3.6}$$

By plotting the left side in the equation (3.6) vs. Log(t), the slope of the straight line n and the intersection K, the kinetic coefficient can be obtained.

The deposition half-time ($t_{1/2}$) is defined as the time at which the degree of deposition (δ_t) has reached 50% of the maximum achievable deposition, and can be calculated from the measured kinetics parameters,

$$t_{1/2} = \left(\frac{\ln 2}{K}\right)^{1/n} \tag{3.7}$$

The deposition half-time is a parameter for understanding the rate of deposition. Both the Avrami exponent and the deposition half-time will be used to evaluate the deposition process in the OBC. An example of calculation work is presented in Appendix A.

CHAPTER 4

RESULTS AND DISCUSSION

Chapter 4 presents the experimental results and discussions of the deposition of paraffin wax in an OBC, and is divided into five main sections. The effects of operating parameters such as the oscillation frequencies and amplitudes on the deposition of wax are discussed in Section 4.1. The effect of the volume of the oil-wax solution in the OBC is given in Section 4.2. Section 4.3 presents the effect of paraffin wax content on the deposition whereas, Section 4.4 examines the effects of solvent carbon numbers. Lastly, section 4.5 investigates the effects of baffle materials and structures on the deposition.

4.1 Effects of oscillatory parameters on the deposition

This section reports and discusses the results obtained from the experiments on the investigation of the effects of the operational parameters on the deposition. In the experiments, four oscillation frequencies, *f*, were tested, *i.e.* 1, 2, 4 and 6 Hz. Oscillation frequency of 8 Hz was tried in the OBC but was observed to cause severe vibrations to the apparatus; hence, the maximum operating frequency for the OBC was taken as 6 Hz. Four centre-to-peak oscillation amplitudes, x_o, were tested, *i.e.* 2.5, 5.0, 10.0 and 15.0 mm; and achieved by using the threaded and predrilled holes on the flywheel attached to the motor shaft.

The baffles used in these experiments were made of stainless steel with the dimensions explained in Section 3.1. Paraffin wax content was set at 10 wt.% and dissolved in diesel as the solvent or oil phase. The hot water bath was set at 50 °C and cold water bath at 10 °C. The cold water flow rate was fixed by setting the speed of the peristaltic pump to 100 rpm and was estimated at 0.87 l/min. The volume of the wax and oil mixture solution was fixed at 60 ml. Results are presented in terms of the temperature profiles studies, deposition as a function of time and the Avrami kinetic studies focusing on the Avrami exponent, *n*, and the deposition half time ($t_{1/2}$).

4.1.1 Studies of temperature profile

Figure 4.1 shows the typical cooling temperature profiles for the effects of varying the oscillation amplitude for each frequency tested. From the graphs it can be observed that at every frequency, the temperatures for experiments with no oscillation were always the highest in comparison to the rest. Temperature profiles of varying the oscillation frequency for each amplitude are given in Figure 4.2 and have similar trends. The important messages from Figures 4.1 and 4.2 are a) the cooling rates used are not linear, but consistent for all oscillatory conditions; b) the starting and the finishing temperature are similar from 50 °C to 10 °C for all experiments.

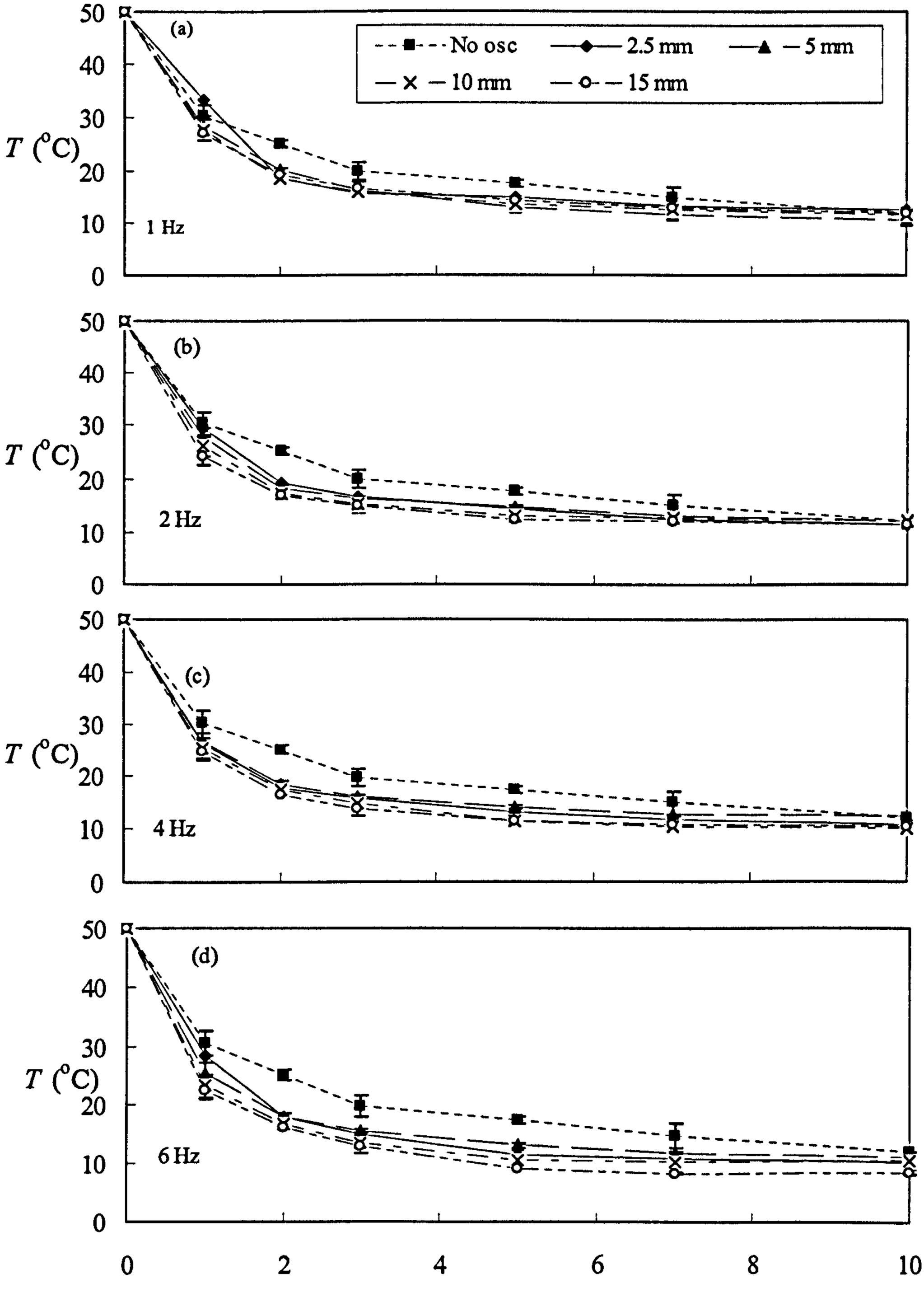

Figure 4.1 Effect of oscillation amplitudes on temperature profiles for each frequency tested

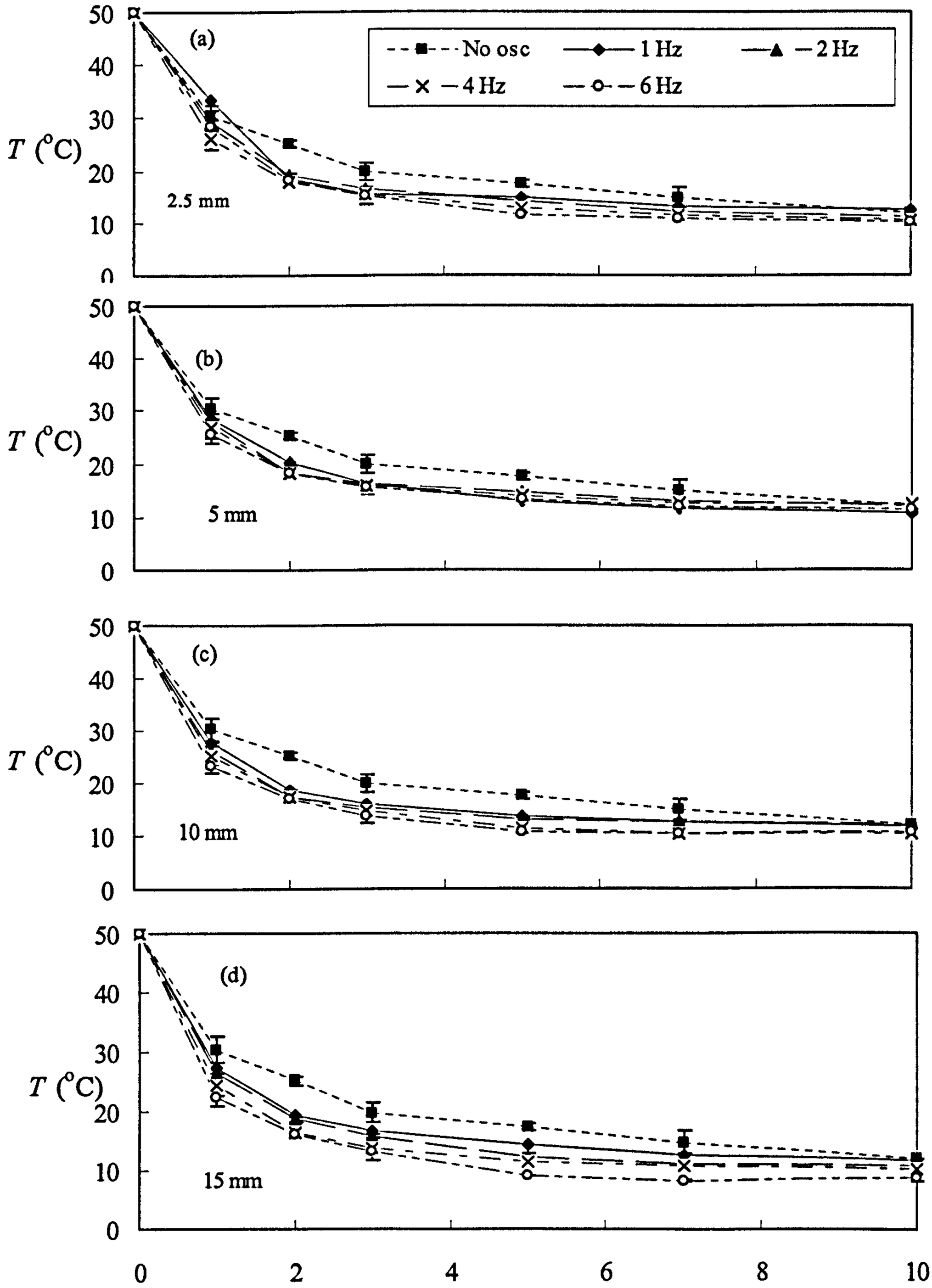

Figure 4.2 Effect of oscillation frequency on temperature profiles for each amplitude

4.1.2 Effects of amplitude and frequency on the deposition

In this subsection, experimental results on the deposition in the OBC are reported and the effects of oscillation amplitudes and frequencies are examined. Figure 4.3 shows the effect of oscillation frequency on the deposition, δ (wt.%), for the experimental duration of 10 minutes and for each oscillation amplitude tested. The dotted lines represent the deposition behaviours with no oscillation, where the deposition of wax increased with time and 100% deposition was always achieved. The case without oscillation is taken as the basis for subsequent comparison. Generally the graphs show that by oscillating the baffles, the deposition was reduced and the asymptotic deposition, *i.e.* the final maximum deposition, was smaller than 100% as in the cases without oscillation. At the shortest amplitude of 2.5 mm (Figure 4.3(a)), the asymptotic depositions were reached at later times compared to these when using other amplitudes, suggesting that greater reduction of the deposition is achieved with increased amplitudes. Similarly the reduction of the deposition also increased with the increase of oscillation frequency at the fixed amplitudes, except at the smallest amplitude of 2.5 mm (Figure 4.3(a)) where the opposite effect was observed. The reason for this is not entirely clear.

The effect of oscillation amplitude on the deposition at each oscillation frequency (presented in Figure 4.4) is similar to that of oscillation frequency as described earlier, with the general trend applying to more or less all operational conditions. In spite of scattering in the data, the important message from the results is that significant reduction of the deposition can be achieved using appropriate oscillation in the presence of baffles.

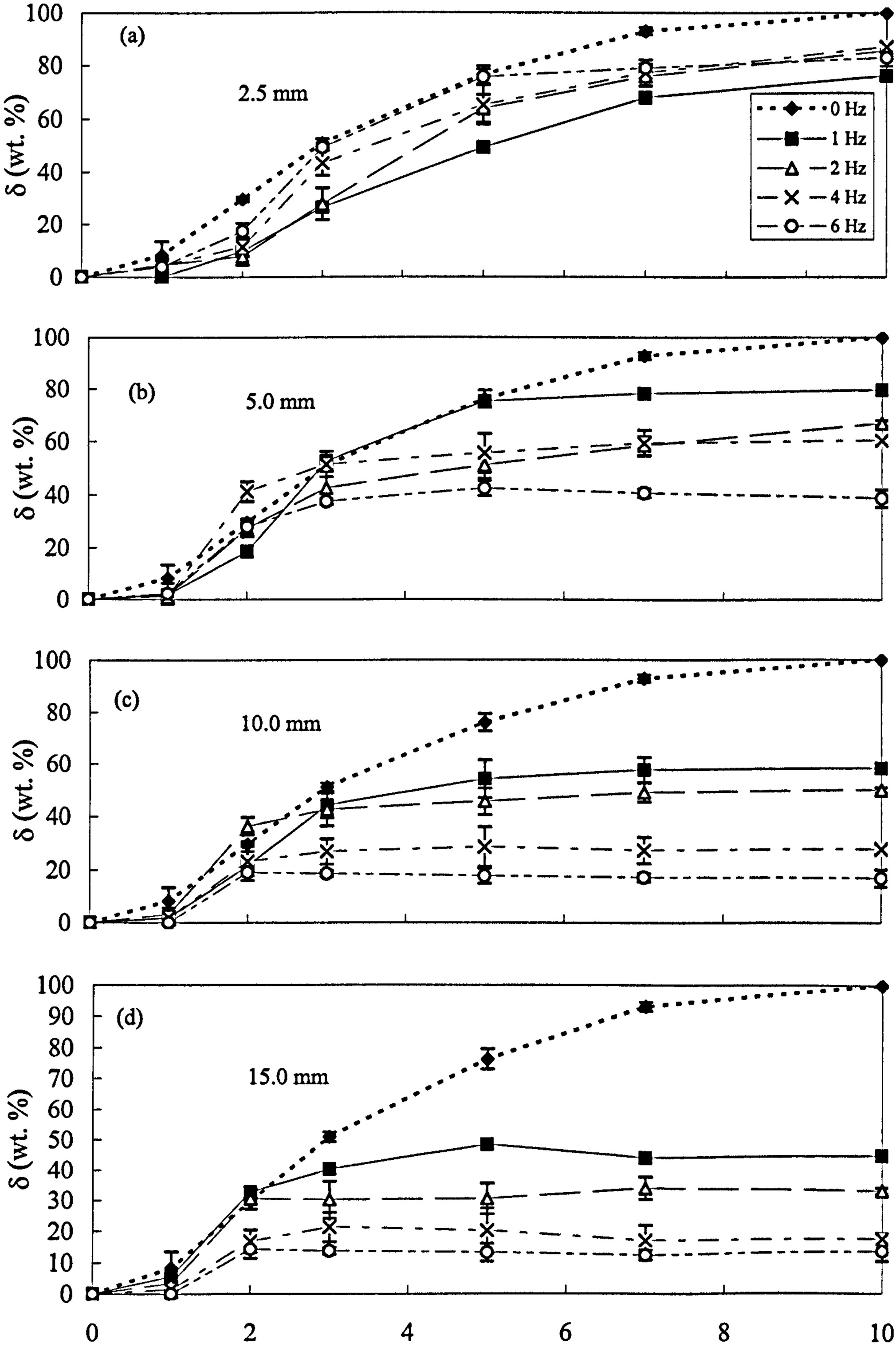

Figure 4.3 Effect of oscillation frequency on the deposition as a function of time. The *y*-axis represents the percentage of wax deposited where a maximum 100% deposition means that all of the wax and oil mixture solution is in the form of a gel or solid deposit inside the column

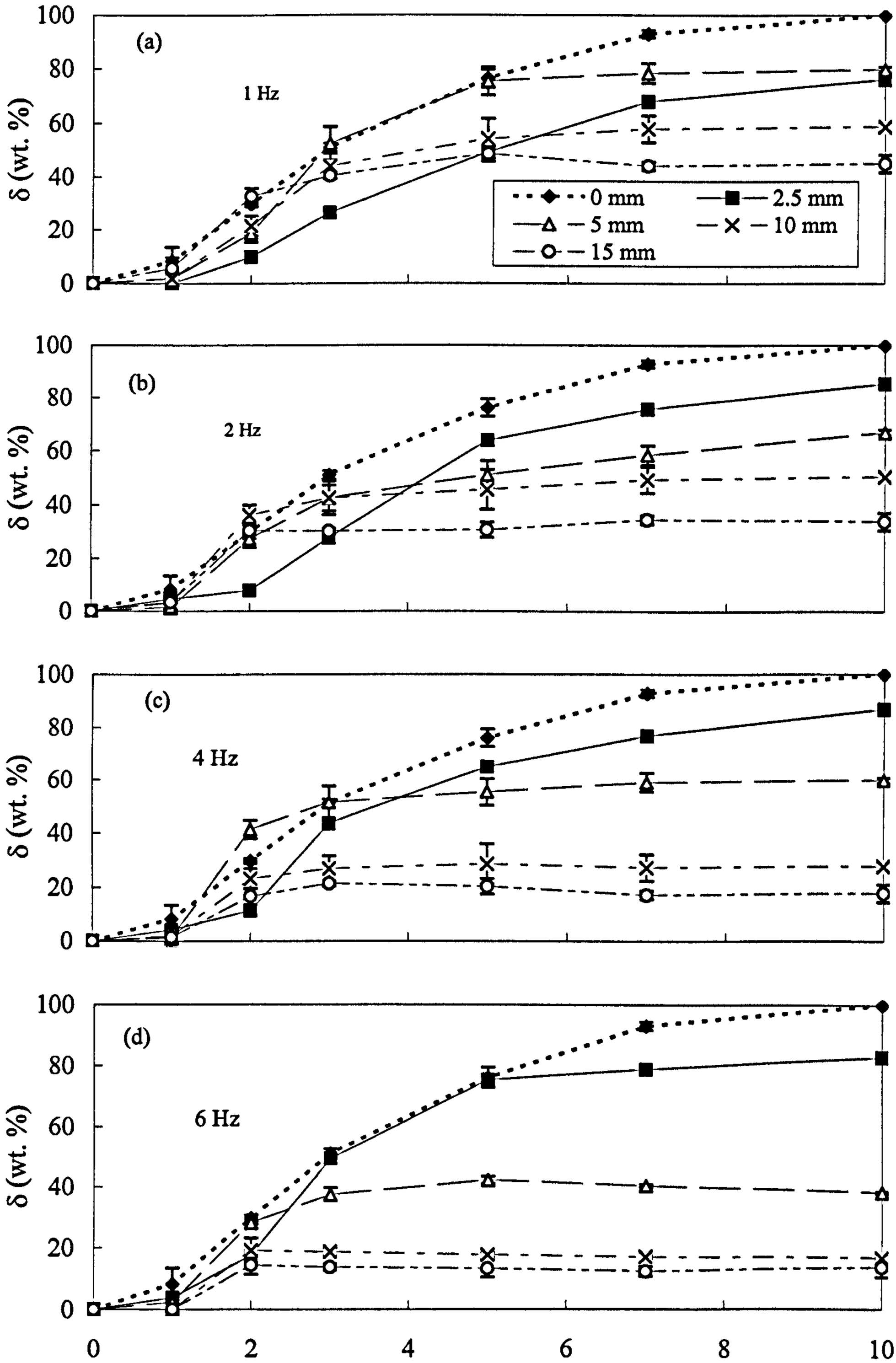

Figure 4.4 Effect of oscillation amplitude on the deposition as a function of time. The *y*-axis represents the percentage of wax deposited where a maximum 100% deposition means that all of the wax and oil mixture solution is in the form of a gel or solid deposit inside the column

4.1.3 Avrami kinetic analysis

Avrami kinetic analyses were conducted by plotting a graph using Equation (3.6), as explained in Section 3.6 as well as Appendix A, and Figure 4.5 is the Avrami plot for each amplitude and frequency tested in this study. From the straight lines, the slopes can be obtained and give the Avrami exponents (n). The intersections of the straight lines with y-axis are the Avrami rate constant (K (min^{-n})). The Avrami exponent, n, provides information on the structure of the crystal as well as on the nature of nucleation and can be used as the phenomenological index of crystallisation to distinguish between different mechanisms of crystallisation; while the Avrami rate constant, K, represents the growth rate over the entire duration and is used to calculate the half time of deposition as $t_{1/2} = (\ln 2/K)^{1/n}$. From the deposition profiles in Figures 4.3 – 4.4, significant kinetics information is embedded in the period of time up to a 50% deposition has been reached, *i.e.* the half time of deposition. It is for this reason that $t_{1/2}$ is a useful tool for evaluation of the rate of deposition. The extracted data from the plots are summarised in Table 4.1.

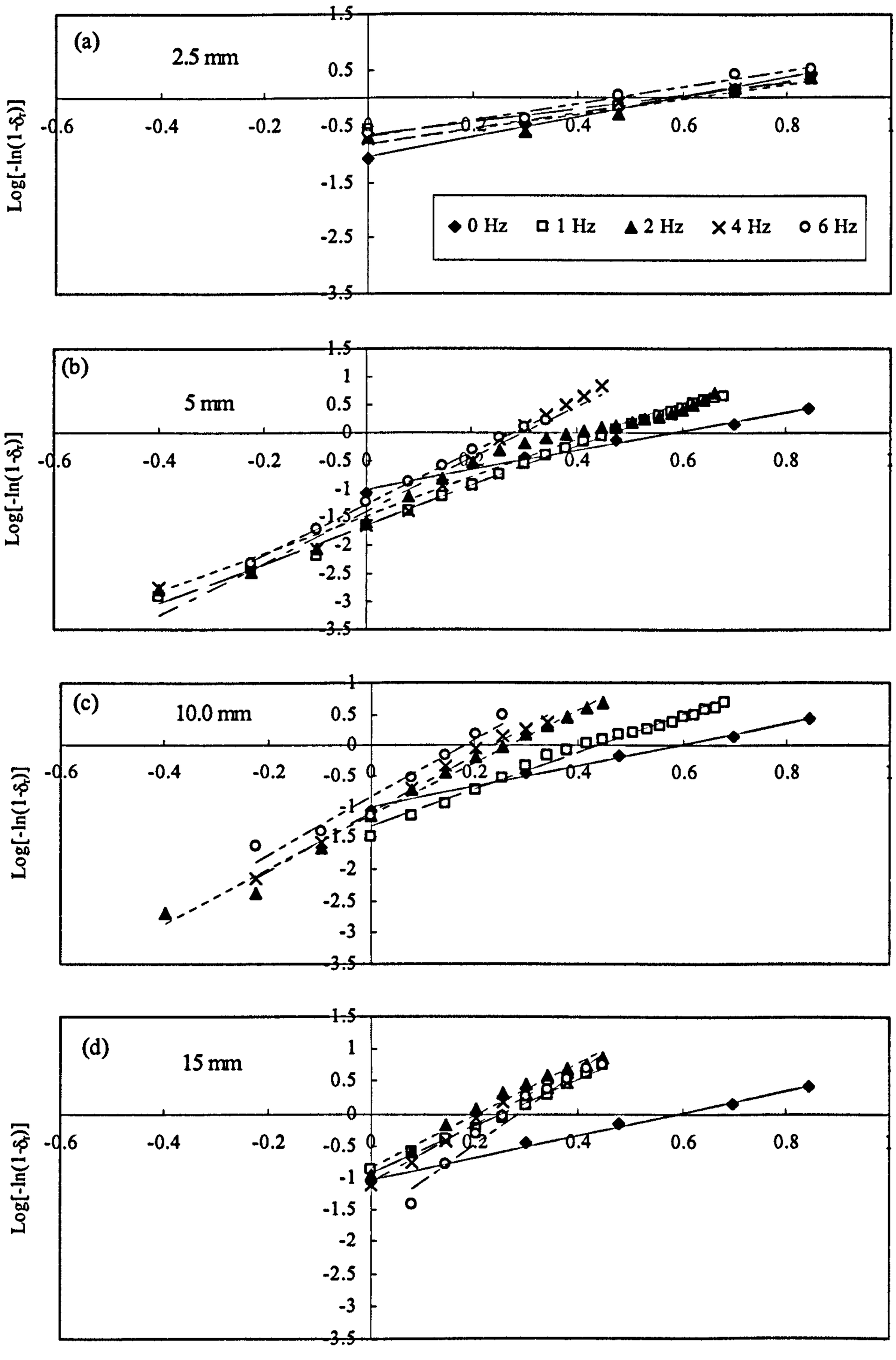

Figure 4.5 Plot of Log[-Ln(1-δ_t)] vs. Log(t) to obtain the Avrami parameters

Table 4.1 Extracted Avrami parameters from Figure 4.5

x_o (mm)	f=0 Hz			f=1 Hz			f=2 Hz			f=4 Hz			f=6 Hz		
	n	K (min^{-n})	$t_{1/2}$ (min)	n	K (min^{-n})	$t_{1/2}$ (min)	n	K (min^{-n})	$t_{1/2}$ (min)	n	K (min^{-n})	$t_{1/2}$ (min)	n	K (min^{-n})	$t_{1/2}$ (min)
2.5				1.14	0.23	2.66	1.33	0.15	3.11	1.37	0.16	2.94	1.45	0.21	2.30
5.0	1.73	0.10	3.15	3.46	0.02	2.68	3.80	0.05	1.96	4.64	0.04	1.84	4.47	0.05	1.77
10.0				3.04	0.05	2.43	3.83	0.10	1.67	4.65	0.08	1.59	4.72	0.14	1.40
15.0				3.05	0.12	1.77	3.70	0.13	1.56	4.08	0.14	1.48	4.43	0.07	1.68

From Table 4.1 it can be seen that in the experiment in the absence of oscillation, the Avrami exponent value (n) was 1.73 indicating that wax crystals produced were of one-dimensional, rod-like or needle-like type as suggested by Hay (1971) in Table 3.1. Figure 4.10 shows the microscopy image of crystals from the control experiments without oscillation, and needle type crystals are clearly seen. For the experiments at the shortest amplitude of 2.5 mm, there is no significant difference in the n values for all frequencies compared to the data from the control experiment with no oscillation and the type of crystals produced would be similar to that in Figure 4.6. When larger amplitudes were used, a step change in the n values can then be observed with higher oscillation amplitudes and frequencies leading to larger n values. This would suggest that the growth mechanism of crystals under these conditions changed from a one- to a multi-dimensional event and crystals are of clustered-plate-like shapes (Figure 4.7). The step increase in the Avrami exponent is contributed to by the change in the type of nucleation, from instantaneous to more sporadic.

From the half time of deposition data in Table 4.1, it can be observed that the highest $t_{1/2}$ of 3.15 minutes was obtained when no oscillation was applied in the control experiment. Increasing either the amplitude or frequency generally decreased the half time of deposition, $t_{1/2}$, with some scattering suggesting that increasing the amplitude and/or frequency accelerated the rate of deposition, as the smaller the $t_{1/2}$, the faster the rate of deposition. However it is worth mentioning that increasing the amplitude and/or frequency had a significant impact in decreasing the overall deposition as explained earlier, hence fluid oscillation can be beneficial in reducing the deposition.

Figure 4.6 Microscopic image of wax crystals from the control experiment without oscillation

Figure 4.7 Microscopic image of wax crystals from the experiment with oscillation (x_o = 15 mm, f = 1 Hz)

4.2 Effects of the volume of wax and oil mixture solution

During the oscillation of the baffles it is possible that either one or both of the baffles are submerged in the liquid. To investigate the effect of one baffle being lifted up from the liquid surface at the top of the stroke, the volume of wax/diesel sample, *i.e.* the height of the working liquid, can be used as an experimental variable. An advantage of this approach is that the effect of the available surface area of the vessel wall can be investigated, which is an important parameter for the batch process, especially when related to the bulk volume.

In these experiments the values for the oscillation frequencies (f) examined were 1, 2 and 4 Hz, whereas for the amplitudes (x_o) were 5, 10 and 15 mm. Four volumes have been tested, *e.g.* 10, 20, 40 and 60 ml of wax-diesel solution with a constant paraffin wax content (w) of 10 % by weight, *i.e.* the wax concentration is fixed for all the oil-wax solutions used in the experiment, whilst the volume changed. The initial hot temperature (T_1) was set at 50 °C which was well above the cloud point of the wax and oil mixture solution, and the final cold temperature (T_2) was selected at 10 °C. Note that the final temperature (T_2) has to be lower than the wax appearance temperature, which was measured around 28 °C by observing the onset of the cloudiness of the solution. The speed of the cooling water pump (C_w) was set at 100 rpm ensuring a fixed cooling water temperature for all experiments.

The typical experimental duration was 10 minutes, and three deposition measurements were made at an interval of 1 minute for the initial 3 minutes, followed by two measurements taken at an interval of 2 minutes for the middle 4 minutes, and

finally one measurement taken at the end of the experiment time of 10 minutes. The experimental results are divided into four main sections: a) the effect of the volume of the wax and oil mixture solution; b) the effects of oscillation frequencies and amplitudes on the overall deposition; and c) the Avrami kinetic analysis.

4.2.1 Without oscillation

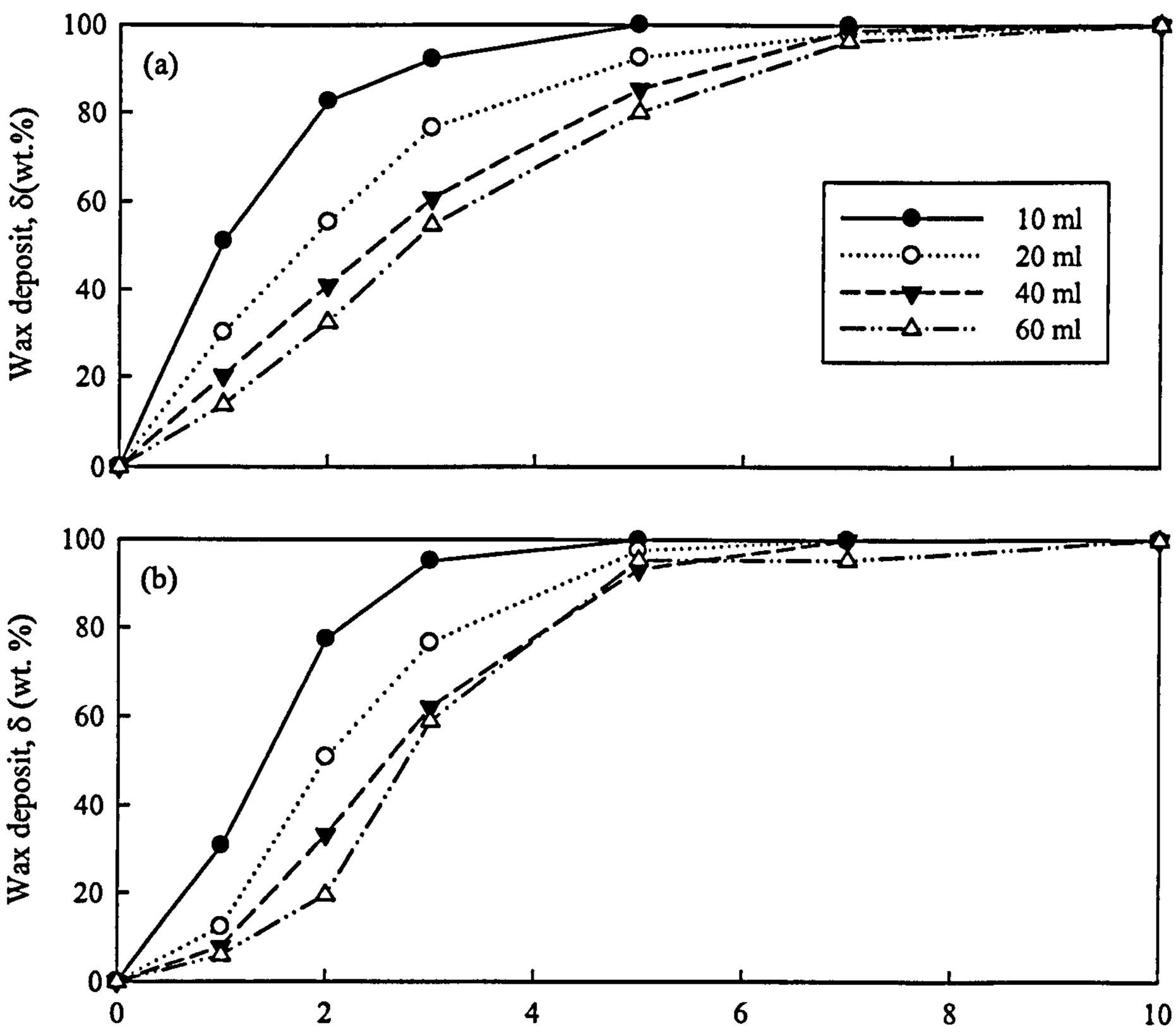

Figure 4.8 Effect of wax and oil mixture volume on the deposition in absence of oscillation (a) without baffles, (b) with baffles

Two sets of control experiments were performed: no baffles without oscillation and with baffles without oscillation. In the experiments without baffles it was visually observed that the wax deposit was in the form of a gel, not hard crystals. At the end of these experiments the liquid that was removed from the column was a clear fluid and the gel-like wax was adhered to the wall of the column. For the experiments with baffles but no oscillation, wax was found to be adhered to the baffles as well as the column walls. Figure 4.8 shows the percentage of the deposition for different volumes of wax and oil mixture solutions without both baffles and oscillation (Figure 4.8(a)), as well as these with baffles in absence of oscillation (Figure 4.8(b)). In Figure 4.8, the *y*-axis represents the percentage amount of wax deposited where a maximum 100% deposition means that all of the wax and oil mixture solution is in the form of a gel or solid deposit inside the column. It can clearly be seen that the smaller the volume used, the greater the fraction of wax deposit produced at any given time; the quicker the crystallisation rate of the paraffin wax and the faster complete deposition that was reached. The results are expected as the smaller the volume, the less the heat-load of the solution, the quicker the cooling (due to larger specific area) and the faster the deposition. As the volume increases, deposits produced act as a layer of insulation and hence could slow down the cooling and, in turn, the percentage of the deposition.

The difference in the total the deposition between the case with neither baffles nor oscillation and the case with baffles in absence of oscillation appears very small, suggesting that the presence of baffles does not necessarily enhance the deposition, while the increased surface area that arises from having baffles does lead to more rapid deposition. Since in the case with baffles that do not oscillate, there is deposition on the baffles, the distributions of deposit on the surfaces of walls and baffles have been

measured (Table 4.2). The mean percentage of deposition is similar for the baffles and the column wall, and the presence of the stationary baffles merely provides additional surface area for the share of the total deposition. The results in Figure 4.12 and Table 4.2 will be used as the basis for comparison with other results in this section.

Table 4.2 Mean percentage of deposition on the baffles and the column wall

	Without both baffles and oscillation	**With baffles without oscillation**	**Relative surface area**
Column wall	100%	50.7%	0.95
Baffles surfaces	0%	49.3%	0.80

4.2.2 With baffles and oscillation

4.2.2.1 Oscillation frequency

These experiments were designed to study the effect of oscillation frequency on the deposition for a range of different wax and oil mixture volumes. The selected frequencies were 1, 2 and 4 Hz. The duration of each experiment was 10 minutes based on the findings of test runs using a 10% paraffin wax solution for 30 minutes, where the typical time for reaching 100% deposition was around 8 minutes. Measurements of wax deposit were taken in the same way as been explained earlier in the control experiments. The viscosity of the wax and oil mixture solution changed during the course of each experiment, as such, it was impossible to calculate the exact oscillatory Reynolds

numbers. However, the average of the initial and final viscosities has been used to provide an estimate of the viscosity in the system.

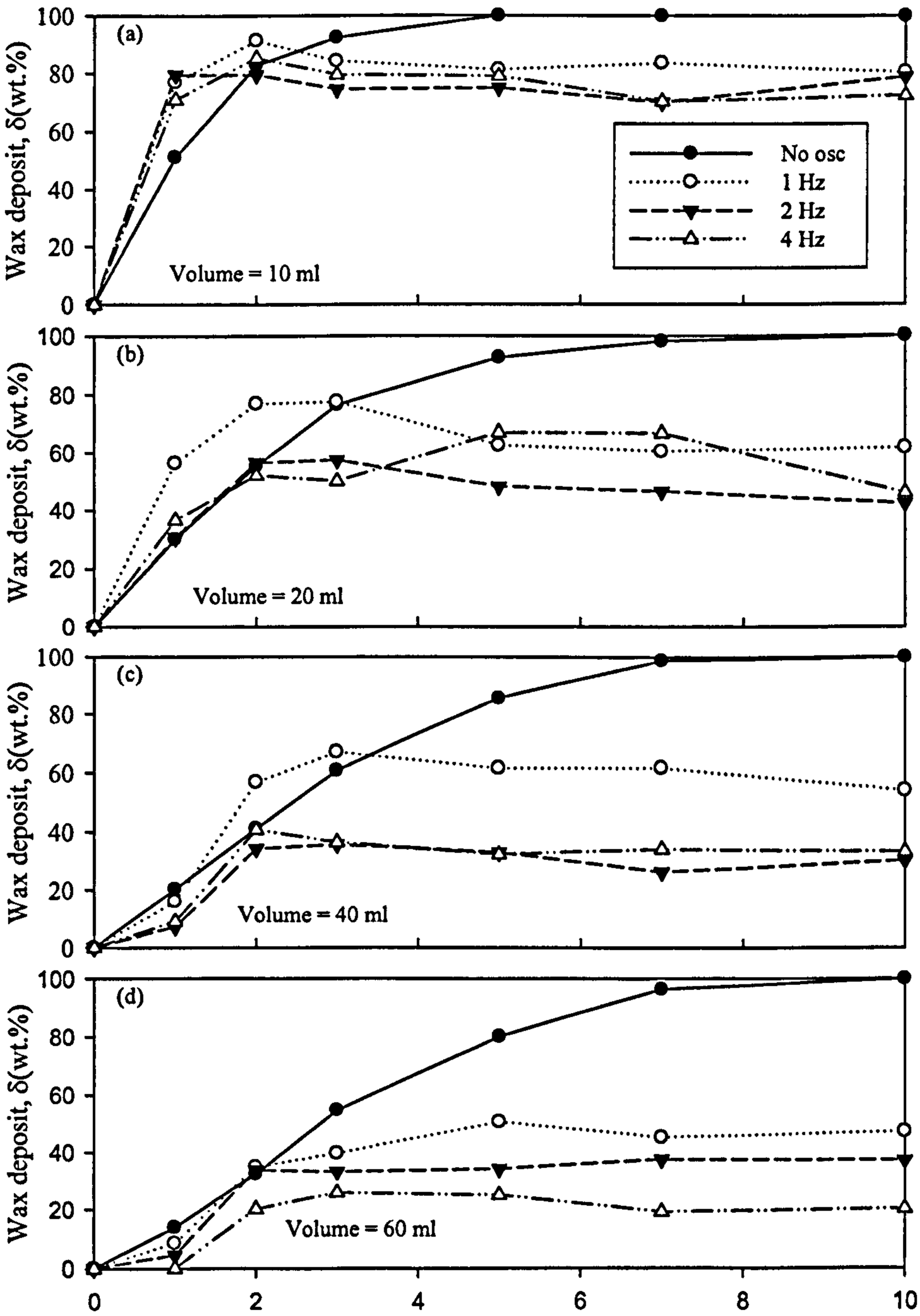

Figure 4.9 Effect of oscillation frequencies on the deposition for different volumes (x_o = 15 mm)

The percentage deposition as a function of time for all wax and oil mixture volumes and oscillation frequencies is shown in Figure 4.9, and for these experiments the amplitude of oscillation was fixed at 15 mm. The estimated oscillatory Reynolds numbers were 2024, 4048 and 8096 for 1, 2 and 4 Hz respectively. Note that the overall deposition shown in Figure 4.9 is comprised of two parts: deposition on the baffles and deposition on the column wall, which have not been separated here. The individual parts will be discussed later. Visually, the liquid produced was cloudier than that in the benchmark experiments. This is due to the fact that wax crystals formed during the cooling process were mixed and dispersed into the bulk fluid leading to the cloudiness.

From the graphs in Figure 4.9, two distinct features can be noted. Firstly, oscillation of the baffles reduced the percentage of wax deposit in comparison to those obtained from the benchmark experiments, while there were significant reductions for increasing volumes of wax and oil mixture solution, and 100% deposition was prevented from occurring for all experiments involving oscillation. Although some of the effects fluctuated with time, the general trend is that the higher the oscillation frequency, the lower the percentage of wax deposited. The reduction in deposition with increasing volume arises from a combination of two effects: the increase in the ratio between the sample volume and the available surface area as the sample volume increases (Table 4.3), and the effect of having both baffles submerged in the solution for the whole oscillation stroke for the larger volumes. The latter effect increases the mixing effect and reduces the temperature gradient from the column wall to the centre.

Secondly, at smaller sample volume the application of baffle oscillation increased the rate of deposition. One contribution to this may be the effect of splashing

of the mixture onto the column wall above the liquid surface as the upper baffle passes through the liquid surface. These splashes quickly solidify on the cooler surface.

Table 4.3 Ratio of surface area per total volume of wax and oil mixture solution

Liquid volume (ml)	Column surface area per volume of liquids (mm^2/mm^3)	Baffles surface area per volume of liquids (mm^2/mm^3)
10	0.1057	0.0718
20	0.0592	0.0359
40	0.0360	0.0359
60	0.0283	0.0239

The rate of wax crystallisation decreased as the volumes of the wax and oil mixture solutions increased; at higher oscillation frequencies and larger volumes, the rates of wax crystallisation are much lower than that without baffles oscillation. By rearranging Figure 4.9, the effect of the sample volume on the deposition for different volumes is shown in Figure 4.10, clearly the reduction in the deposition is greater for increasing both the volume of wax and oil mixture solution and oscillation frequencies. The results are important; suggesting that the deposition can be reduced by incorporating oscillatory motion, in this study via oscillating baffles in the column.

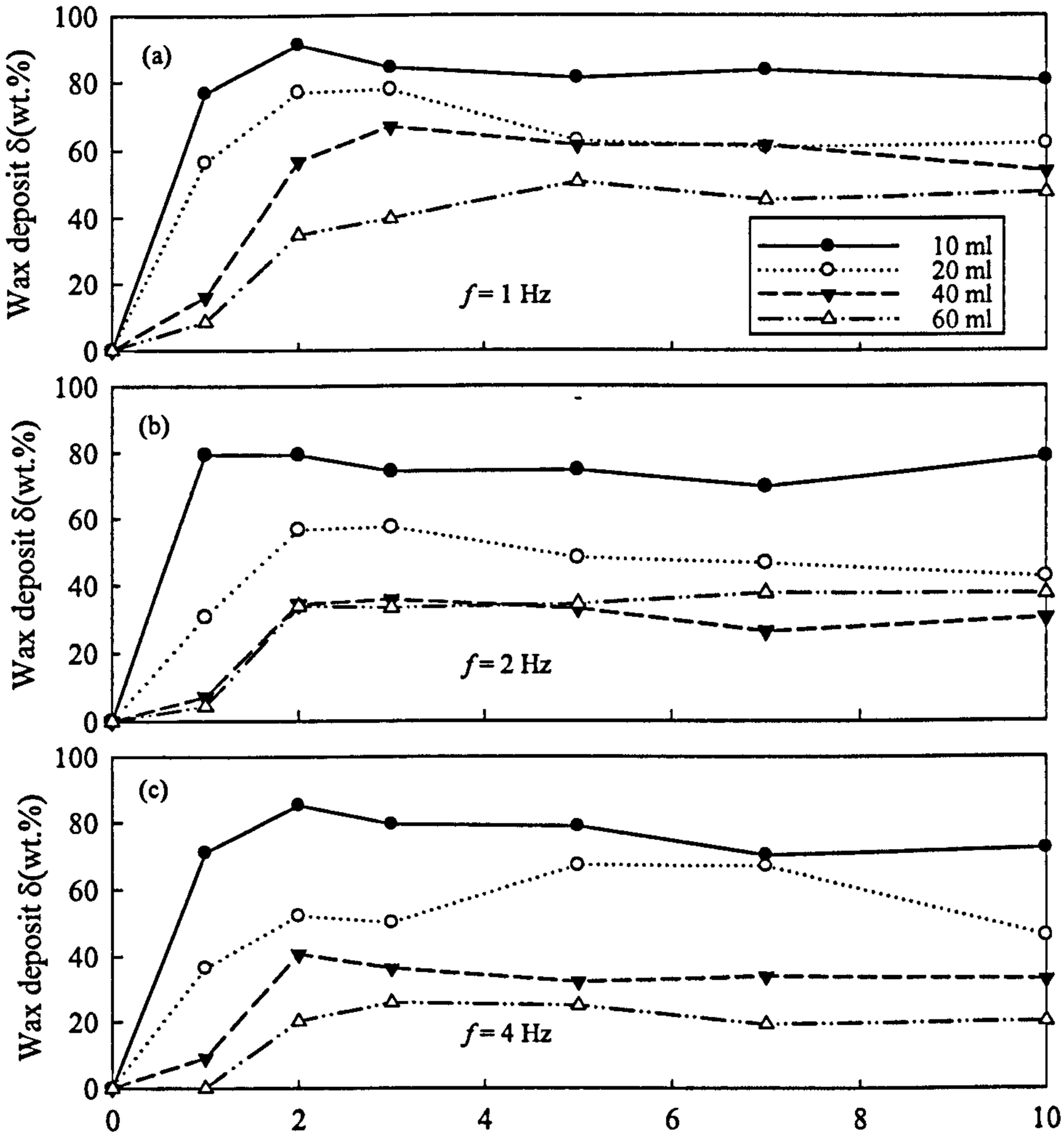

Figure 4.10 Effect of sample volumes on the deposition for different frequencies (x_o = 15 mm)

As mentioned earlier, the percentage of wax deposit shown in Figures 4.9 and 4.10 consists of depositions on the walls and the baffles. From the control experiments it is obvious that stationary baffles only serve to provide additional surface area for the share of the total deposition. For the oscillating baffles it is desirable to understand the effect oscillation has on the distribution of the deposit between the column walls and the baffles. In order to present concise information, we adopted the arithmetic means of the percentage of deposition throughout each experiment. The arithmetic mean is

calculated by averaging the deposition curve of each frequency and sample volume. Table 4.4 contains the necessary data.

Table 4.4 Mean values of percentage deposition on the baffles and the column wall (x_o = 15 mm)

Sample volume (ml)	Oscillation Frequency (Hz)	Mean of deposition (wt.%)		Overall mean for each volume (wt.%)	
		Baffles	Column wall	Baffles	Column wall
10	1	20.8	79.2	25.5	74.5
	2	26.3	73.7		
	4	29.3	70.7		
20	1	14.3	85.7	30.2	69.8
	2	29.3	70.7		
	4	47.1	52.9		
40	1	16.6	83.4	27.7	72.3
	2	26.0	73.9		
	4	40.6	59.4		
60	1	28.2	71.8	32.6	67.4
	2	36.8	63.2		
	4	32.7	67.3		

It can be noted that the deposition is consistently greater on the walls of the column than on the baffles, and this difference is the greatest at the lowest oscillation frequency. However, the mean deposition on the baffles surfaces generally increases with oscillation frequency for different volumes of wax and oil mixture solutions.

4.2.2.2 Oscillation amplitude

In these experiments, the main objective is to understand the effect of oscillation amplitude on the deposition. The centre-to-peak amplitudes of 5, 10 and 15 mm were used at a fixed oscillation frequency of 2 Hz, giving equivalent oscillatory Reynolds numbers of 1349, 2699 and 4048 respectively. Figure 4.11 shows the percentage of deposition over time as a function of oscillation amplitude for a range of volumes, where the 'no osc.' line represents the control results.

From Figure 4.11, similar features to that of the oscillation frequency experiments can be extracted. Firstly, the greater the amplitude of oscillation, the lower the amount of deposition observed. So, in tandem with the oscillation frequency results, this means that high oscillation frequency and high amplitude lead to greater reduction of deposition. It is also clear that 100% deposition was prevented with all amplitudes tested. The main reason for these results is due to eddy motions that are generated in the fluid, which strip off and suspend some of the deposit from the walls. Secondly, for the experiments with oscillating baffles, the smaller the volumes of wax and oil mixture solutions, the higher the initial slopes of the curves. This could again be a consequence of splashing onto the wall of the column above the liquid surface as the upper baffle passes through the liquid surface. Generally, there is a greater reduction in the deposition for increasing both the volume of wax and oil mixture solution and oscillation amplitudes; however, the extent of reduction diminishes with larger volumes.

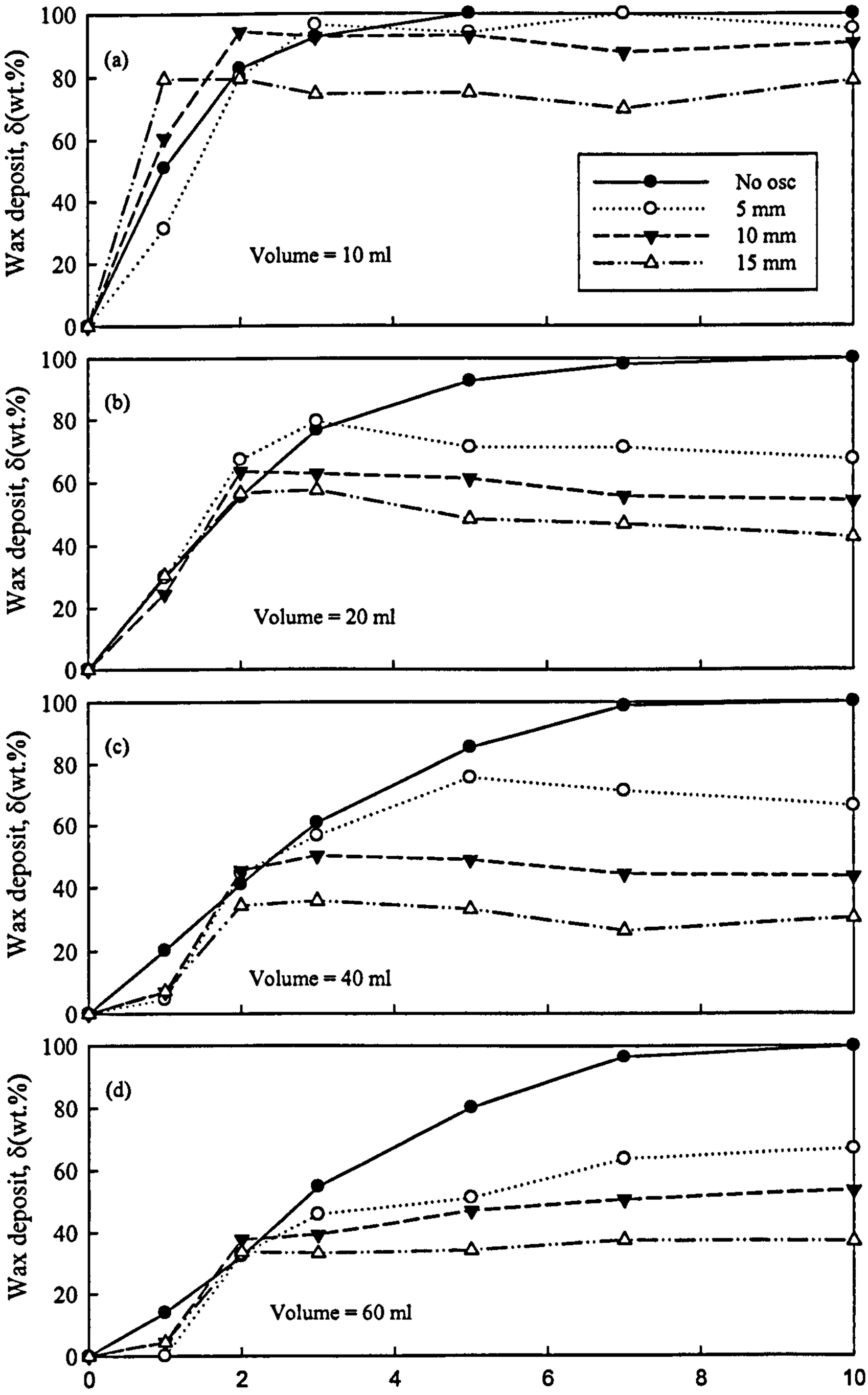

Figure 4.11 Effect of oscillation amplitudes on the deposition for different volumes (f = 2 Hz)

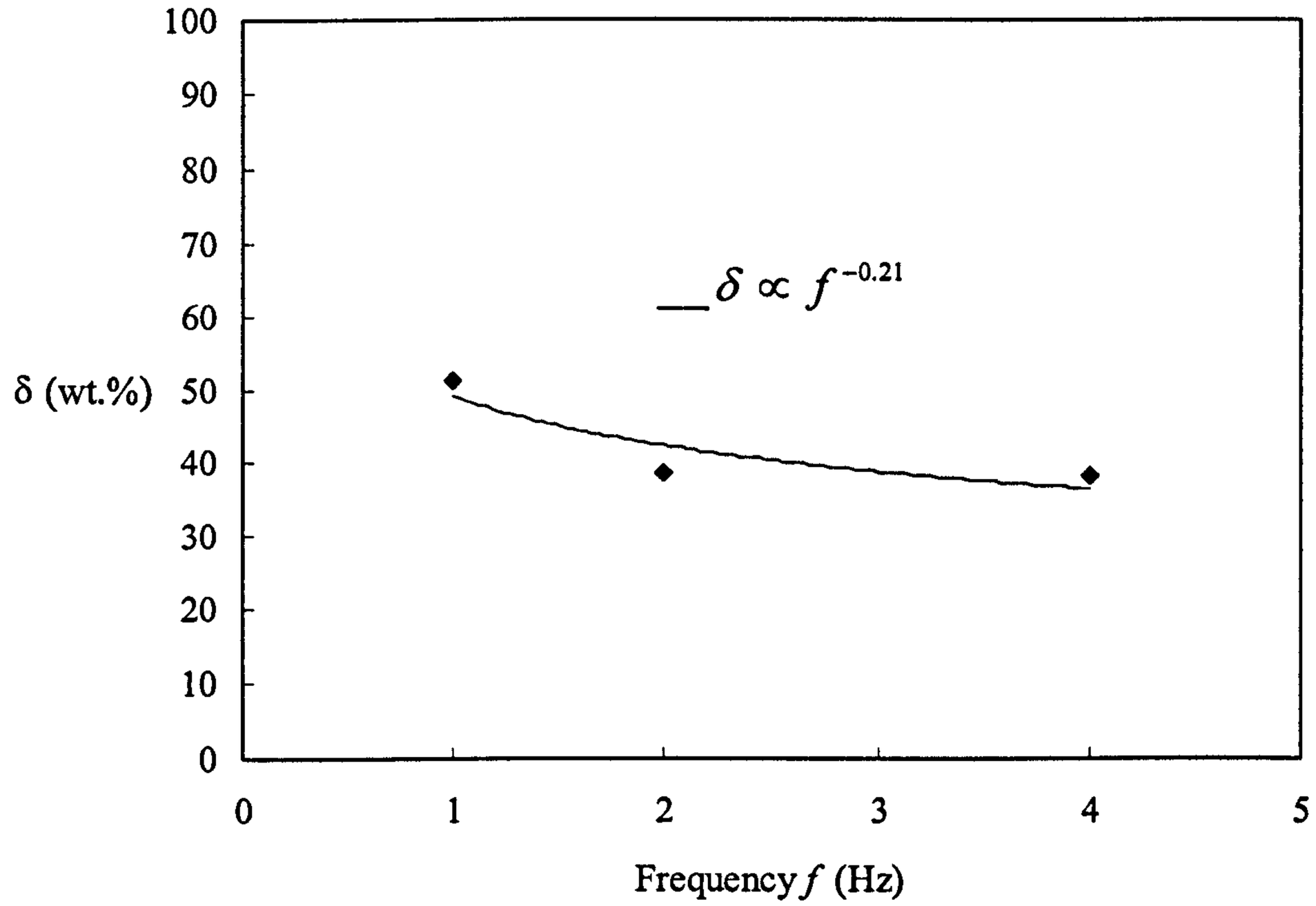

Figure 4.12 Effect of oscillation frequency on the mean deposition (x_o = 15 mm)

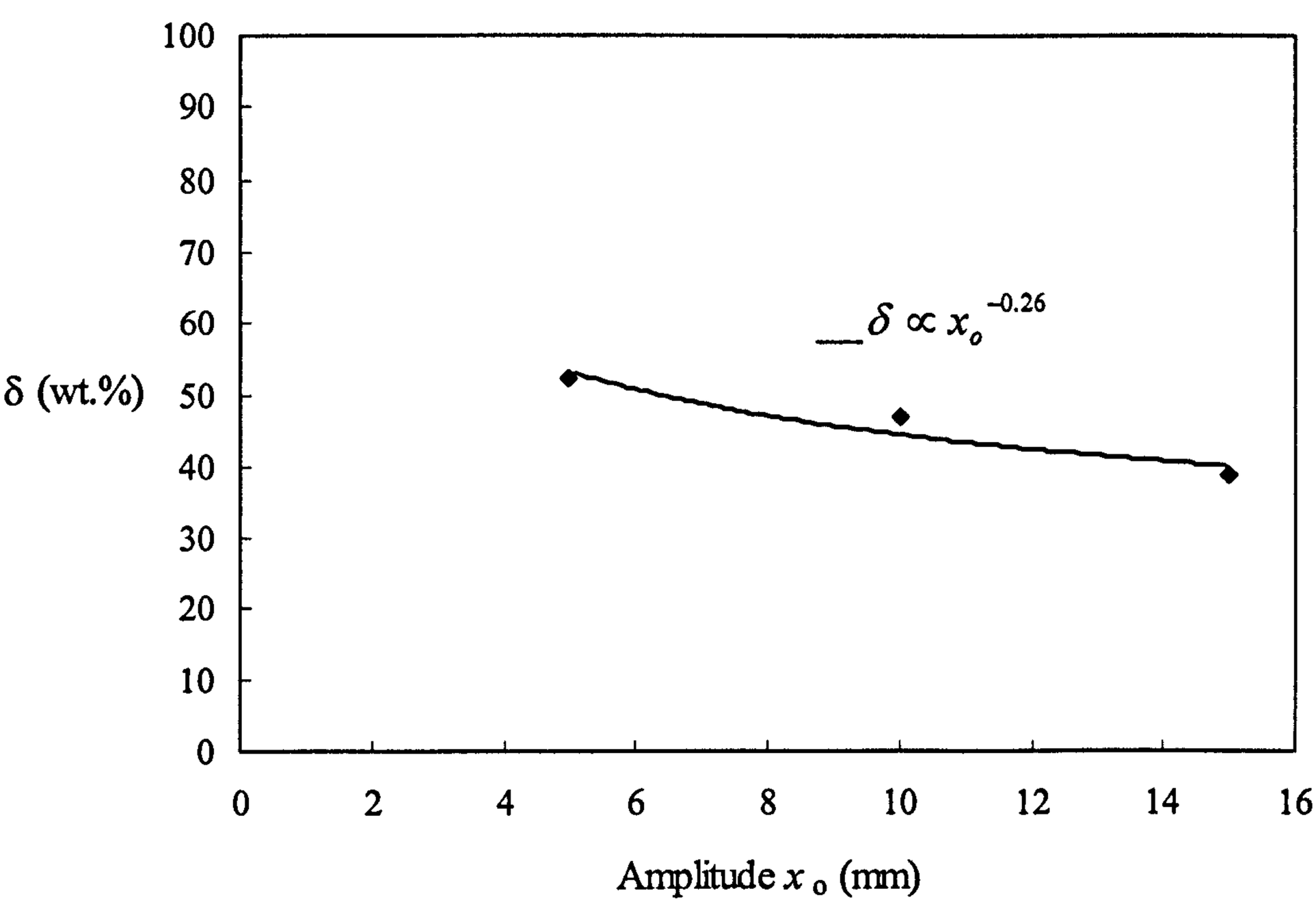

Figure 4.13 Effect of oscillation amplitude on the mean deposition (f = 2Hz)

It can be seen that the effects of oscillation frequency and amplitude on average deposition are similar. However, the magnitude of the power index calculated in Figures 4.12 and 4.13 indicates that changing oscillation amplitude has a greater impact than changing frequency. The relationship between the deposition and the oscillatory Reynolds number is evaluated in Figure 4.14. Increasing oscillation intensity makes a dramatic reduction in the deposition in the range of $Re_o < 4000$. At $Re_o > 4000$ the effect is less dramatic, possibly because the optimum mixing is generated under this fluid dynamical condition.

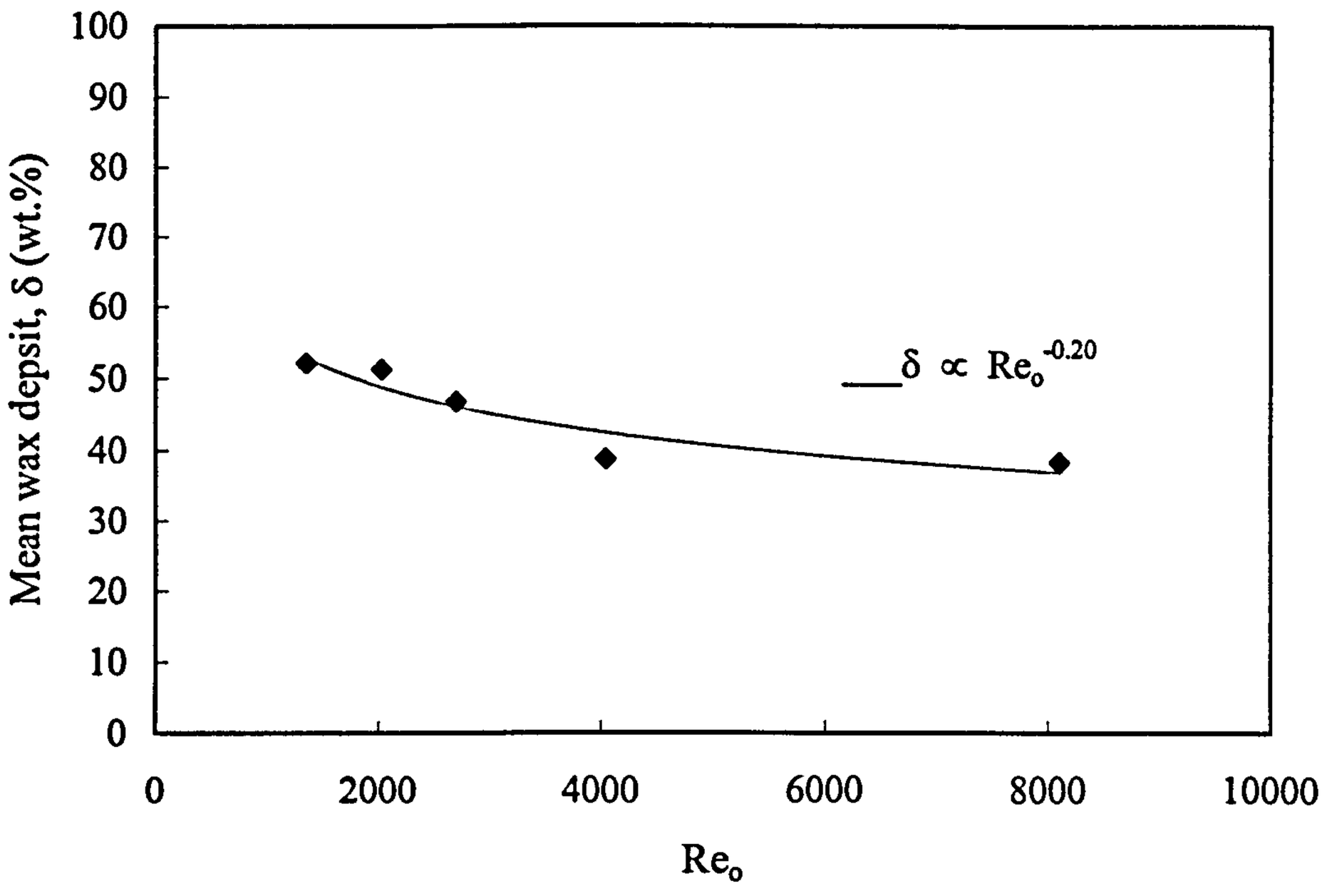

Figure 4.14 Correlation of mean wax deposit and oscillatory Reynolds number

For the individual deposition, Table 4.5 lists the calculated arithmetic means of the percentage of the deposition on the baffles and the column respectively for the experiments with different amplitudes.

Table 4.5 Mean values of percentage deposition on the baffles and the column wall with different amplitudes (f = 2 Hz)

Sample volume (ml)	Oscillation amplitude (mm)	Mean deposition (wt.%)		Overall mean for each volume (wt.%)	
		Baffles	Column wall	Baffles	Column wall
10	5	15.5	84.5	19.2	80.8
	10	15.8	84.2		
	15	26.3	73.7		
20	5	11.3	88.7	17.9	82.1
	10	13.1	86.9		
	15	29.3	70.7		
40	5	32.9	67.1	28.1	71.9
	10	25.2	74.8		
	15	26.1	73.9		
60	5	39.8	60.2	38.0	62.0
	10	37.5	62.5		
	15	36.8	63.2		

From Table 4.5, it can be observed that

a) the deposition is consistently greater on the walls of the column than on the baffles, with an average of 74.2% on the walls and 25.8% on the baffles;

b) mean percentage deposit on the wall generally decreases with the increase in volume of sample, whereby the fraction on the baffles increases.

In some of the examples described in the introduction (*e.g.* oil transmission lines), the implementation of oscillatory motion via the means of oscillating baffles in existing equipment may be impossible or impractical, however, similar mixing conditions would be achieved using tubes/pipes with furrowed or wavy walls (Bellhouse *et al.*, 1973; Nishimura *et al*, 2004) at the appropriate flow rate of crude oil, *e.g.* the production rate. Hence an equivalent level of reduction in the deposition would be realised. Since the fluid mechanical conditions in a batch OBC can easily and directly be applied to continuous processes, the results would have a profound effect on transportation pipelines. The irony is that the inclusion of any inserts/restrictions, such as baffles/corrugated walls, in pipe lines immediately relates to the concept of increasing surface areas available for deposition, the results of this work however indicate that the appropriate balance of tube/pipe insertions/restrictions together with a sufficient bulk flow rate can in fact reduce the wax deposition.

4.2.3 Avrami kinetic analysis

Avrami kinetics analysis has been conducted by plotting the graph using Equation (3.6), explained in Section 3.6 and Appendix B. Figures 4.15 and 4.16 show the Avrami plot for each amplitude, frequency and volume tested in this study. The slope of the straight lines gives the Avrami exponent, n. The intersection of the straight lines with y-axis provides the Avrami kinetics coefficient, K. From n and K, the deposition half time, $t_{1/2}$ (min), can be calculated as explained in Section 3.6 and Appendix A, can be used as a tool to investigate the deposition rate.

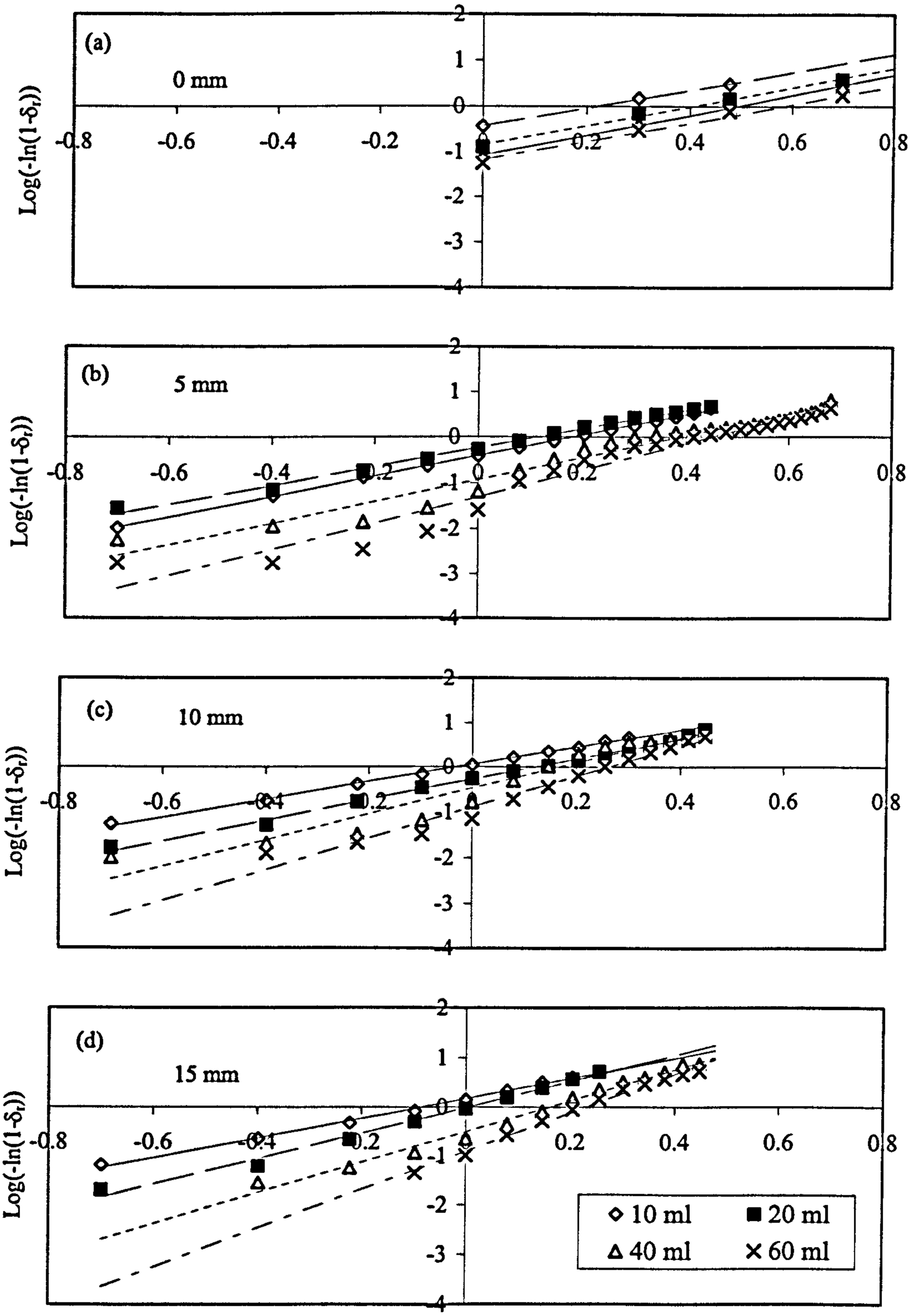

Figure 4.15 The Avrami plot of Log(-ln(1-δ_r)) vs. Log(t) for each amplitude and volume tested (f = 2 Hz)

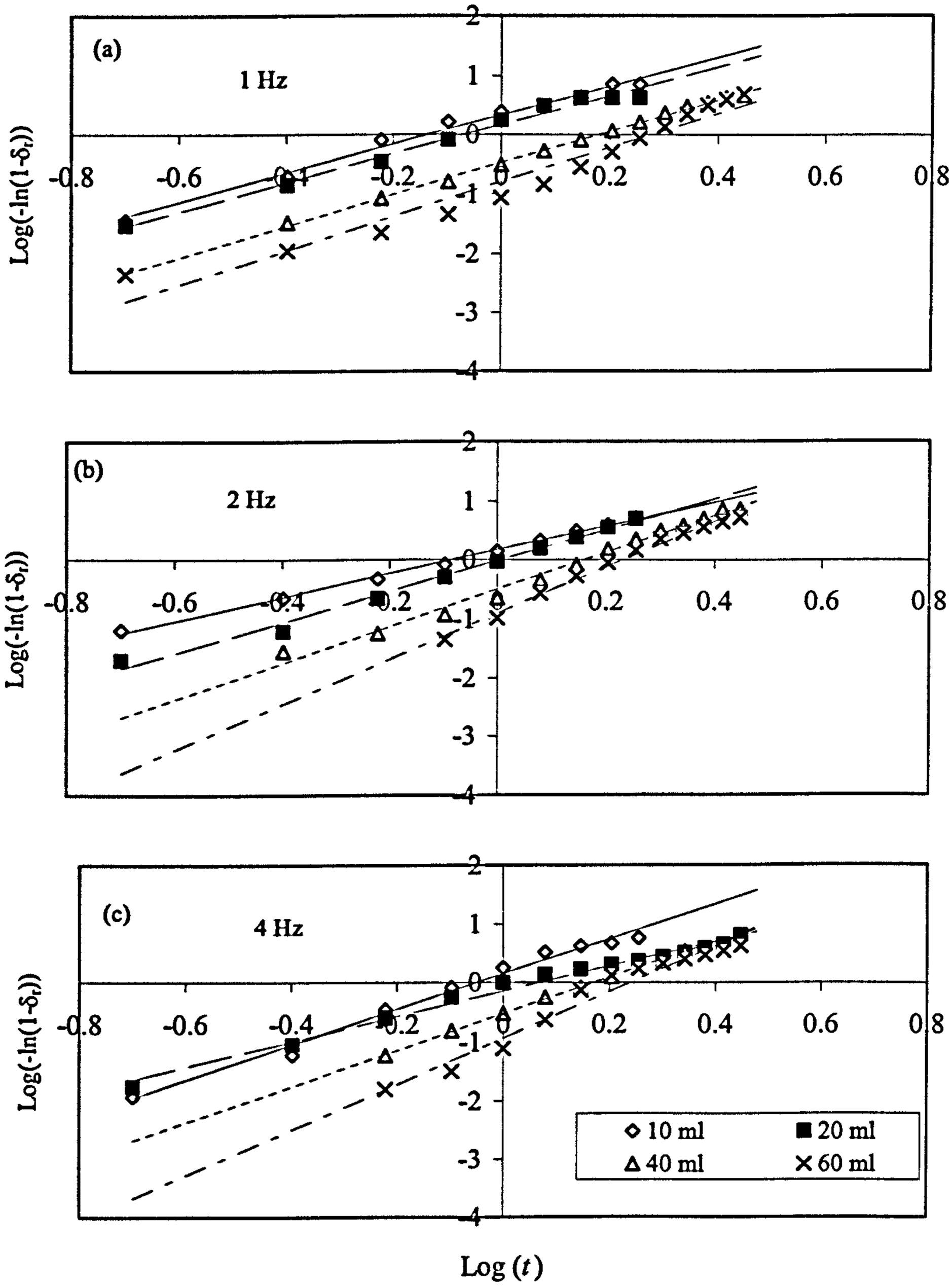

Figure 4.16 The Avrami plot of Log(-ln(1-δ_r)) vs. Log(t) for each frequency and volume tested (x_o = 15 mm)

Table 4.6 Avrami data for the effect of amplitude extracted from Figure 4.15

Volume	$x_o = 0$ mm			$x_o = 5$ mm			$x_o = 10$ mm			$x_o = 15$ mm		
(ml)	n	K (min^{-n})	$t_{1/2}$ (min)	n	K (min^{-n})	$t_{1/2}$ (min)	n	K (min^{-n})	$t_{1/2}$ (min)	n	K (min^{-n})	$t_{1/2}$ (min)
10	1.93	0.37	1.38	2.24	0.39	1.29	1.94	1.14	0.77	2.02	1.48	0.69
20	2.08	0.14	2.14	2.05	0.58	1.09	2.25	0.53	1.13	2.62	0.97	0.88
40	2.19	0.08	2.62	2.39	0.12	2.11	2.82	0.33	1.29	3.15	0.32	1.28
60	1.73	0.10	3.15	2.90	0.05	2.49	3.40	0.13	1.64	3.70	0.13	1.57

Table 4.7 Avrami data for the effect of frequency extracted from Figure 4.16

Volume (ml)	f=0 Hz			f=1 Hz			f=2 Hz			f=4 Hz		
	n	K(min^{-n})	$t_{1/2}$ (min)	n	K(min^{-n})	$t_{1/2}$ (min)	n	K(min^{-n})	$t_{1/2}$ (min)	n	K(min^{-n})	$t_{1/2}$ (min)
10	1.93	0.37	1.38	2.45	2.16	0.63	2.02	1.48	0.69	3.00	1.41	0.79
20	2.08	0.14	2.14	2.45	1.48	0.73	2.62	0.97	0.88	2.14	0.72	0.98
40	2.19	0.08	2.62	2.66	0.34	1.31	3.15	0.32	1.28	3.09	0.30	1.31
60	1.73	0.10	3.15	3.05	0.12	1.77	3.70	0.13	1.57	4.08	0.14	1.48

Tables 4.6 and 4.7 show the extracted Avrami parameters of the Avrami exponent (n), rate constant (K) and the half time ($t_{1/2}$) for the effect of amplitude from Figures 4.15 and 4.16. From Table 4.6 it can be seen that in control experiments without oscillation, the values for n are around 2 indicating one-dimensional type of crystals are produced when no oscillation is applied (Hay, 1971)(Figure 4.17). Generally, increasing the oscillation amplitude increased the n values, but the effect is lower for smaller volumes. The highest n value of 3.70 was observed for the largest volume of 60 ml and the longest amplitude of 15 mm, where the mechanism of crystal growth is of multi-dimensional (Figure 4.18).

The deposition half-time, $t_{1/2}$, can provide information on the rate of deposition in such a way that the smaller the $t_{1/2}$ value, the faster the deposition rate. From Table 4.2, it can be seen that for all volumes, the effect of oscillating the wax and oil mixture solution led to the $t_{1/2}$ values to decrease as compared to that from the control experiments. Hence, the deposition or crystallisation rate was increased due to the mixing effect of oscillation that leads to better cooling of the fluids. Although this initially caused a negative impact on the prevention of wax deposition, applying fluid oscillation significantly lowered the overall deposition (as explained in Section 4.2.2) as well as improved the efficiency of wax prevention (as explained in Section 4.2.3). On the effect of volume, it is evident that increasing the wax and oil mixture volume has increased the deposition half-time suggesting that the deposition rates were reduced. This is in line with expectation. Table 4.7 presents the Avrami parameters for the effect of frequency extracted from Figure 4.16, and outcomes similar to those for the effect of amplitude are observed. In summary, the larger the volume, the lower the deposition observed.

Figure 4.17 Microscopic image of wax crystals from the experiment with no oscillation

Figure 4.18 Microscopic image of wax crystals from the experiment with oscillations

4.3 Effect of paraffin wax content

The main focus of this investigation was on the effect of paraffin wax content of the wax-diesel solution used in the OBC together with the effect of oscillation frequency (f) and amplitude (x_o). Four paraffin contents have been tested, *i.e.* 10, 20, 40 and 60 percent by weight, represent four different supersaturation levels in terms of the crystallisation process. The values for the oscillation frequencies (f) examined were 1, 2 and 4 Hz, whereas for the amplitude (x_o) were 5, 10 and 15 mm, giving the oscillatory Reynolds numbers from 1359 to 8155 for 10% wax concentration; from 822 to 4934 for 20%; from 164 to 984 for 40% and from 37 to 224 for 60%. In the experiments to examine the effect of oscillation frequency, the amplitude was fixed at 15 mm whilst in the experiments to investigate the effect of oscillation amplitude, the frequency was fixed at 2 Hz. The initial hot temperature (T_1) was set at 50 °C which was well above the cloud point of the wax and oil mixture solutions where no cloudiness is observed for all solutions, and the final cold temperature (T_2) was selected at 10 °C. The speed of the cooling water pump (C_w) was set at 100 rpm ensuring a fixed cooling rate for all experiments. The cooling starts at $t = 0$ s.

The longest experimental duration is 10 minutes, and three wax deposit measurements were conducted at an interval of 1 minute for the initial 3 minutes, followed by two measurements taken at an interval of 2 minutes for the middle 4 minutes, and finally one measurement taken at the end of the experiment time of 10 minutes. When carrying out measurements of wax deposit, the experiment was stopped, the column was dismantled from its supporting platform and the non-crystallised wax and oil mixture was drained out of the column to a beaker and weighed. The crystallised

wax inside the column was determined by the difference between the weight of the empty column and the weight of the column with the deposit. The deposit was then calculated as a percentage from the total wax and oil mixture solution used. After the measurement, the experiment was restarted by recombining the solid deposit with the liquid part and the mixture was reheated to 50 °C. The experimental results are divided into two main sections: a) the deposition study and b) Avrami kinetic analysis.

4.3.1 Deposition study

In order to assess the effect of baffle oscillation on the deposition, control experiments were carried out in the OBC with the presence of baffles, but without oscillation. Observations from the experiments were that the wax deposit was in the form of an oil gel, and the hardness of the gel increased with the content of the paraffin wax. The gel-like wax was adhered to the baffle surfaces and the wall of the column, while the liquid that flowed out from the centre of the column was a clear fluid. When 100% deposition has been reached, the gel-like wax filled the whole tube and became solidified. Figure 4.19 shows the percentage of the deposition for different contents of paraffin wax in the control runs, where the *y*-axis corresponds to the percentage of wax deposited. Some of the experiments were repeated for the purpose of consistency; these data also provided the error bars in Figure 4.19.

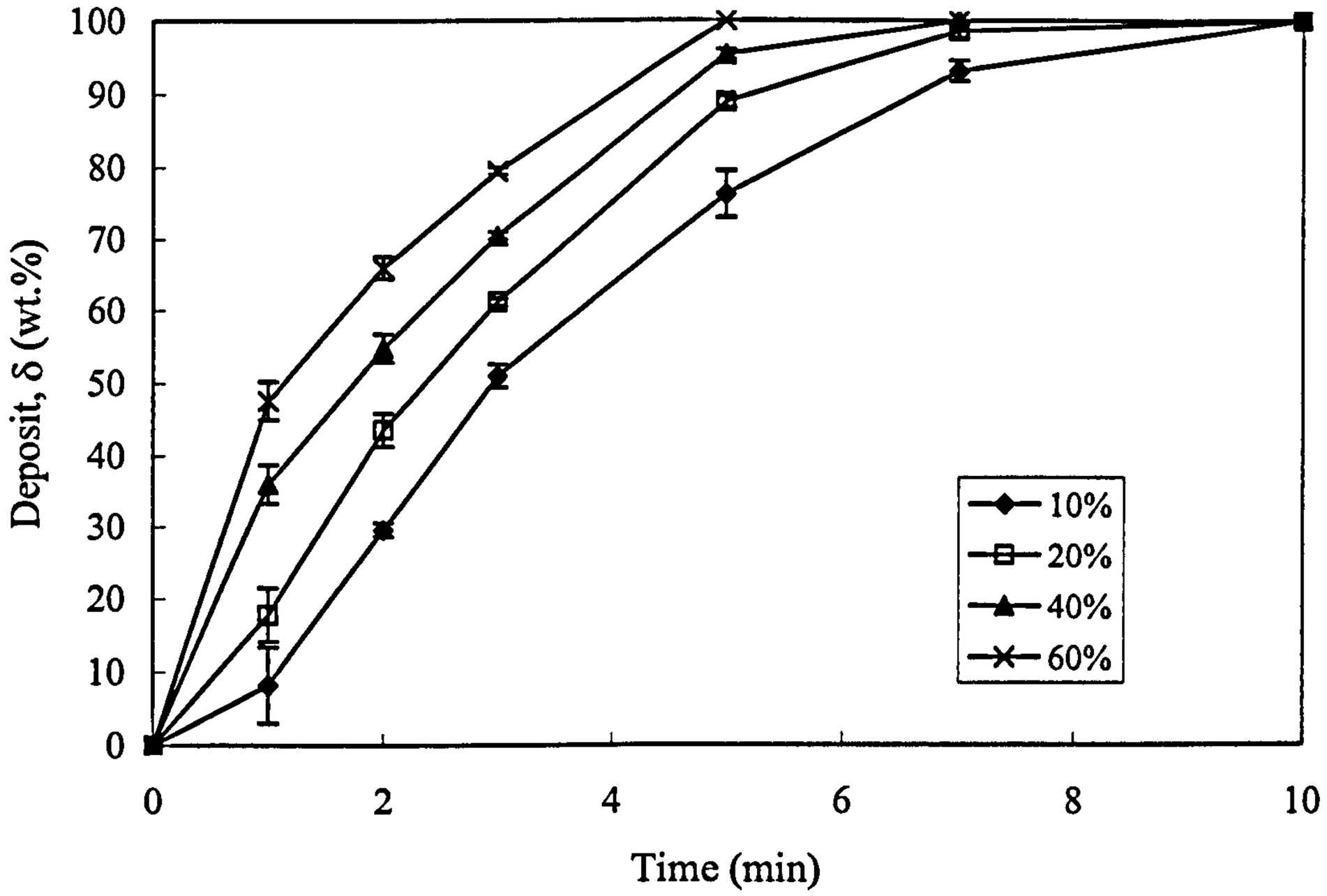

Figure 4.19 Effect of paraffin wax content on deposition in absence of oscillation

From the graph it can clearly be observed that the higher the paraffin content (the supersaturation level), the more wax deposit produced at any given time; the faster the deposition rates; and the quicker it reaches 100% deposition. These results are expected: with the increase of the paraffin wax content in solution, there are more wax molecules available to produce wax crystals.

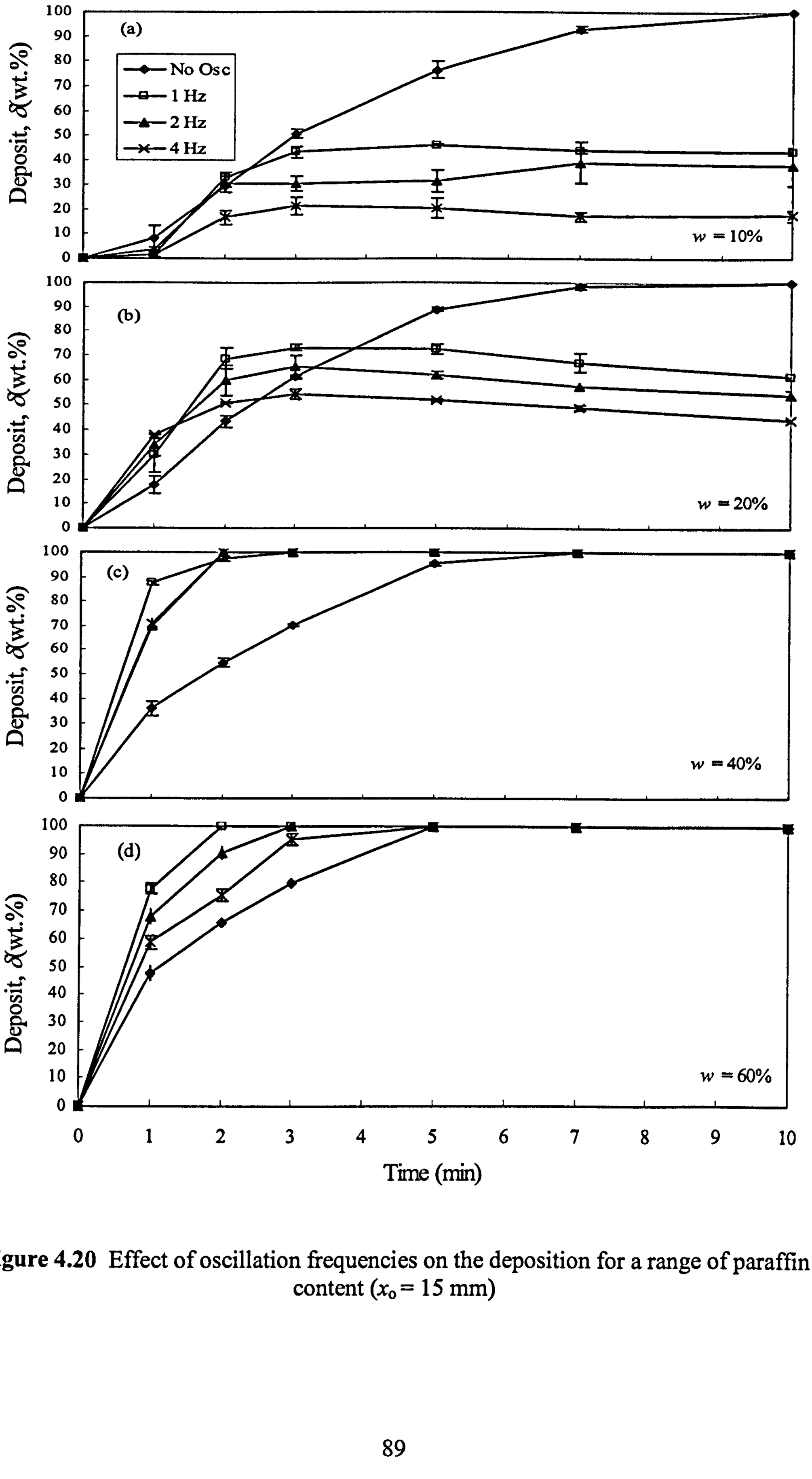

Figure 4.20 Effect of oscillation frequencies on the deposition for a range of paraffin content (x_o = 15 mm)

Figure 4.20 compares the percentage depositions from the control runs with those from the oscillation experiments for the wax content of 10, 20, 40 and 60% at a fixed oscillation amplitude. In Figure 4.20(a) with 10% paraffin wax content, the oscillatory motion reduced the deposition in comparison to the control results. At the end of experiments, the degree of the reduction is remarkable, *e.g.* about 60% reduction for 1 Hz; 70% for 2 Hz and over 80% for 4 Hz. Oscillatory motion effectively enables the wax crystals to remain suspended in the liquid, which minimises the contact time for crystals with the surface of the OBC. In all cases 100% deposition has been avoided. The results clearly demonstrated that oscillatory motion has a beneficial effect in reducing the deposition without the use of any solvent or wax inhibitor.

Figure 4.20(b) shows the corresponding deposition curves for experiments with 20% paraffin wax content. The reduction of the deposition is still clearly seen, *e.g.* about 30% for 1 Hz, 40% for 2 Hz and 50% for 4 Hz, and once again 100% deposition has been prevented. However the extent of reduction is less in comparison to Figure 4.20(a), reinforcing that the wax content of the solution or supersaturation level plays a major role in the deposition process. In fact, the oscillatory motion in this condition gave faster rates of deposition in the first 2 minutes than in the control runs. The situation becomes more pronounced when the wax content is increased to 40% (Figure 4.20(c)) and 60% (Figure 4.20(d)), where the oscillation exhibits the opposite effect, *i.e.* enhancing the deposition on surfaces, not only with faster rates, but also with much shorter time to reach 100% deposition in comparison to the results of the control runs. The possible explanation would be that the enhancement of mixing encourages the cooling process of the solution in the OBC, hence allowing wax crystals in contact with internal surfaces more frequently at much shorter time and effectively promoting either

instantaneous or sporadic nucleation. Note that the trend of the percentage deposition in Figure 4.20(d) is that there is a faster deposition rate for 1 Hz than that for 4 Hz. This is likely due to the fact that reduced agitation led to longer contact time with the wall at this supersaturation level.

The effect of oscillation amplitude on percentage deposition as shown in Figure 4.21 is similar to that in Figure 4.20, but with lesser effective reduction of the deposition. The results indicate that the oscillatory motion can have either beneficial or detrimental effect on the percentage deposition depending on the wax content in solution. For the wax content of 10~20%, the beneficial effect prevails. On the other hand, for the wax content greater than 20%, the detrimental effect dominates. In the real world, the wax content of crude oil is generally less than 20%, *e.g.* Leontaritis and Mansoori (1988) reported that the Venezuelan Boscan crude contained around 17% waxy materials, 12.4% wax content in the crude oil from Bu Hasa oil-field near Abu Dhabi (Al-Marzouqi *et al.*, 2007) and 11.0% wax content in the crude oil from Shengli oil-field, East China (Hao *et al.*, 2004).

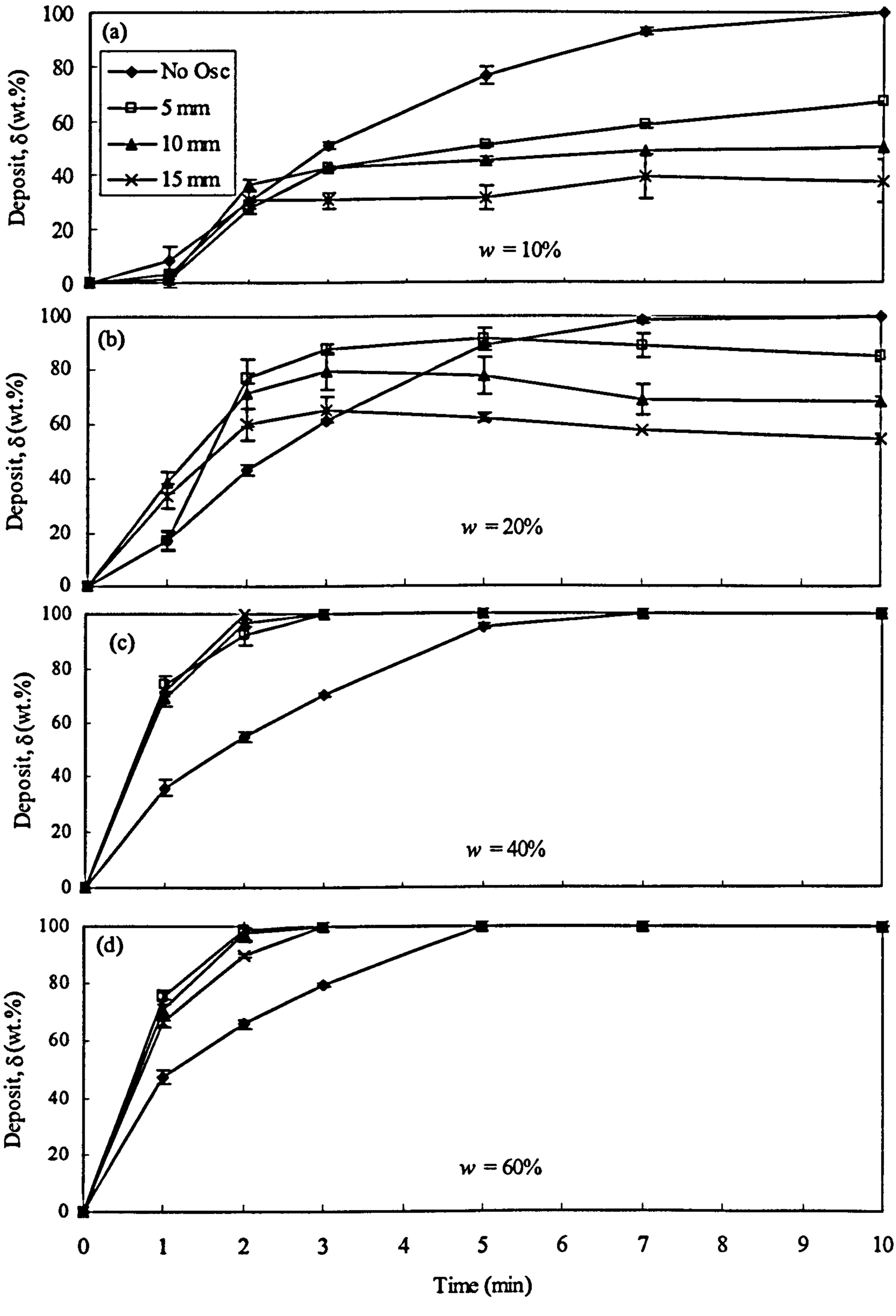

Figure 4.21 Effect of oscillation amplitude on the deposition for a range of paraffin content (f = 2 Hz)

4.3.2 Avrami kinetic analysis

From the deposition profiles presented earlier, wax formation can generally be divided into three main sections: the nucleation phase, the growth phase and the quasi-steady (or the asymptotic) state. As nucleation is too fast to measure, the first and second sections are combined as a single step in most related studies. Typically the growth phase took place in the first 2 or 3 minutes of the experiments for most of the wax-diesel solutions. By analysing the growth phase curves using the Avrami theory as explained in Section 3.6 and Appendix A, some crystallisation/deposition kinetics can be extracted. Figures 4.22 and 4.23 plot $\log[-\ln(1-\delta_t)]$ vs. $\log(t)$ for the effect of oscillation frequency and amplitude respectively. From these figures, good linearity can be seen for both cases, indicating the effectiveness of the Avrami methodology. The Avrami exponent (n), and the half time of deposition ($t_{1/2}$) are extracted from the plots and summarised in Tables 4.8 and 4.9.

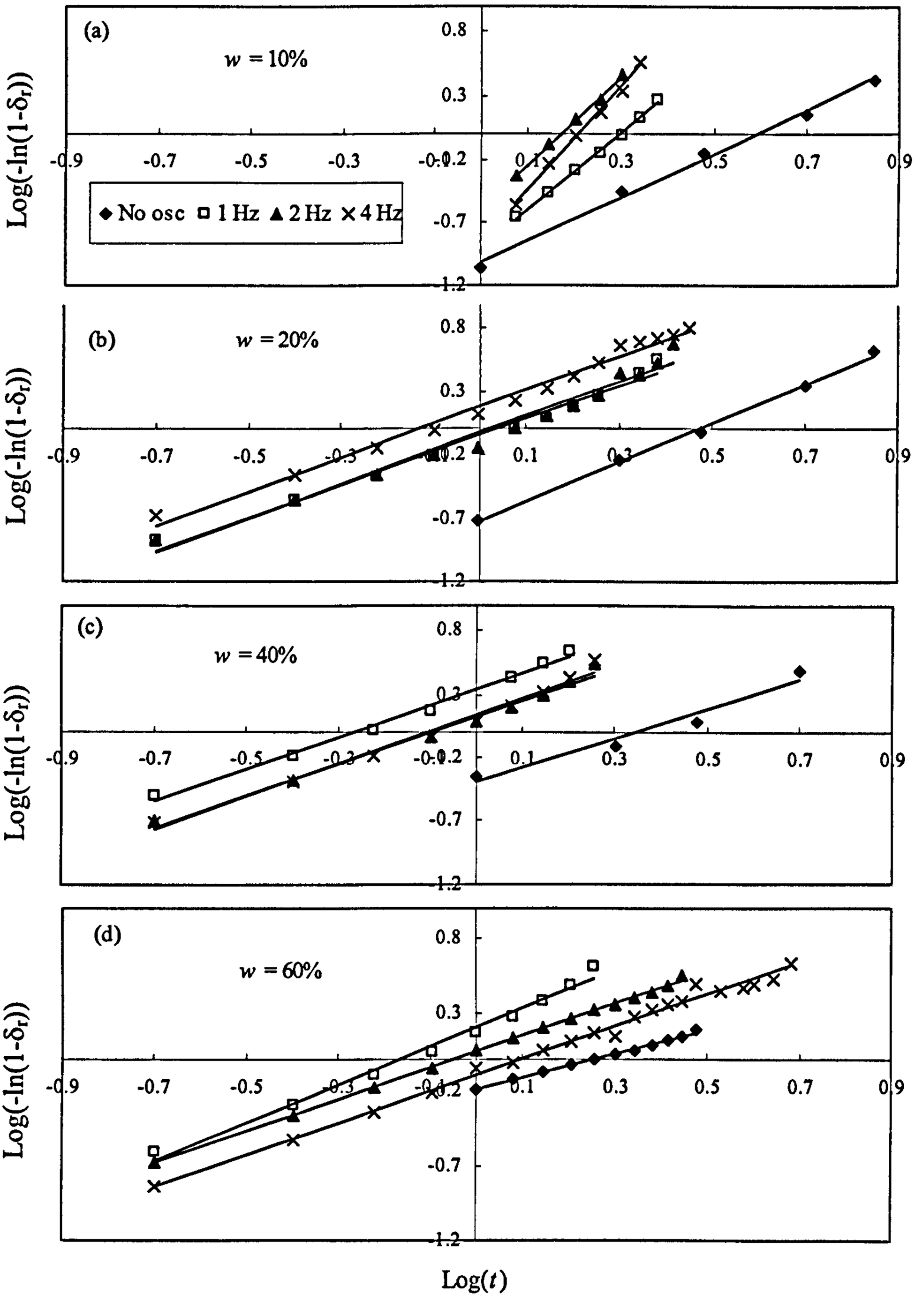

Figure 4.22 The Avrami plots for different wax content showing the effect of oscillation frequencies (x_o = 15 mm)

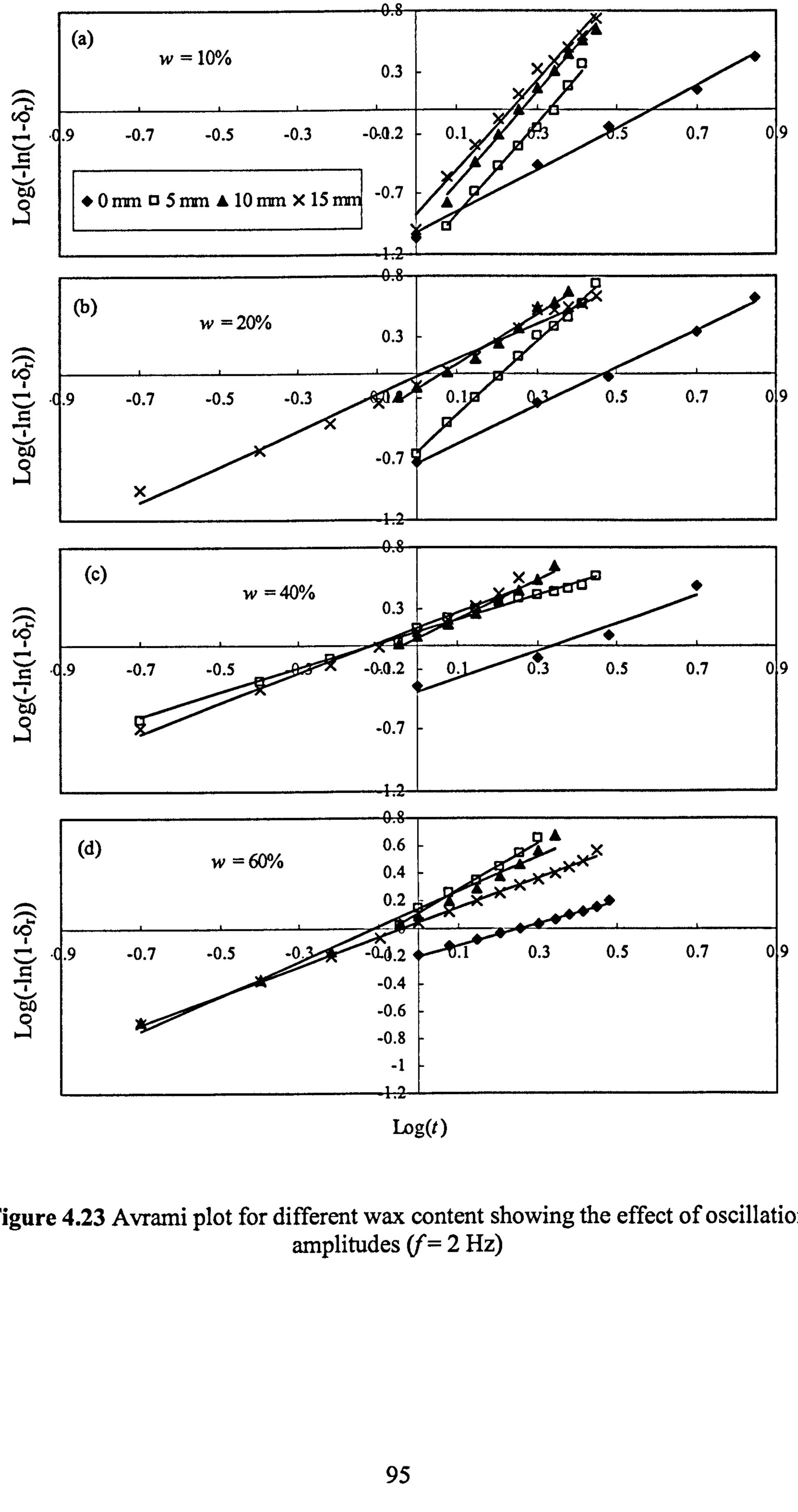

Figure 4.23 Avrami plot for different wax content showing the effect of oscillation amplitudes ($f = 2$ Hz)

Table 4.8 Extracted Avrami parameters for the effect of oscillation frequency (x_o = 15 mm)

Wax content (wt. %)	f = 0 Hz		f = 1 Hz		f = 2 Hz		f = 4 Hz	
	n	$t_{1/2}$ (min)	n	$t_{1/2}$ (min)	n	$t_{1/2}$ (min)	n	$t_{1/2}$ (min)
10	1.73	3.15	3.05	1.77	3.70	1.57	4.08	1.48
20	1.56	2.30	1.28	0.82	1.34	0.80	1.34	0.56
40	1.17	1.61	1.28	0.41	1.26	0.57	1.31	0.59
60	0.78	1.11	1.26	0.75	1.07	0.65	1.06	0.88

Table 4.9 Extracted Avrami parameters for the effect of oscillation amplitude (f = 2 Hz)

Wax content (wt. %)	x_o = 0 mm		x_o = 5 mm		x_o = 10 mm		x_o = 15 mm	
	n	$t_{1/2}$ (min)	n	$t_{1/2}$ (min)	n	$t_{1/2}$ (min)	n	$t_{1/2}$ (min)
10	1.73	3.15	3.80	1.96	3.83	1.67	3.70	1.56
20	1.56	2.30	3.03	1.45	2.08	0.98	1.46	0.82
40	1.17	1.61	1.01	0.54	1.58	0.73	1.26	0.57
60	0.78	1.11	1.70	0.69	1.27	0.58	1.07	0.65

In both tables, some general trends can be observed. Firstly, the half time of deposition, $t_{1/2}$, generally decreases with the wax content in solution or supersaturation level (with some exceptions) indicating that the growth rate generally increases. This is expected, as the higher wax concentration or supersaturation, the more wax crystals, the higher the crystallisation rate. Secondly, the Avrami exponent decreases with the increase of the wax concentration in solution. This suggests different growth forms of crystals for different wax concentrations. Thirdly, for higher wax concentrations or supersaturations, both n and $t_{1/2}$ are largely similar for different frequencies and amplitudes, suggesting that the effect of oscillation on the crystallisation mechanism is insignificant under these conditions. As the 10% wax concentration in solution is closely associated with the real crude oil systems, both n and $t_{1/2}$ values are further analysed.

The most noticeable increase in n in Tables 4.8 and 4.9 can be seen for the 10% wax concentration, where a step change is clearly visible between the cases with and without oscillation. Using both n and $t_{1/2}$ as the diagnostic tool of crystallisation mechanism, Hay (1971) derived a model for spheres, discs and rods, representing three-, two- and one-dimensional forms of growth, which were summarised in Table 3.1. It suggests that the wax crystals produced in the presence of oscillation tend to be disc-like, in comparison to needle-like shape in the absence of oscillation. The results may underline the transition mechanism for the beneficial effect of oscillatory motion on the reduction of the deposition. Without the oscillation, the wax crystals would be of rod-like shape in one-dimensional growth; these rods would spread to the walls and baffle surfaces, resulting in gel-formation and crystals precipitated out of solution.

When the oscillatory motion is applied at 10% wax concentration, the Avrami exponents approach 4 suggesting sporadic nucleation, and the net result of the motion is to change the rod-like crystals into clustered, disc-like crystals. With the help of a light microscope, Figure 4.24 shows the microscopic shapes of the crystals obtained with and without oscillation. Clearly the shapes of the crystals shown in Figure 4.24 are matched well with the kinetic evaluations. It seems that the clustered, disc-like crystals are less likely to be adhered to the internal surfaces of the OBC; however, it is not fully understood as to why the changes in the crystallisation mechanism would cause the reduction of the deposition.

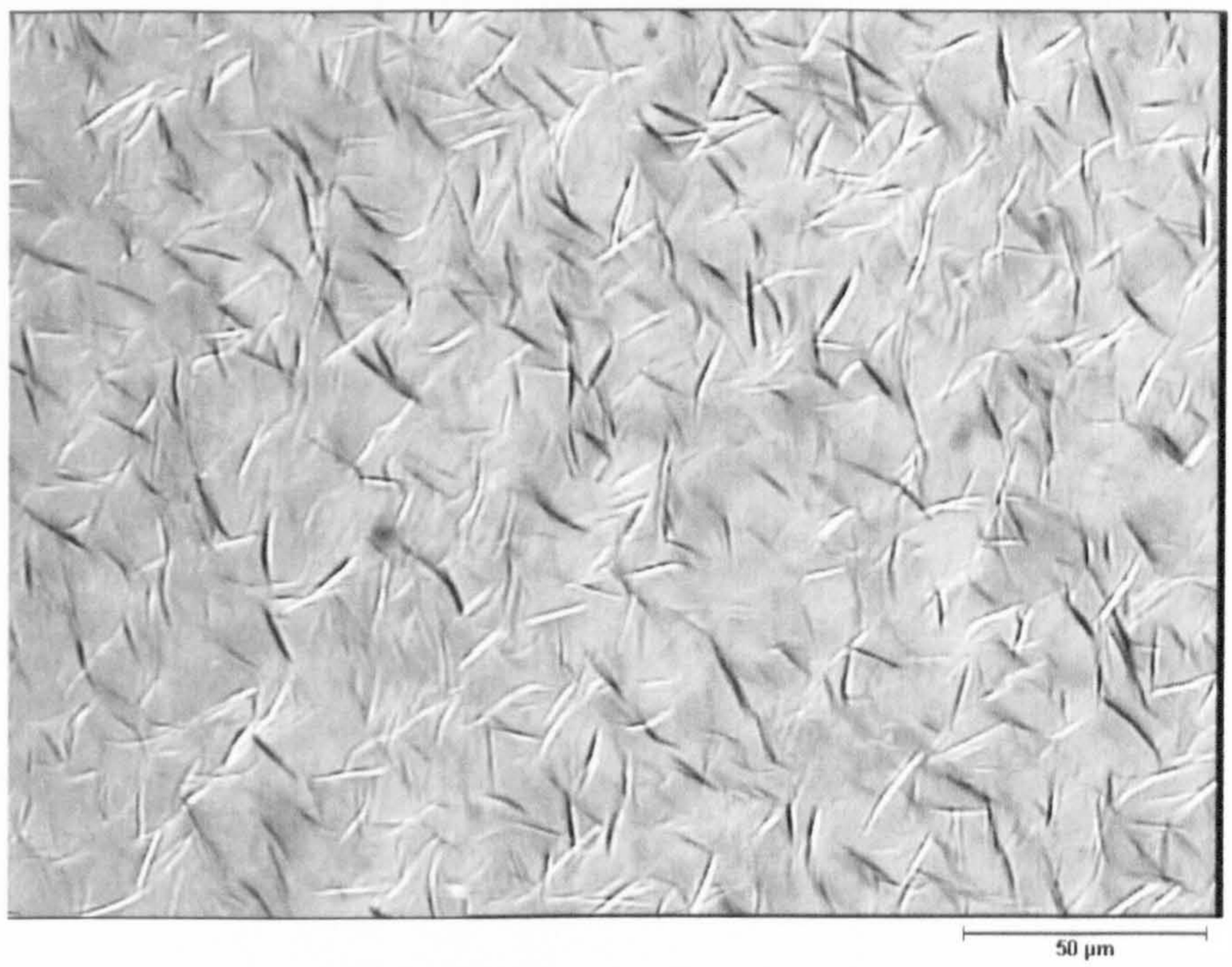

(a) Without oscillation (magnification = 60 x)

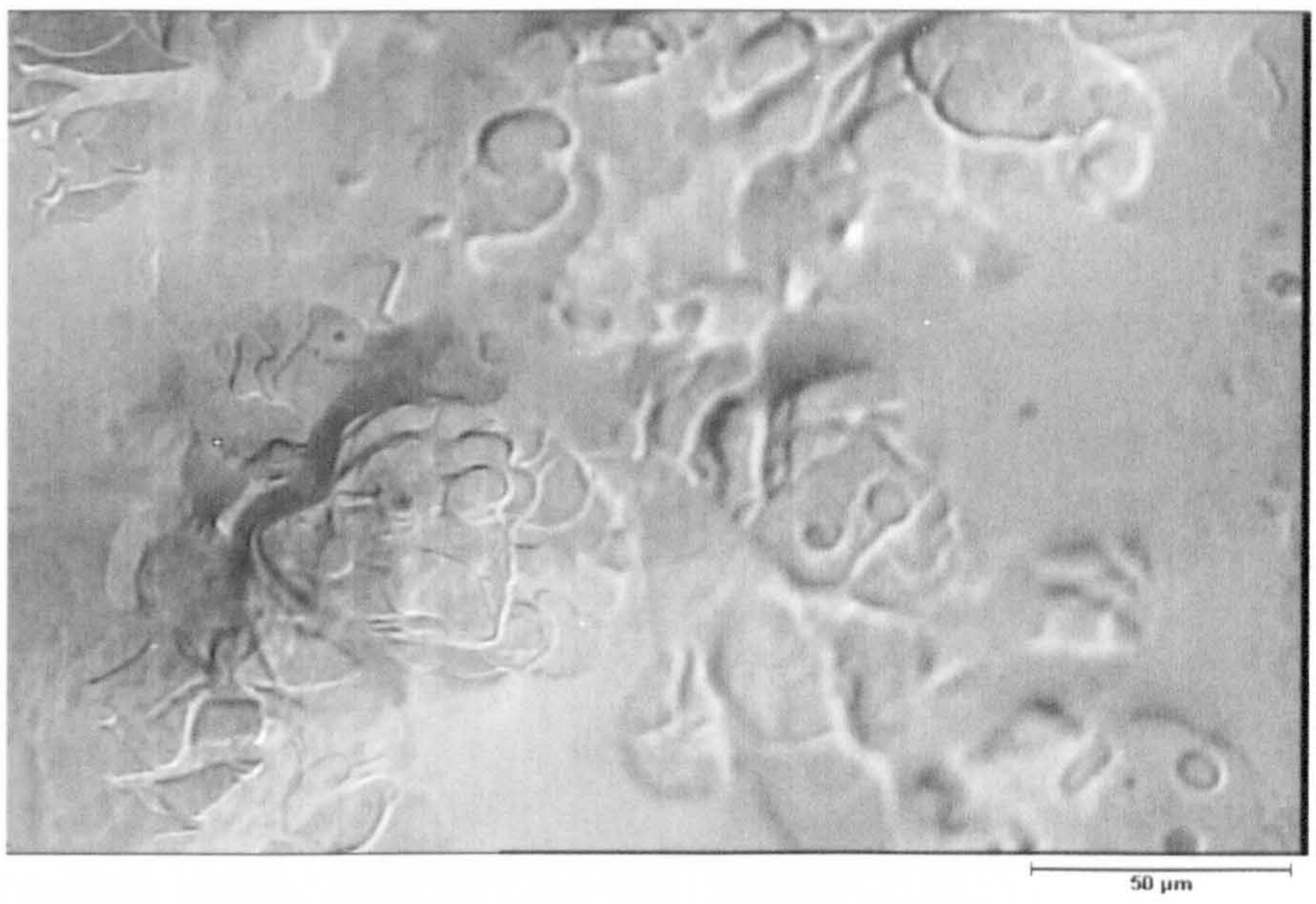

(b) With oscillation (x_o = 15 mm, f = 1 Hz)

Figure 4.24 Microscopic images of samples taken from solution containing 10% wax (magnification = 60 x)

4.4 Effect of solvent carbon numbers

In this section, results are discussed on the systematic investigation of the effects of solvent types particularly the carbon numbers of the paraffinic solvent ranging from *n*-octane (C_8), *n*-decane (C_{10}) and dodecane (C_{12}) to tetradecane (C_{14}). The main objective of this work is to examine the impact of solvent carbon numbers on the mechanism of deposition as well as the influence of oscillation frequency and amplitude. Oscillation frequencies (f) examined were 1, 2 and 4 Hz, whereas for the amplitudes (x_o) were 5, 10 and 15 mm. The wax content was fixed at 20% for all experiments. The initial hot temperature (T_1) was set at 50 °C which was tested for all solutions and found to be well above the cloud point and the final cold temperature (T_2) was selected at 10 °C. The speed of the cooling water pump (C_w) was set at 100 rpm (0.87 l/min) and the cooling starts at t = 0 s. The typical experimental duration was 10 minutes, and three wax deposit measurements were conducted at an interval of 1 minute for the initial 3 minutes, followed by two measurements taken at an interval of 2 minutes for the middle 4 minutes, and finally one measurement taken at the end of the experiment time of 10 minutes. Results are presented in terms of deposition studies and the Avrami kinetic analysis.

4.4.1 Deposition study

The effects of different solvents on the deposition are examined by comparing with control experiments carried out in the OBC with baffles in static conditions. From the visual observations during experiments, the wax deposits were in the form of an oil gel that adhered to the baffle surfaces and the wall of the column, and the liquid that flowed

out was a clear fluid. After reaching final deposition of 100%, the gel wax and oil mixture deposits became solidified and filled the whole tube. Figure 4.25 shows the percentage of the deposition for different solvents in the control tests, where the *y*-axis corresponds to the percentage of wax deposited.

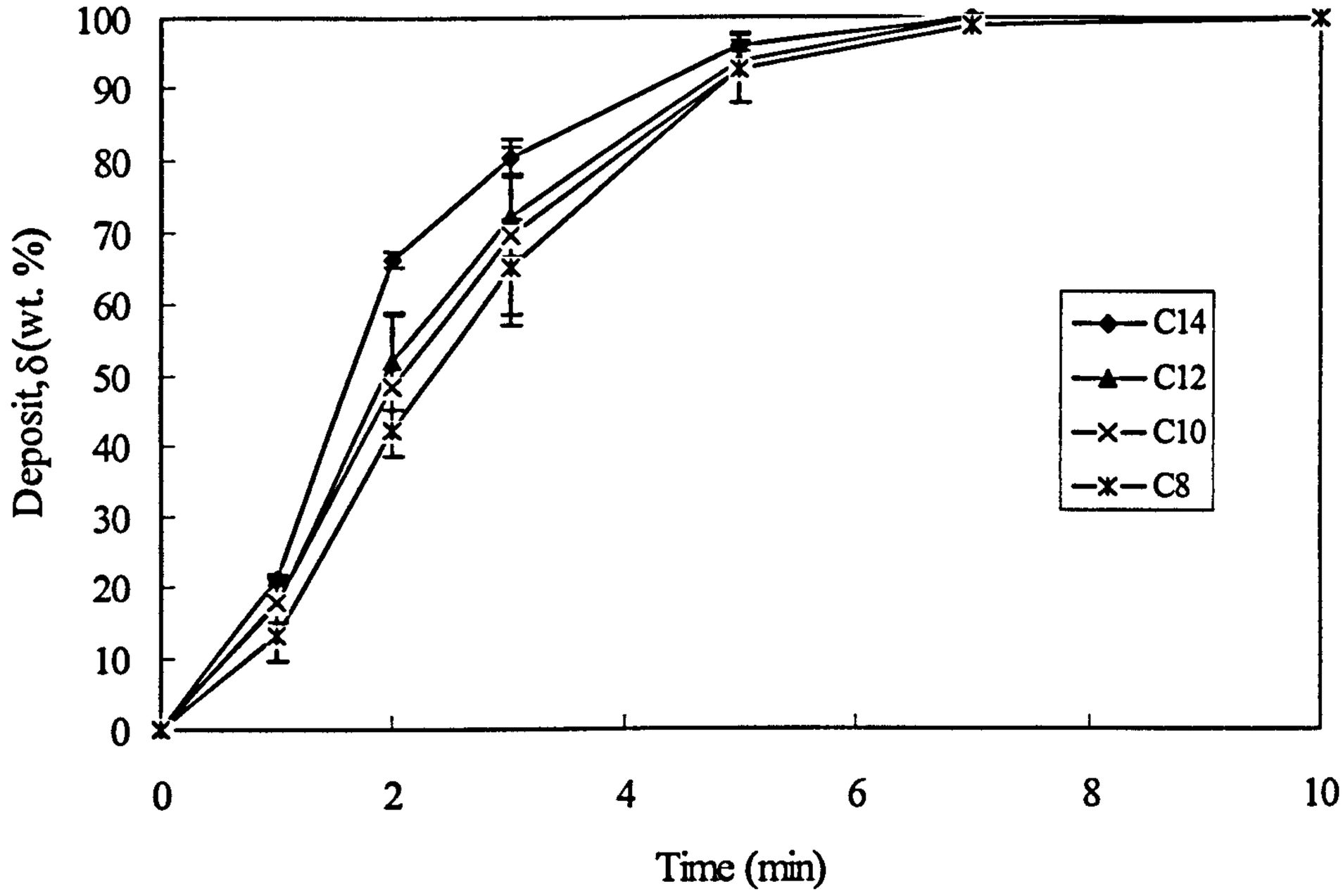

Figure 4.25 Effect of solvent carbon numbers on the deposition in absence of oscillation

From Figure 4.25, it can be observed that the higher the carbon number of the solvent, the more wax gel deposited at any given time and the faster the deposition rates. These results are related to the fact that paraffin waxes are more soluble in lighter hydrocarbons than in heavy hydrocarbons; Jennings and Weispfennig (2005) reported the solubility of *n*-hexatriacontane ($C_{36}H_{74}$) increased as the solvent size decreased due to the ability of the smaller solvent to more effectively contact and solvate the solute (see Figure 4.26). Hence wax molecules were more readily to be precipitated out from solvents having a longer carbon chain.

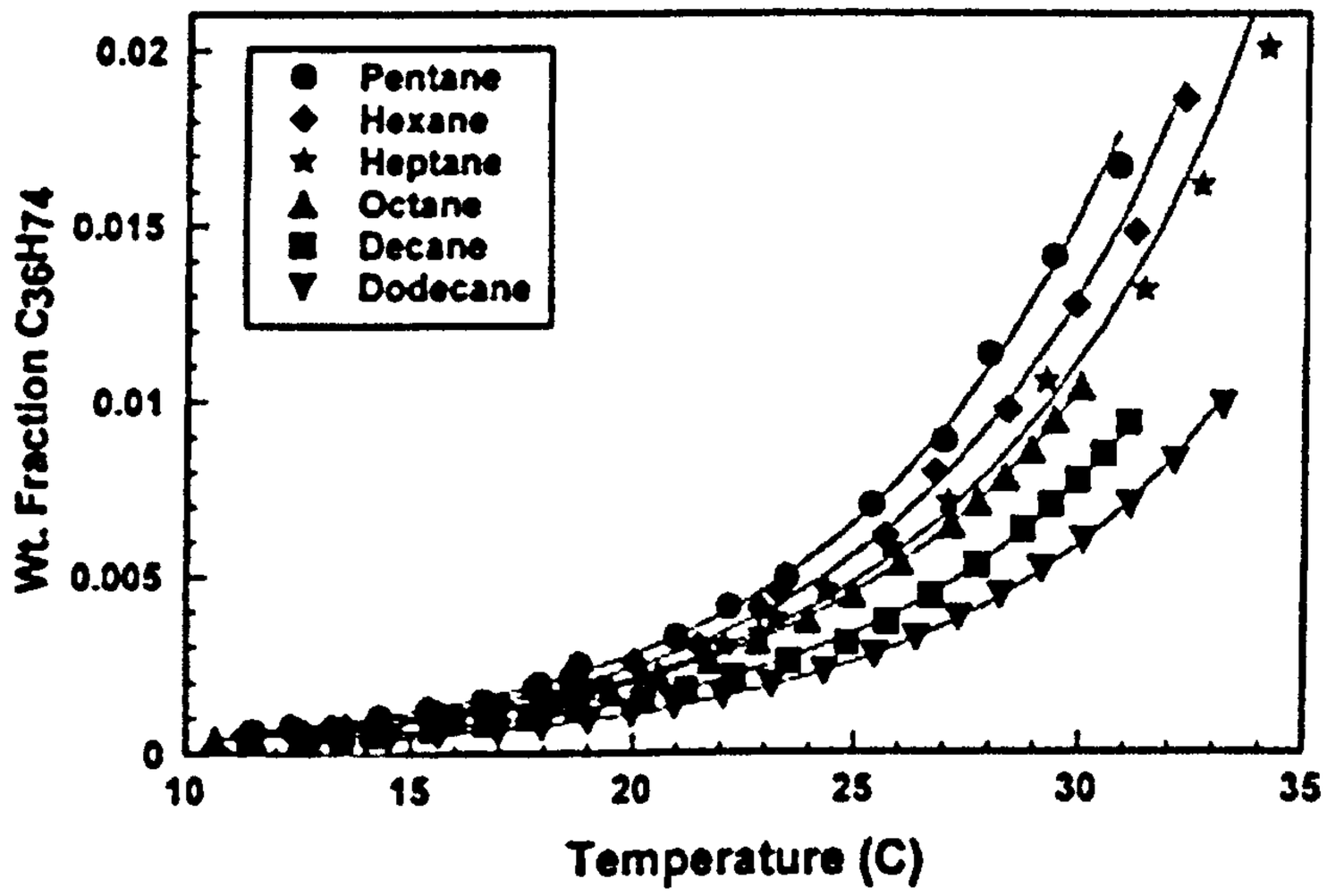

Figure 4.26 Solubility of *n*-hexatriacontane in low molecular weight *n*-alkanes (Jennings and Weispfennig, 2005)

Figure 4.27 compares the percentage depositions from the control runs with those at different frequencies at a fixed oscillation amplitude or Strouhal number (15 mm and 0.133 respectively). In Figure 4.27(a), with *n*-octane (C_8) as a solvent, the oscillatory agitation reduced the deposition by 50% as compared to the control results. The deposition curves for different frequencies seemed to be quite close to each other indicating that changing the oscillation frequency had little effect on the deposition for this solvent.

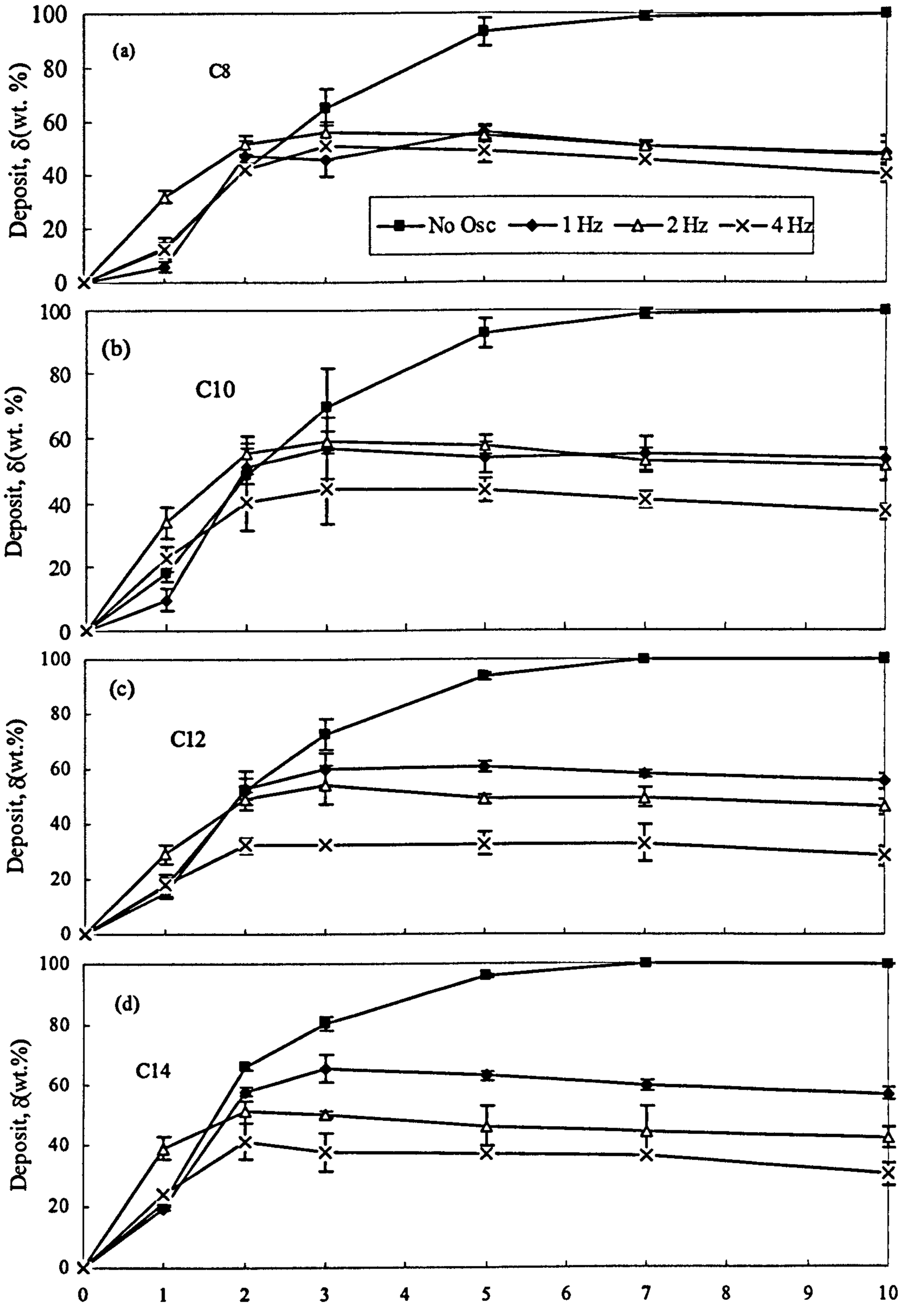

Figure 4.27 Effect of oscillation frequencies on the deposition for a range of different solvent carbon numbers (x_o = 15 mm)

For *n*-decane, C_{10}, the overall depositions were lowered to around 40 to 50% as shown in Figure 4.27(b), with the highest frequency resulted in the lowest overall deposition, while, the difference was not apparent for frequencies of 1 and 2 Hz. Similar results can be seen for C_{12} (Figure 4.27(c)) and C_{14} (Figure 4.27(d)). The general trend for all conditions in Figure 4.27 is that the higher the oscillation frequency, the lower the deposition.

Figure 4.28 shows the similar effect of oscillation amplitude on percentage deposition for the corresponding solvent types, with more reduction in the overall deposition for longer amplitudes. Comparing Figures 4.28(a)-(d), it can be observed that as the carbon number of the solvents increased from C_8 to C_{14}, the degree of reduction in the overall deposition was found to increase. For example, in Figure 4.28(a), the reduction in the overall deposition was from around 30% to 50% by the difference of 20%, whereas in Figure 4.28(d), the reduction was from around 10% to 50% by the difference of 40%.

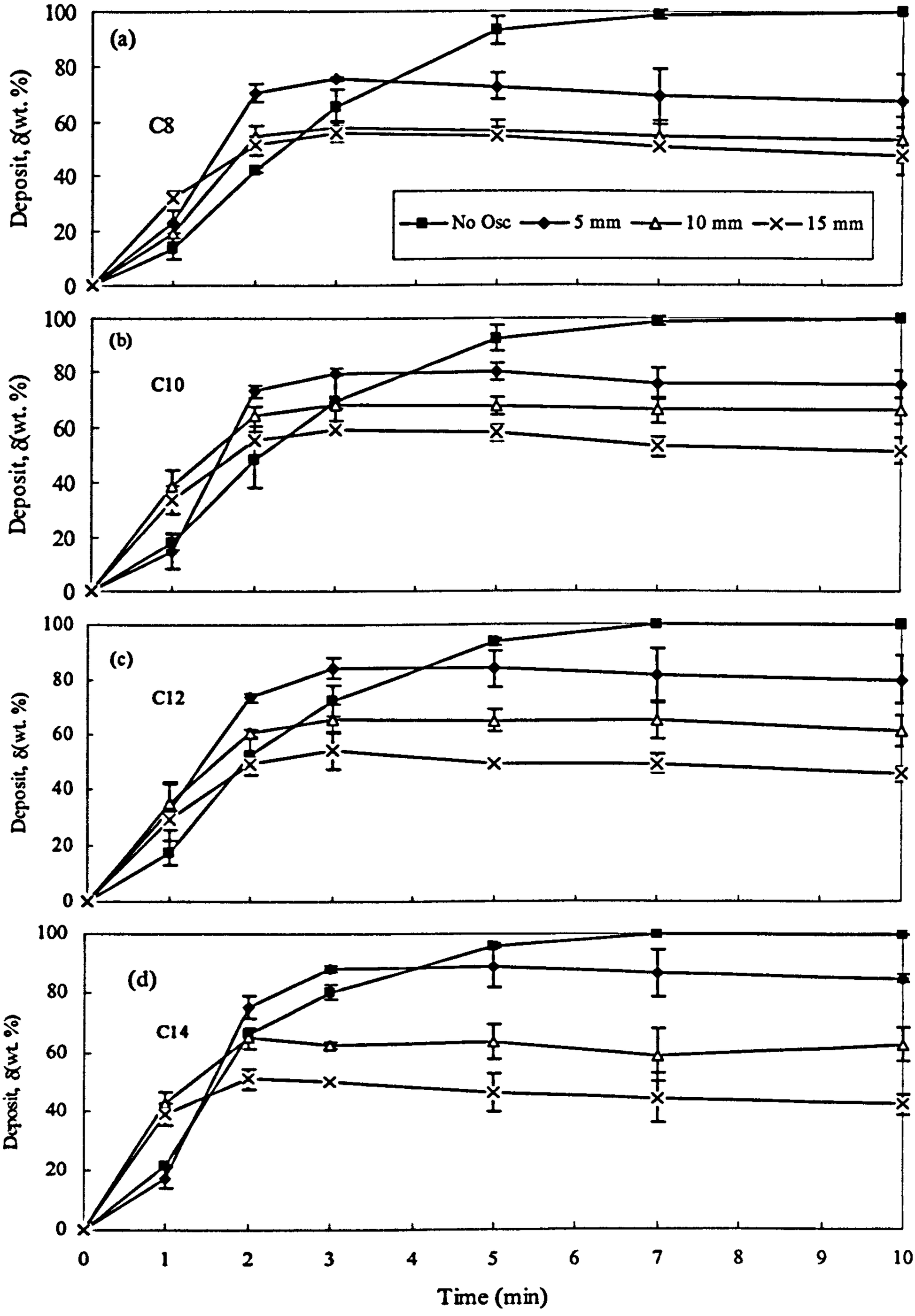

Figure 4.28 Effect of oscillation amplitude on the deposition for a range of different solvent carbon numbers ($f = 2$ Hz)

4.4.2 Avrami kinetic analysis

By examining the growth phase curves in Figures 4.27 and 4.28 using the Avrami theory, some crystallisation and deposition kinetics can be extracted as explained in Section 3.6 and Appendix A. Figures 4.29 and 4.30 plot Log[-ln(1-dr)] vs. Log(t), showing the effects of oscillation frequency and amplitude respectively. From these figures, again, good linearity can be observed for both cases, indicating the effectiveness and relevance of the Avrami methodology. The Avrami exponent (n) and the half time of deposition $t_{1/2}$ are extracted from the plots and presented in Tables 4.10 and 4.11.

In Table 4.10, it can be seen that at the static condition (0 Hz), the highest Avrami exponent value of 2.11 was observed for the solution using C_8 as the solvent whereas for other solvents, the n values were around 1.60, suggesting that at non-oscillated conditions, the crystal growth was one-dimensional (Hay, 1971). This is also confirmed with the microscopic images presented in Figures 4.31(a) – 4.34(a), which show rod or needle-like shapes for all solvent carbon numbers. As the oscillation was applied at the frequency of 1 Hz, the n values were shifted dramatically to around 3 or 4; and the bigger the carbon number of the solvent, the smaller the n values, indicating a different mechanism of crystal growth. The microscopic images taken at the oscillation frequency of 1 Hz (Figures 4.31(b)-4.34(b)) verify the multi-dimensional structures of the wax crystals obtained. For oscillation frequencies of 2 and 4 Hz, the n values were found to fall around 2 with no significant variation or trend, the growth mechanism would be similar to that of the control runs.

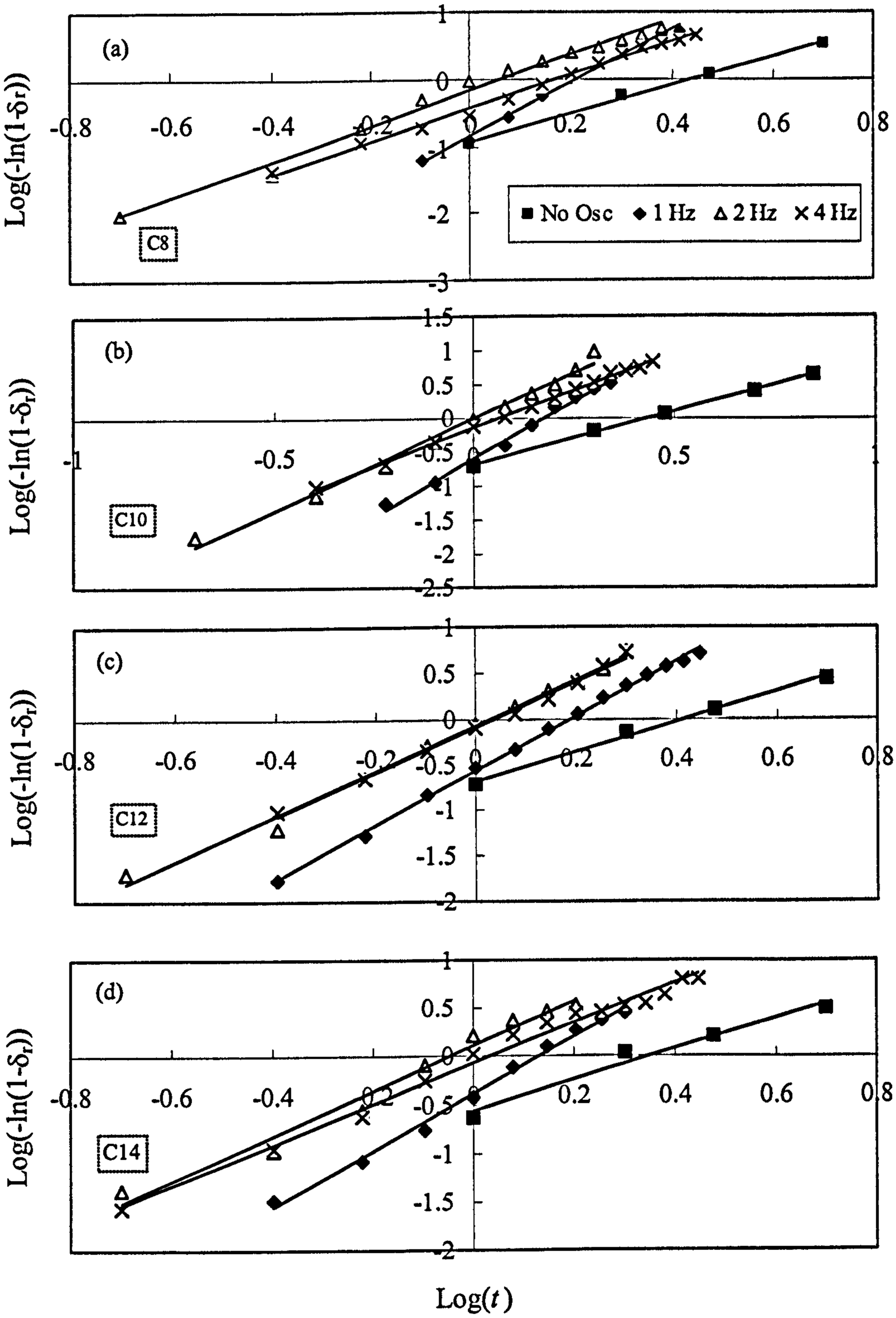

Figure 4.29 The Avrami plots for different solvent type showing effect of oscillation frequencies (x_o = 15 mm)

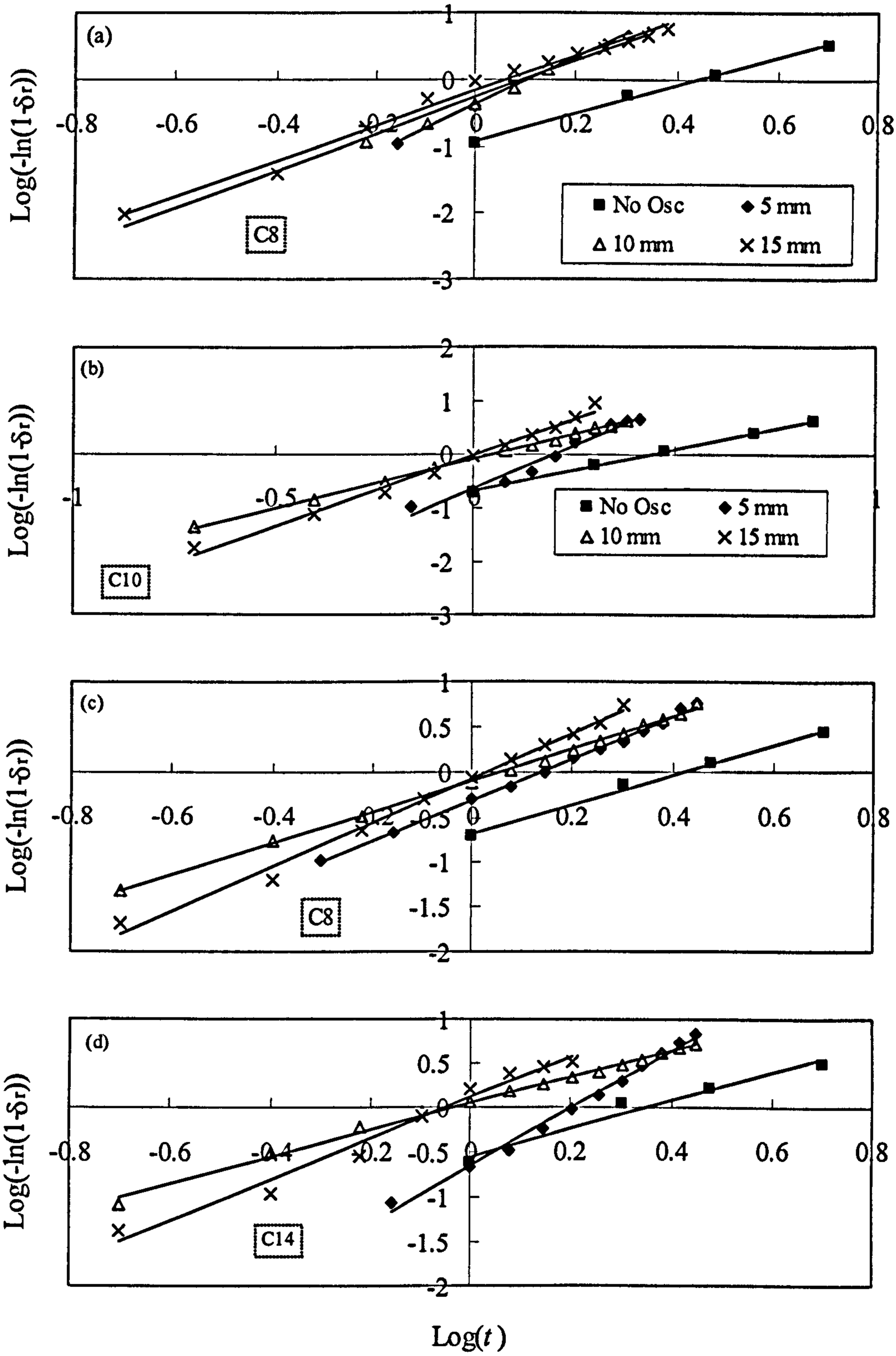

Figure 4.30 Avrami plot for different solvent carbon numbers showing effect of oscillation amplitudes (f = 2Hz)

Table 4.10 Extracted Avrami parameters for the effect of oscillation frequency (x_o = 15 mm)

Solvent	f = 0 Hz		f = 1 Hz		f = 2 Hz		f = 4 Hz	
	n	$t_{1/2}$ (min)	n	$t_{1/2}$ (min)	n	$t_{1/2}$ (min)	n	$t_{1/2}$ (min)
C_8	2.11	2.32	3.99	1.48	2.64	1.01	2.47	1.29
C_{10}	1.59	2.14	3.37	1.35	2.69	0.87	2.22	0.98
C_{12}	1.65	2.08	2.98	1.36	2.48	0.92	2.46	0.93
C_{14}	1.60	1.78	2.93	1.19	2.31	0.77	2.09	0.90

Table 4.11 Extracted Avrami parameters for the effect of oscillation amplitude (f = 2 Hz)

Solvent	x_o = 0 mm		x_o = 5 mm		x_o = 10 mm		x_o = 15 mm	
	n	$t_{1/2}$ (min)	n	$t_{1/2}$ (min)	n	$t_{1/2}$ (min)	n	$t_{1/2}$ (min)
C_8	2.11	2.32	3.59	1.15	2.78	1.10	2.64	1.01
C_{10}	1.59	2.14	3.25	1.39	1.85	0.90	2.69	0.87
C_{12}	1.65	2.08	2.31	1.17	1.77	0.92	2.48	0.92
C_{14}	1.60	1.78	3.26	1.42	1.49	0.72	2.31	0.77

The half time of deposition, $t_{1/2}$, presented in Table 4.10 can be used as a tool to evaluate the deposition rates. It can be observed that in the control experiments with no oscillation, the larger the carbon number of the solvents, the smaller the $t_{1/2}$, indicating higher deposition rates. Therefore, it can be deduced that wax deposits were more rapidly precipitated in the solvents with higher carbon numbers. A general decreasing trend can also be seen for the results obtained from the experiments with oscillations, with the exception of 4 Hz.

Table 4.11 shows the data for the Avrami exponent, n, and the half time of deposition, $t_{1/2}$, for the effect of oscillation amplitude where experiments were conducted at different amplitudes with a fixed oscillation frequency of 2 Hz. Analysing the n values obtained, we can see that there is again a major shift of the values from the static condition to the oscillated condition at 5 mm. However the values fluctuate when the amplitudes increase from 5 to 10 and 15 mm with no apparent trend showing that increasing the amplitudes has less effect on the types of crystals produced. As for the half time of deposition, generally, increasing the oscillation amplitude decreased $t_{1/2}$ for all solvent types used.

(a) C_8 with no oscillation

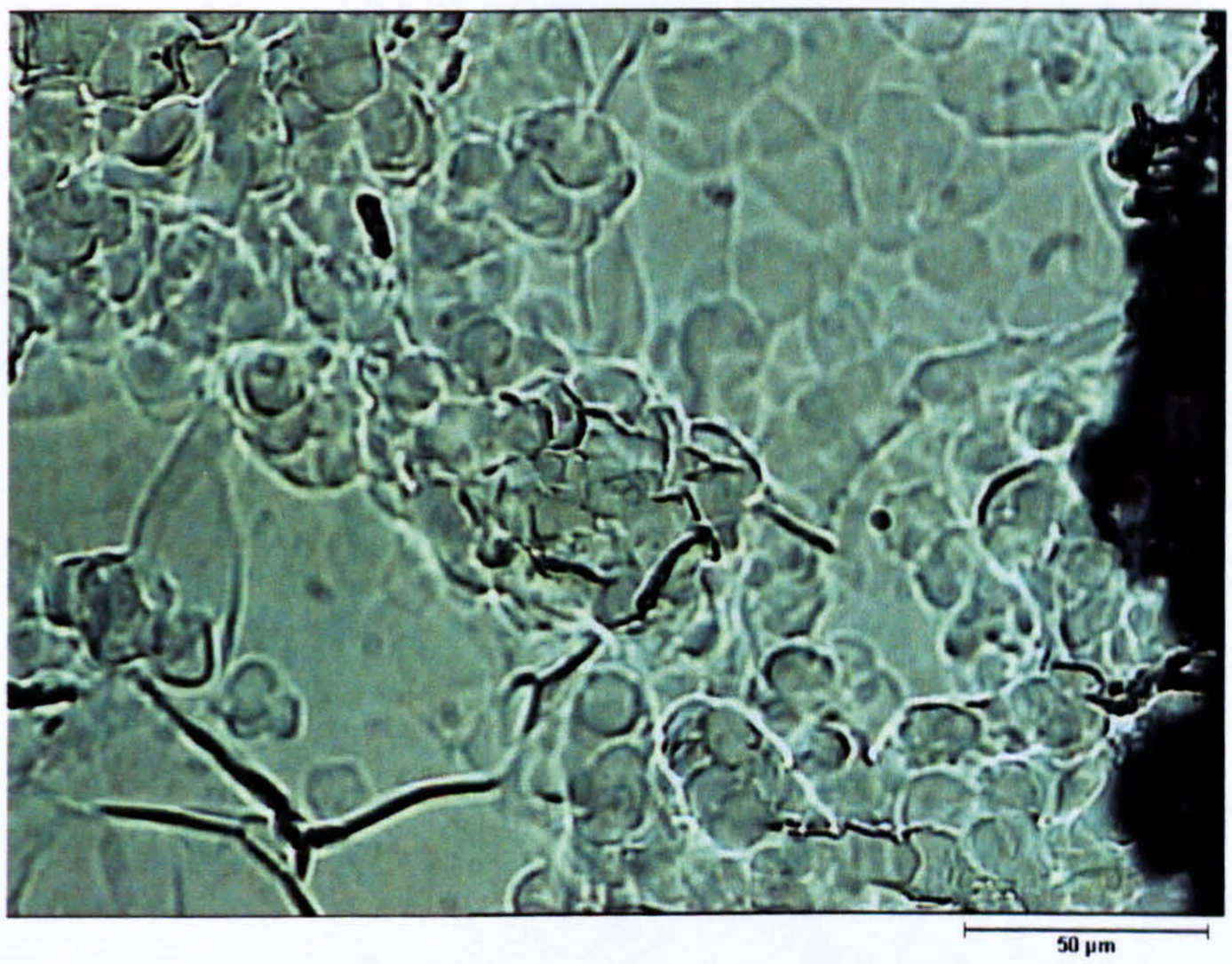

(b) C_8 with oscillation (x_o = 15 mm, f = 1 Hz)

Figure 4.31 Microscopy images for wax in C_8 samples (magnification = 60 x)

(a) C_{10} with no oscillation

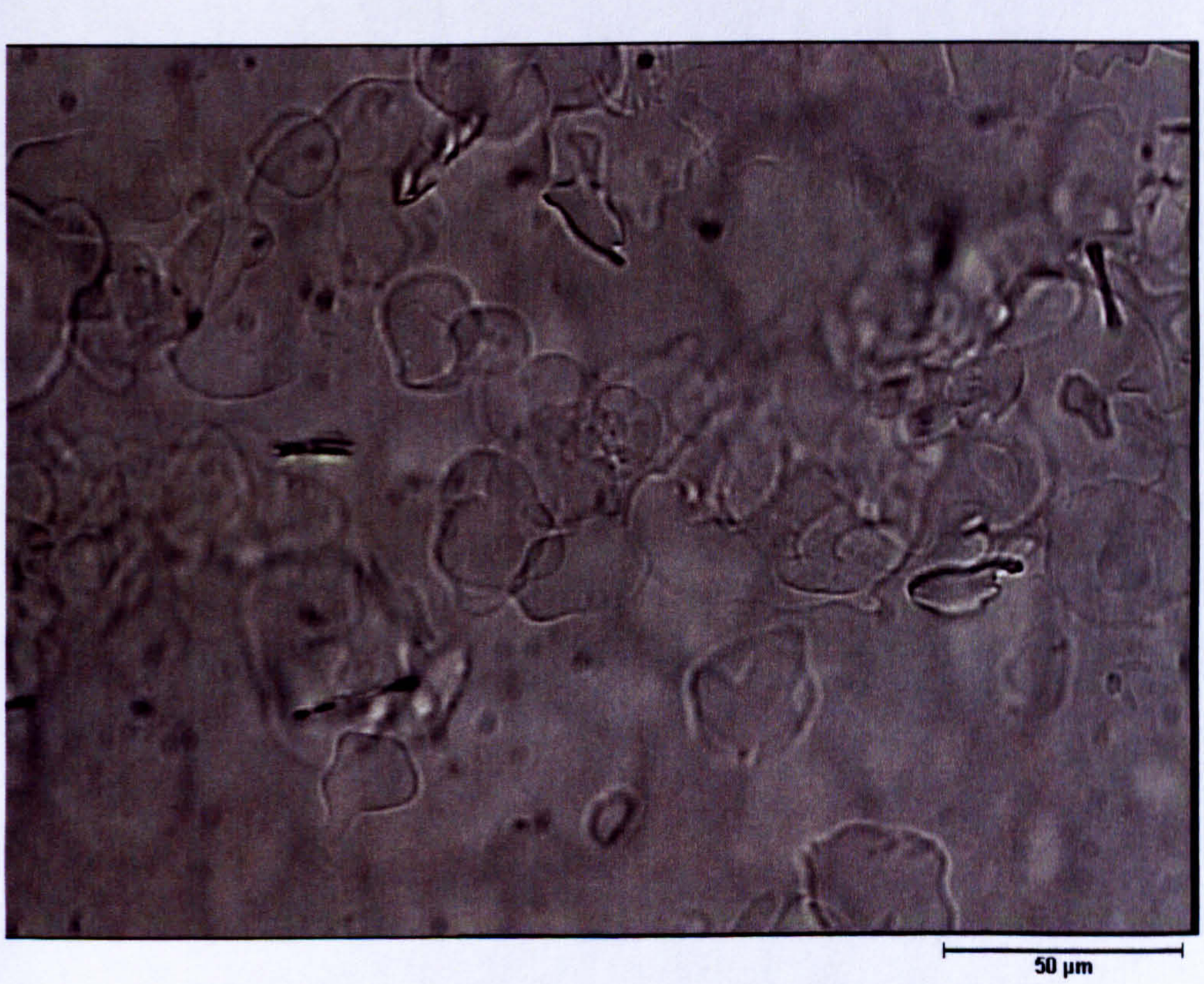

(b) C_{10} with oscillation (x_o = 15 mm, f = 1 Hz)

Figure 4.32 Microscopy images for wax in C_{10} samples (magnification = 60 x)

(a) C_{12} with no oscillation

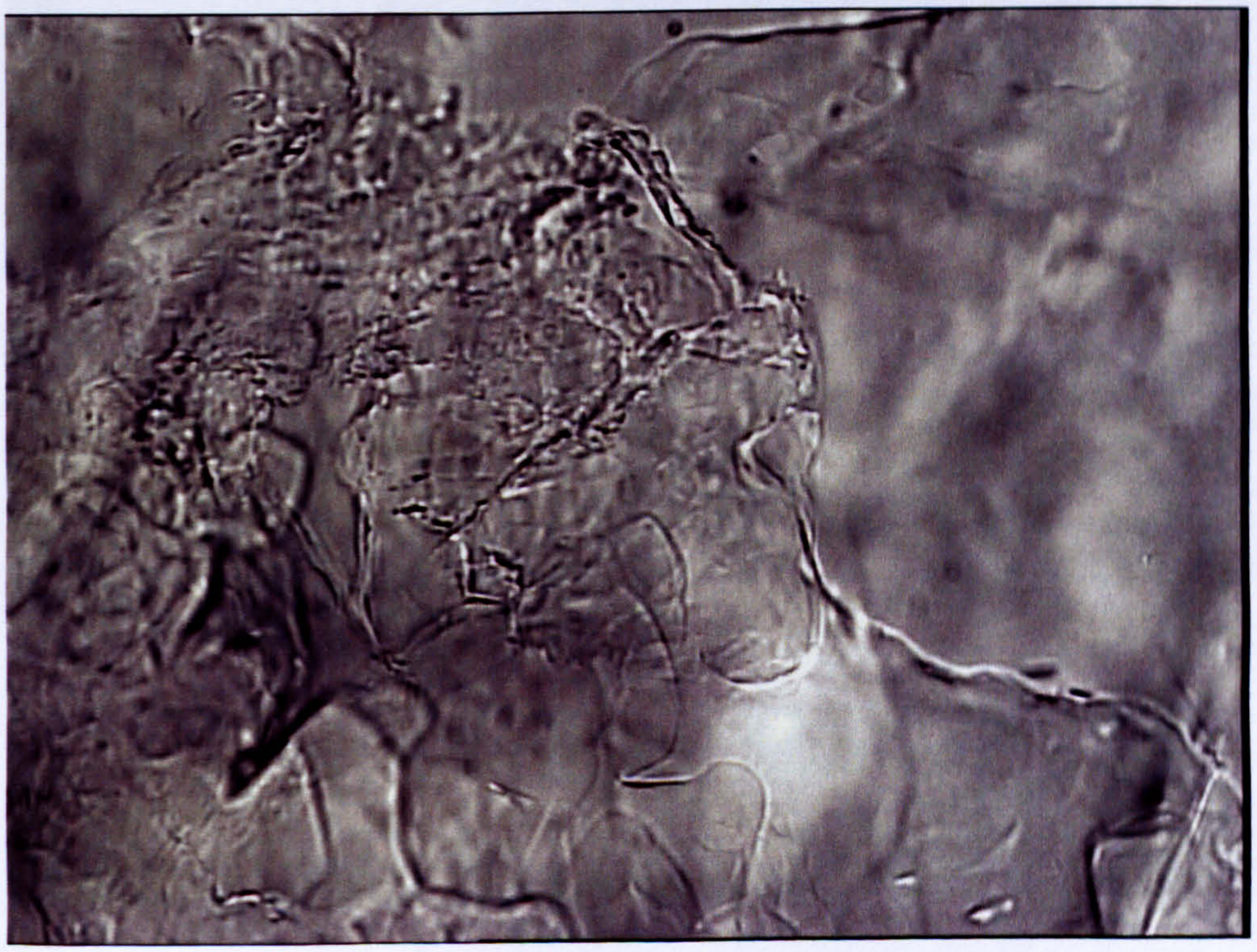

(b) C_{12} with oscillation (x_o = 15 mm, f = 1 Hz)

Figure 4.33 Microscopy images for wax in C_{12} samples (magnification = 60 x)

(a) C_{14} with no oscillation

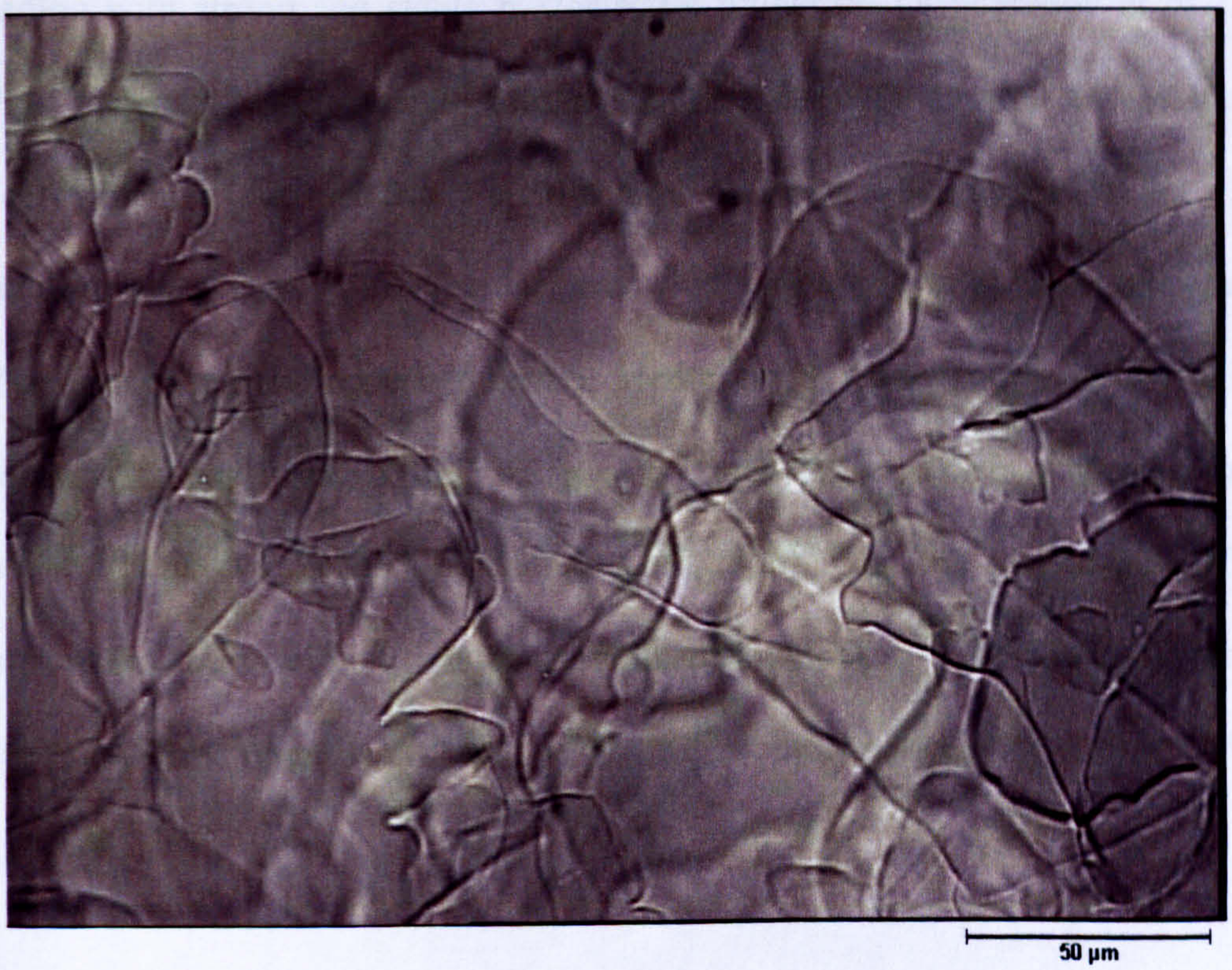

(b) C_{14} with oscillation (x_o = 15 mm, f = 1 Hz)

Figure 4.34 Microscopy images for wax in C_{14} samples (magnification = 60 x)

4.5 Effect of baffle material and structure

This section explains the work done in the investigation of the effect of baffle material and structure. Two baffle structures were tested; baffles with hemispherical dimples and smooth surfaces baffles with no dimple. Three types of baffles materials were examined, *i.e.* stainless steel (abbreviated as SS for baffles without dimple), polyvinylidene difluoride (abbreviated as PVDF) and polytetrafluoroethylene (abbreviated as PTFE). Stainless steel baffles with dimples is abbreviated as SSD whereas for PVDF and PTFE, the abbreviations are PVDFD and PTFED respectively.

PVDF is a semicrystalline, highly non-reactive thermoplastic fluoropolymer (Siripurapu *et al.*, 2002) and considered as a 'smart' material that can detect changes in the loading with strong and stable piezoelectric properties (Vinogradov *et al.*, 2004). PVDF is generally used in applications requiring strength as well as resistance to chemicals such as in external architectural coatings (Schneider *et al.*, 2001). Polytetrafluoroethylene (PTFE) is a synthetic fluoropolymer, well known commercially as Teflon, has extremely low coefficient of friction and is used as a non-stick coating for cookware. It is non-reactive, and so is often used in containers and pipework for reactive and corrosive chemicals (Cheng *et al.*, 2003). The low coefficient of friction results from the ability of its extended chain linear molecules, $-(CF_2-CF_2)_n-$, to form low shear strength films upon its surface and mating counter-faces during sliding (Khedkar *et al.*, 2002).

It is the intention of this study to investigate the effect of these baffle materials on the deposition and also on the effect of having dimple structures on the baffle surfaces, as dimples promote local flow separation. The dimple size was 4.0 mm in diameter and each baffle contains 16 dimples on the bottom and top surfaces. Figure 4.35 shows photographs of the baffles used. In these experiments the solvent used was diesel and two paraffin wax contents were tested, *i.e.* 10% and 20%. The hot initial and cold final temperatures were set at 50 and 10 °C respectively with cooling water flowed at 0.87 l/min (pump speed of 100 rpm). The oscillations were conducted at an amplitude of 10 mm and frequency of 2 Hz for all runs. The total experiment time duration was fixed at 10 minutes and the deposition measurements were carried out at similar time intervals as previous experiments. As usual, results and analyses are presented in terms of deposition and the Avrami kinetic analyses.

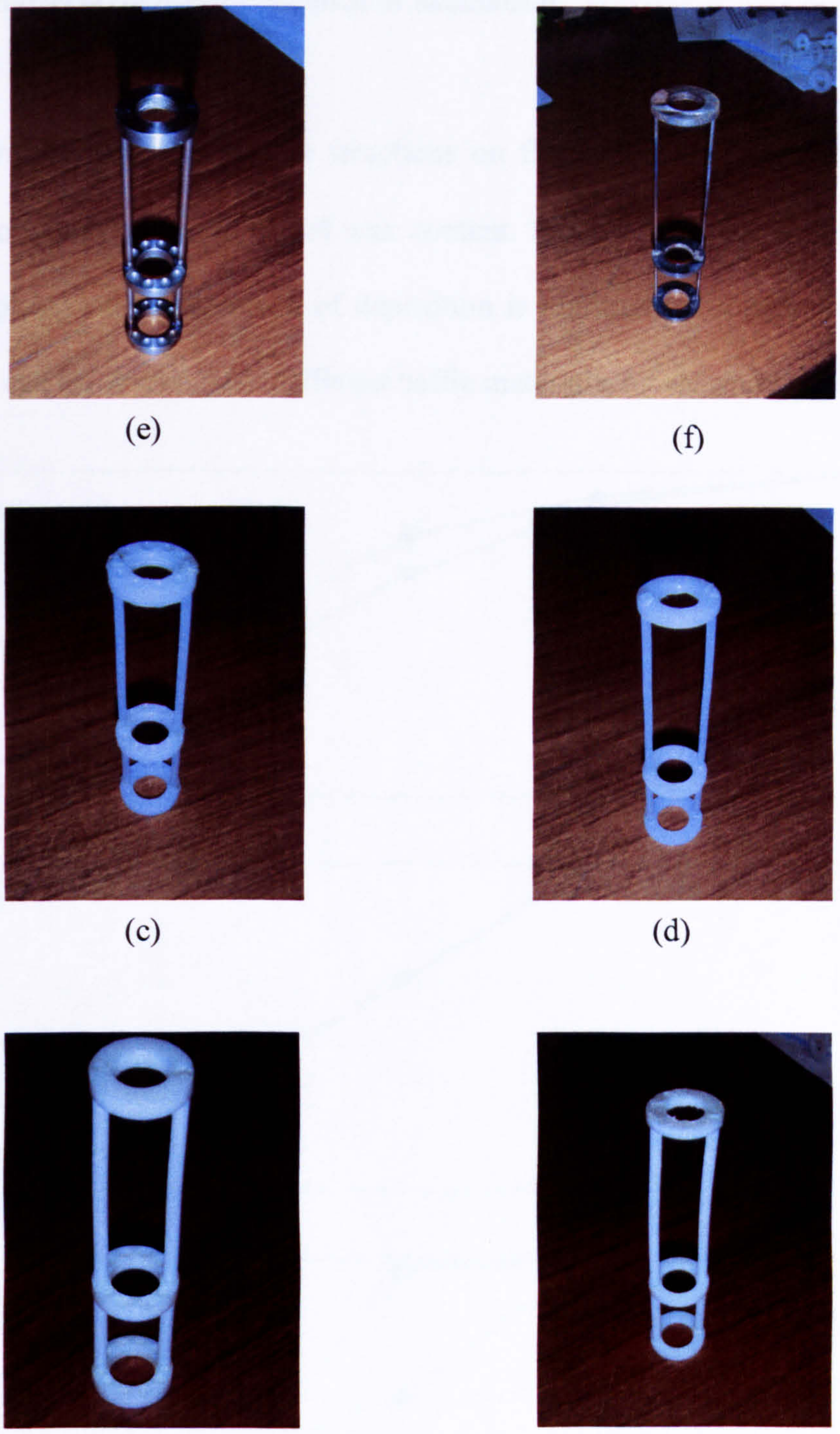

(e) (f)

(c) (d)

(a) (b)

Figure 4.35 Photographs of baffles used in the study. (a) PTFED, (b) PTFE, (c) PVDFD, (d) PVDF, (e) SSD, (f) SS

4.5.1 Effect of baffle structure in absence of oscillation

Figure 4.36 shows the effect of dimple structures on the deposition for experiments conducted with no oscillation and 10% of wax content. From the graphs, it seems that the effect of dimples on the percentage of deposition is minimal, with odd scattering. Similar outcomes can be observed for different baffle materials, as shown in Figure 4.37.

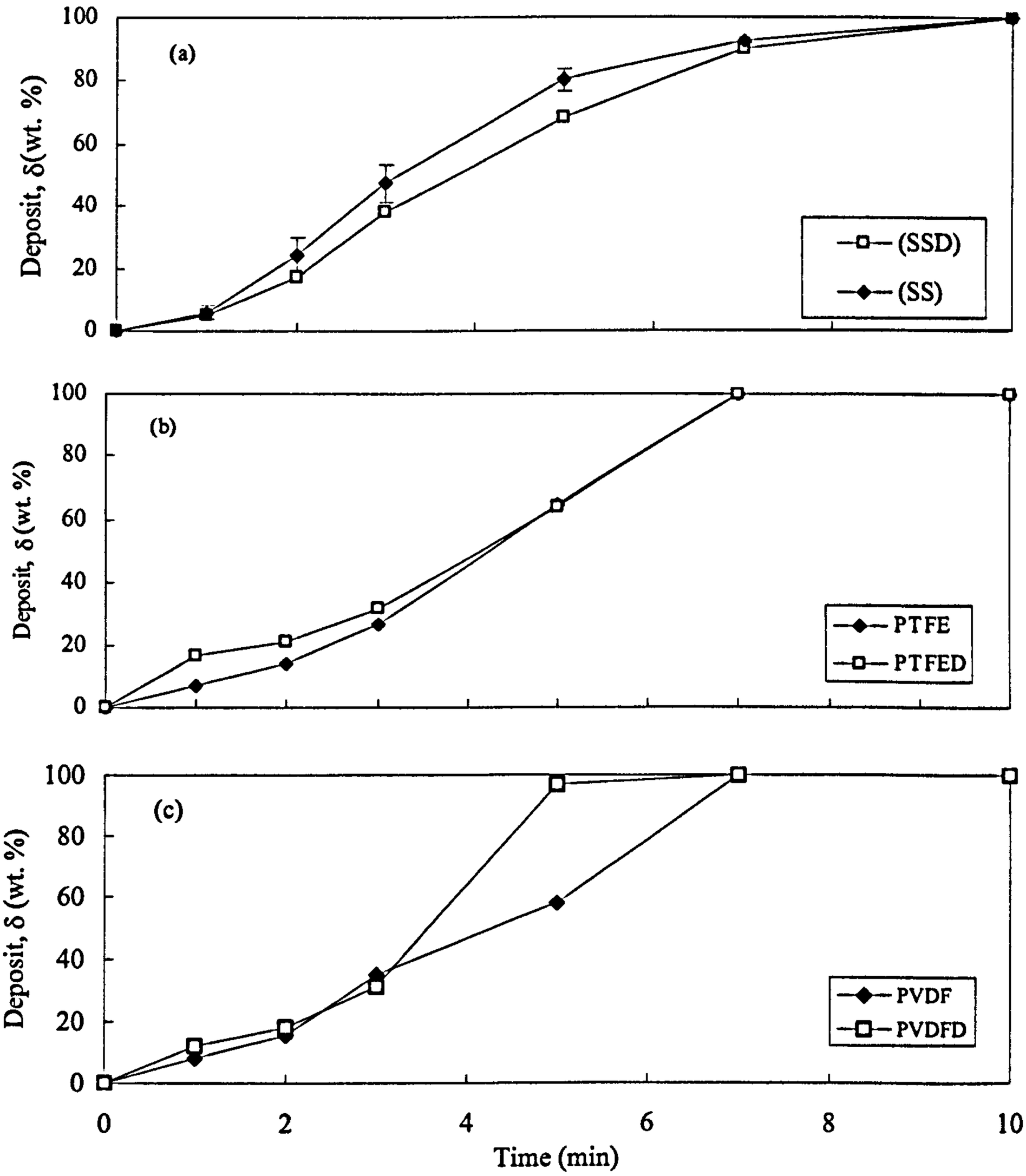

Figure 4.36 Effect of dimples on the deposition in absence of oscillation (wax content = 10 %)

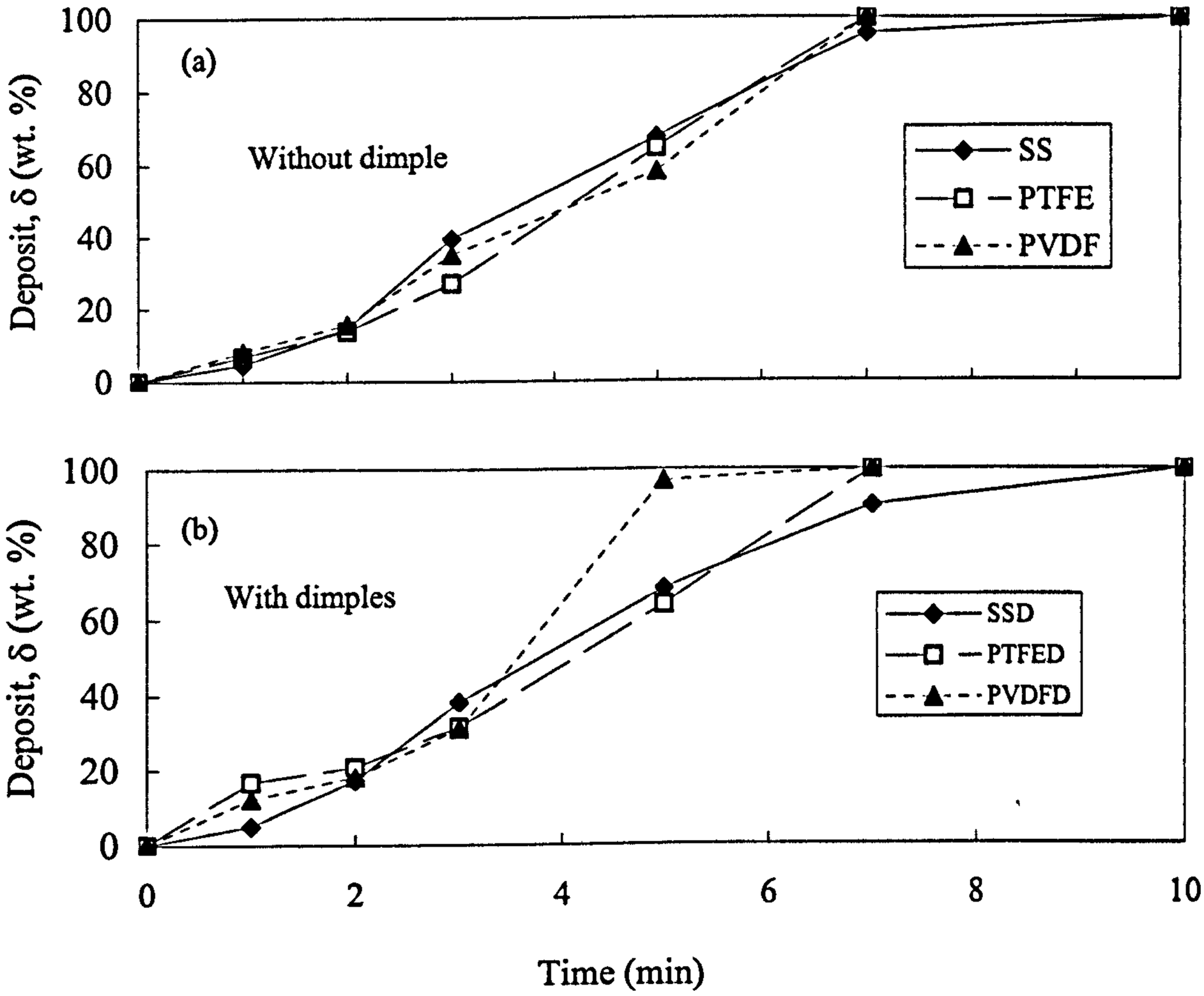

Figure 4.37 Effect of baffle materials on the deposition without oscillation

4.5.2 Deposition with oscillation

When baffle oscillation is present, the effects of baffle structure (with and without dimples) and baffle materials (SS, PVDF and PTFE) on the deposition are again insignificant, see Figures 4.38 and 4.39.

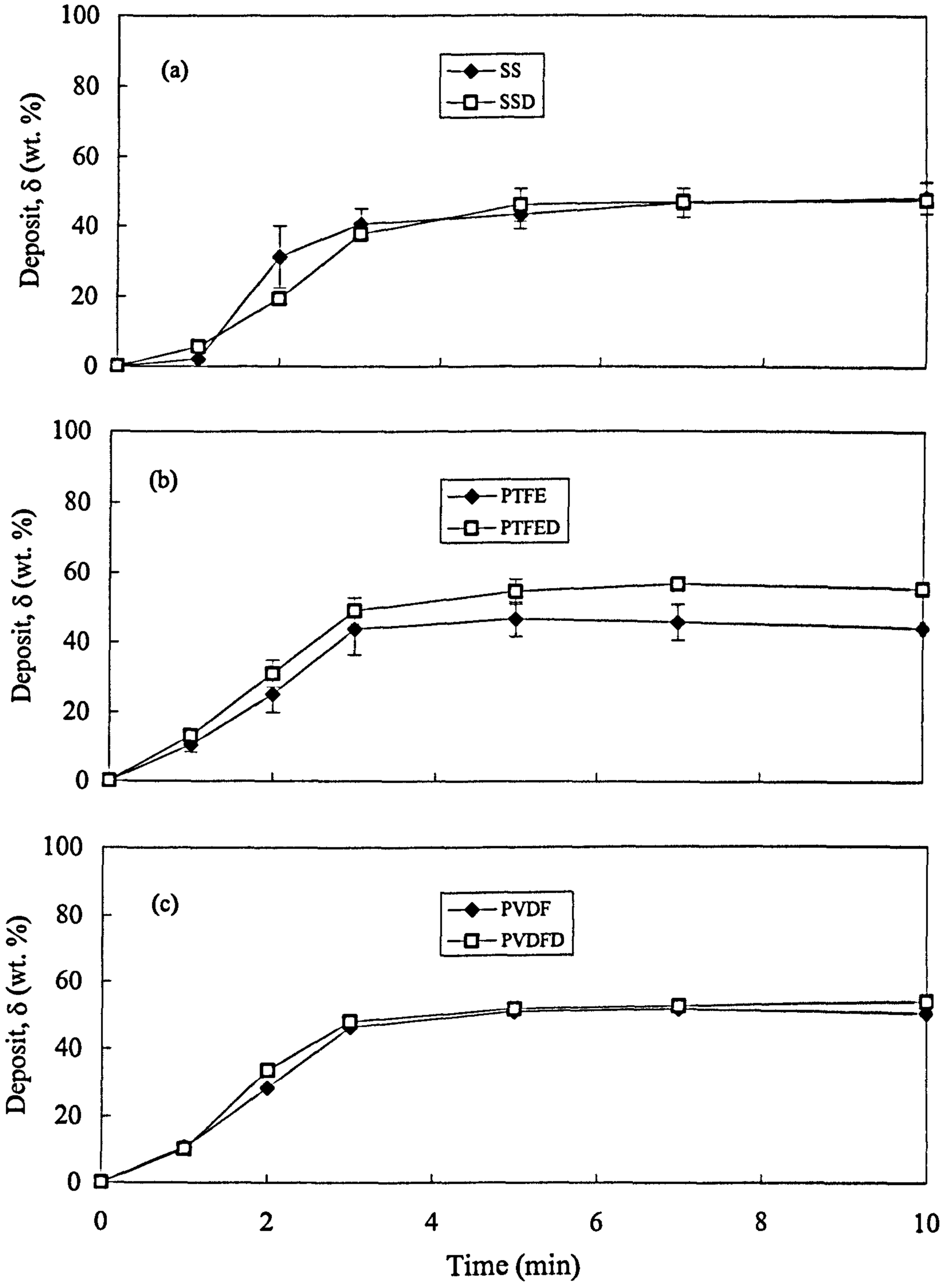

Figure 4.38 Effect of baffle structure on the deposition for each material tested (wax content = 10%, f = 2 Hz, x_o = 10 mm)

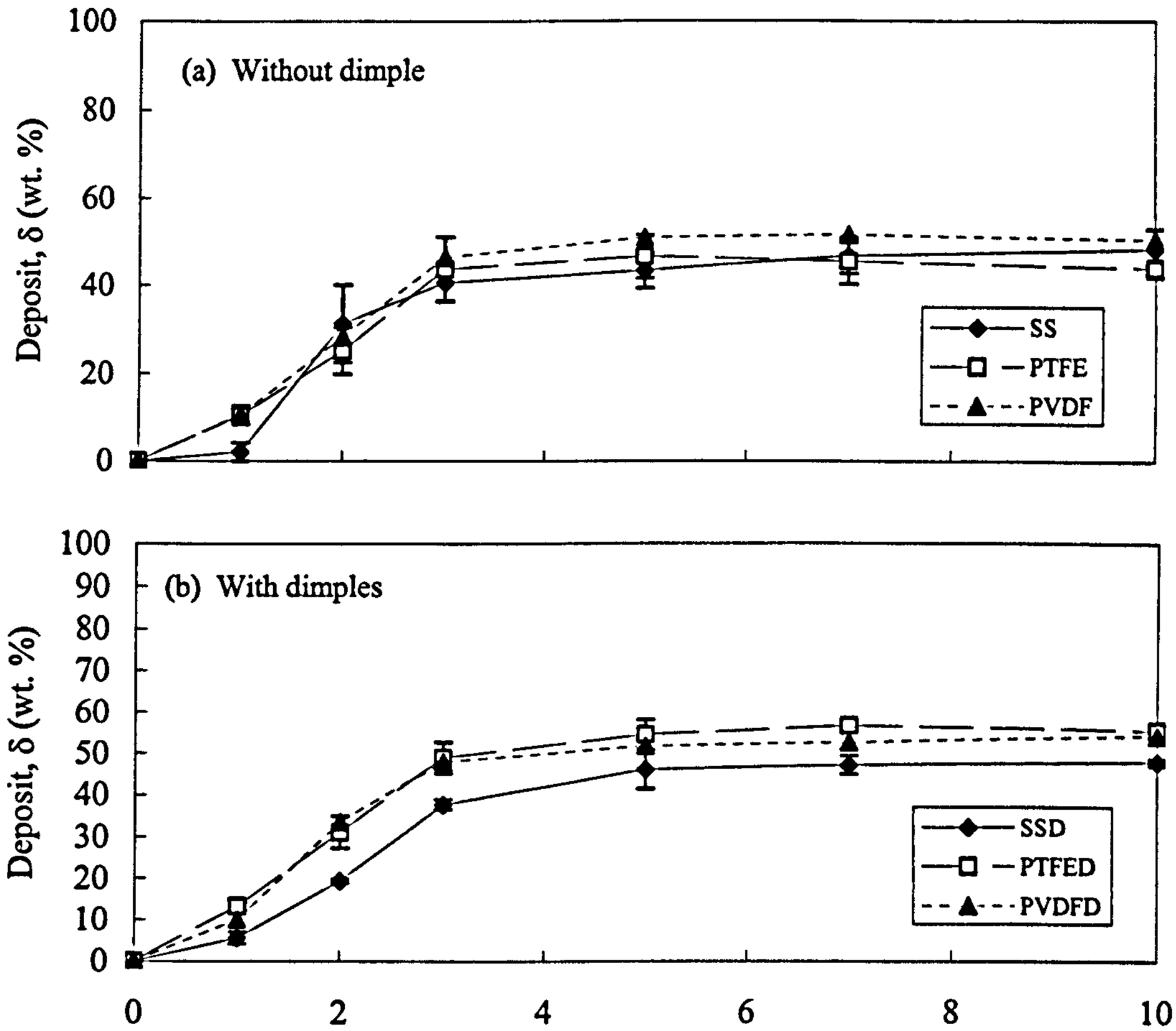

Figure 4.39 Effect of baffle material on the deposition with oscillation (wax content = 10%, f = 2 Hz, x_o = 10 mm)

4.5.3 Wax content of 20%

Experiments were also conducted at 20% wax concentration in order to verify the effects of baffle materials and structure on the deposition. Figure 4.40 shows the effect of dimples on the deposition without oscillation, while Figure 4.41 shows the effect of baffle materials on the deposition in the absence of oscillation. From the graphs it can be seen that no significant effect can be observed on the deposition.

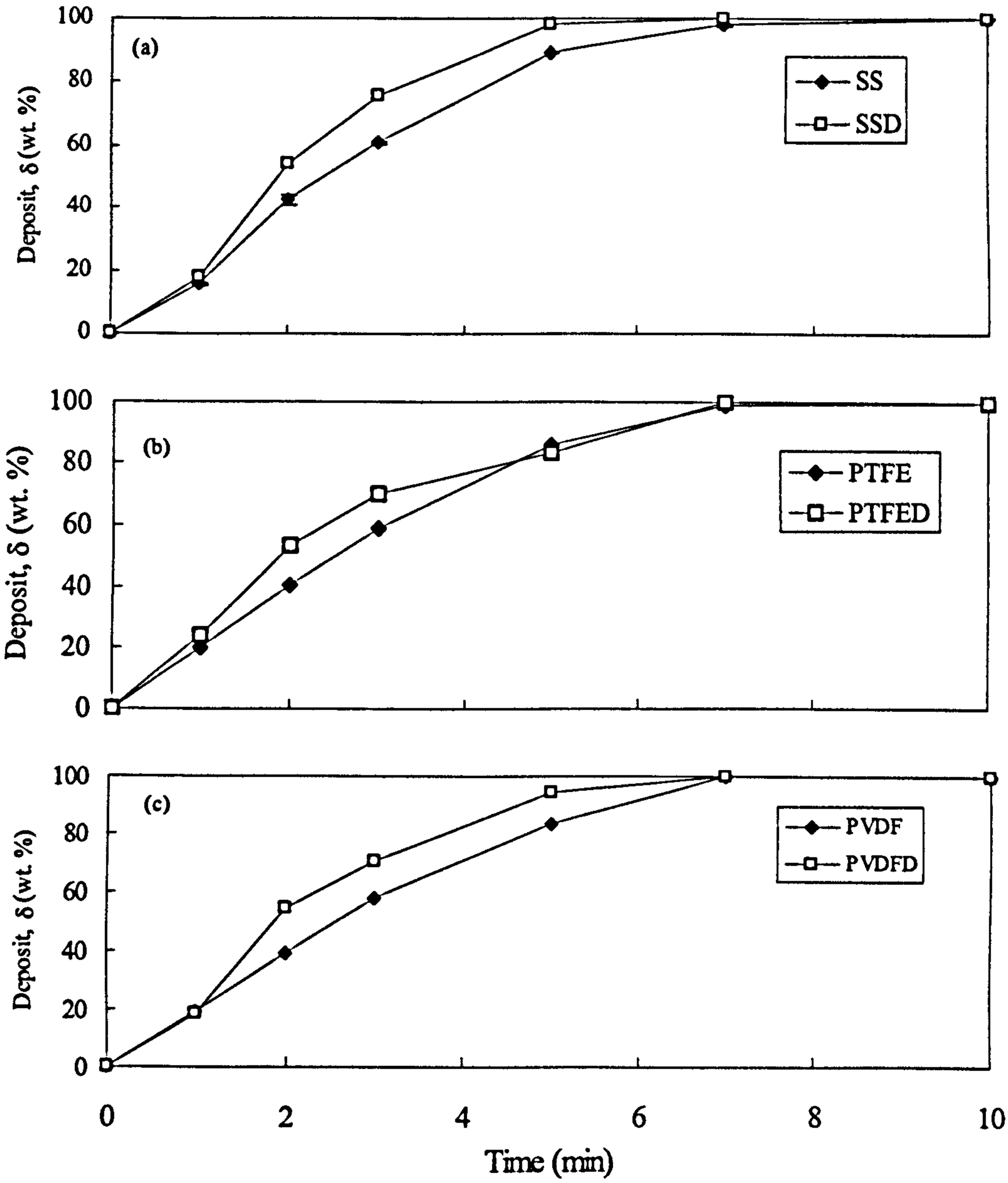

Figure 4.40 Effect of dimples on the deposition in absence of oscillation (wax content = 20 %)

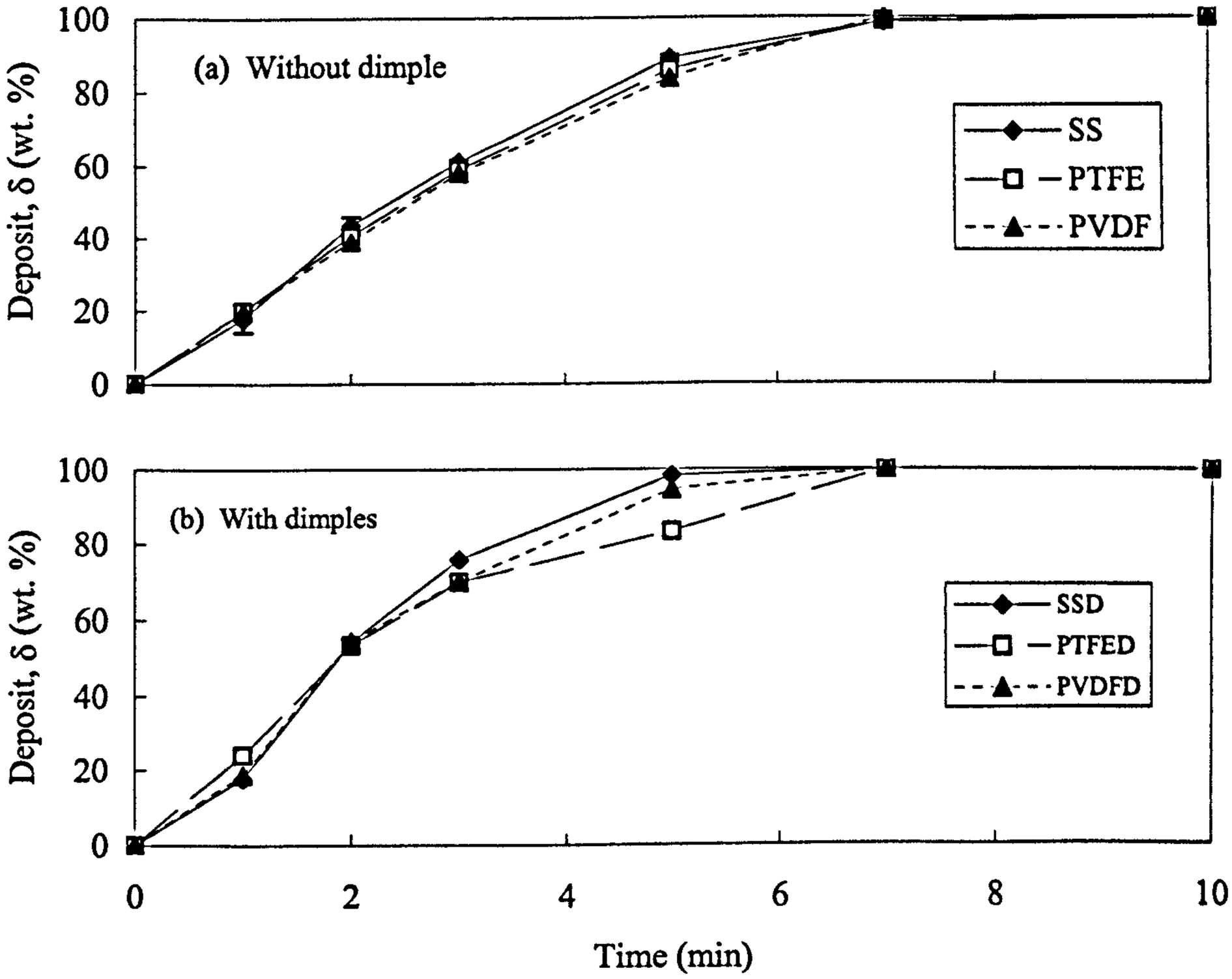

Figure 4.41 Effect of baffle materials on the deposition without oscillation (wax content = 20%)

With the presence of oscillation, once again no apparent difference in the deposition was observed for baffle structures (Figure 4.42) and baffle materials (Figure 4.43). Consequently, there is no kinetic study on these data.

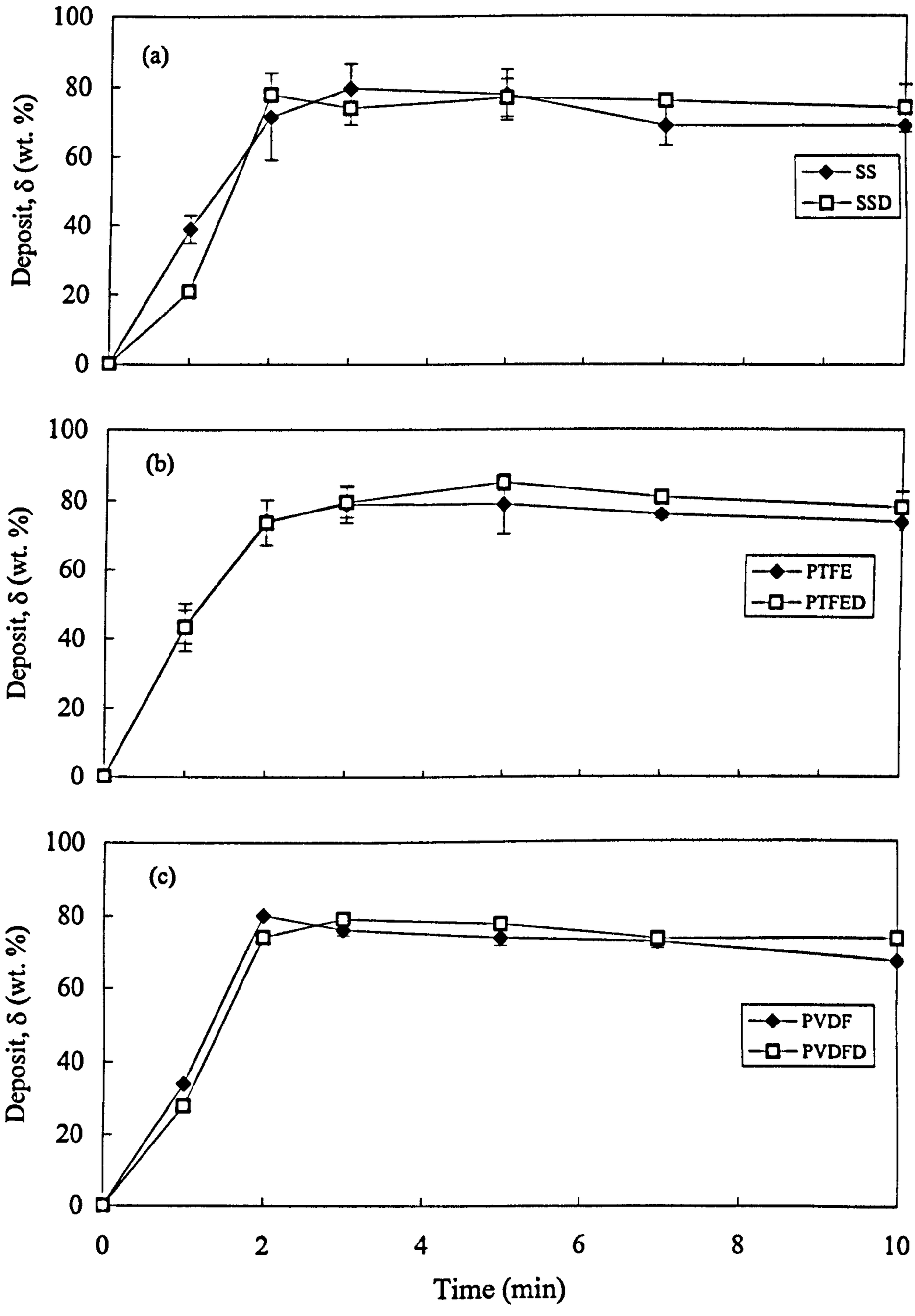

Figure 4.42 Effect of baffle structures on the deposition (wax content = 20%, f = 2 Hz, x_o = 10 mm)

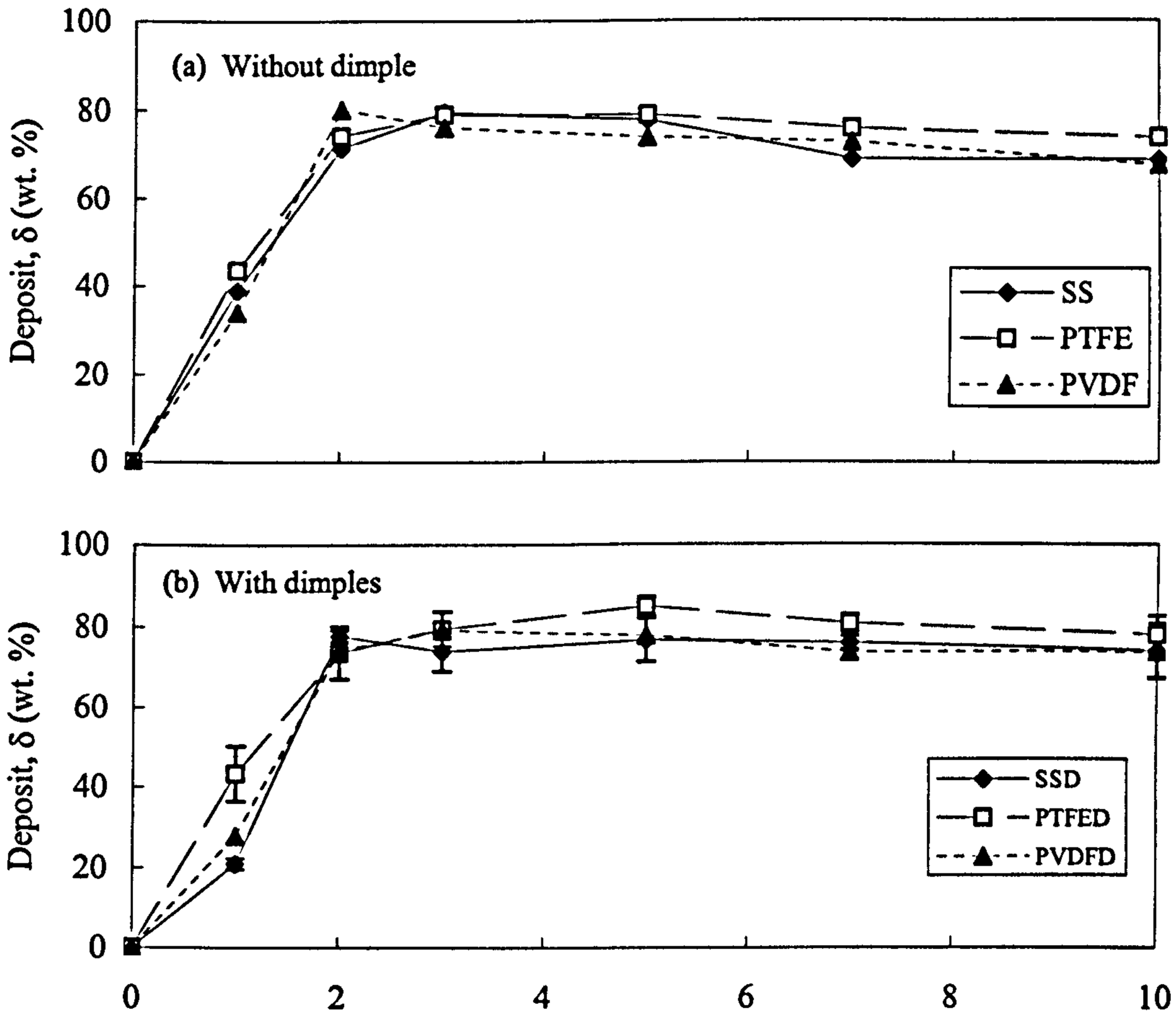

Figure 4.43 Effect of baffle materials on the deposition (wax content = 20%, f = 2 Hz, x_o = 10 mm)

CHAPTER 5

CONCLUSIONS AND FUTURE WORK

5.1 Conclusions

This thesis reports the experimental investigation into the deposition of wax in oscillatory baffled column. The major conclusions of this work are summarised as follows:

- ☐ On the study of the effect of OBC's parameters, it was found that increasing the oscillation frequency and amplitude reduced the overall deposition; baffle oscillation altered the type of wax crystal from needle type to clustered plate-like shapes; and accelerated the rates of deposition.

- ☐ On the effect of wax and oil mixture volume, it was observed that increasing the volume of the sample reduced the deposition, increased n and $t_{1/2}$ values, hence reduced the deposition rates per unit volume.

- ☐ The study on the effect of paraffin wax content revealed that increasing the wax content increased the deposition, reduced n values and caused higher crystallisation rates.

- ☐ In the effect of solvent carbon number, it was found that the higher the carbon numbers, the more wax deposited, reduced n and $t_{1/2}$.

- ☐ Lastly on the study of baffles material and structure, it can be deduced that using different baffle materials and structures has no significant effect on the deposition.

5.2 Future work

The present study has examined some of the parameters on the deposition in an OBC. During the study new issues arose and some areas required further in depth study. These form the basis of the recommendations for future work.

- ☐ Further study can be conducted in a continuous system with oscillatory flow of the fluids.

- ☐ Experiments can be carried out using more realistic oils rather than model oils.

- ☐ Experiments can be carried out using other viscous fluid such as vegetable oil and dairy products, to investigate the suitability of oscillatory flow to solve fluid transport problems.

- ☐ Investigation on other parameters such as the cooling rates using appropriate apparatus with good control of temperature gradient.

- In order to have better data acquisition especially during the growth phase of deposition of crystallisation, another online method of analysis of the deposition should be sought. One example is using heat transfer method as proposed by Cordoba and Schall (2001a).

- Investigation on the effect of additive and anti-wax agents, and develop a rapid screening test for new control chemicals.

Appendix A: Calculation of the Avrami parameters

This example calculation is based on the data obtained from the experiments conducted without baffle oscillation with paraffin wax content of 10% in diesel as the solvent. The deposition curve is shown in Figure A1. By plotting the left side in equation (7) *i.e.* Log[-ln(1-δ_t)], vs. Log(t), the slope of the straight line n (the Avrami exponent) and the intersection K (the kinetic coefficient) can be obtained. The relative deposition, δ_t, is calculated from equation (6), *i.e.* $\delta_r = \frac{\delta_t - \delta_0}{\delta_\infty - \delta_0}$, in this case the initial deposition, $\delta_0 = 0$ and final deposition, $\delta_\infty = 1$ (100% deposition). Tabulated data is shown in Table A1 and the plot of Log[-ln(1-δ_t)] vs. Log(t) is shown in Figure A1.

Table A1 Tabulated data for the calculation of the Avrami parameters

t (min)	Log(t)	δ_t	1-δ_t	Log(-ln(1-δ_t))
0	∞	0.0000	1.0000	∞
1	0.0000	8.2432	0.9176	-1.0654
2	0.3010	29.6237	0.7038	-0.4543
3	0.4771	50.9865	0.4901	-0.1469
5	0.6990	76.2260	0.2377	0.1573
7	0.8451	93.0234	0.0698	0.4253
10	1.0000	100.000	0.0000	∞

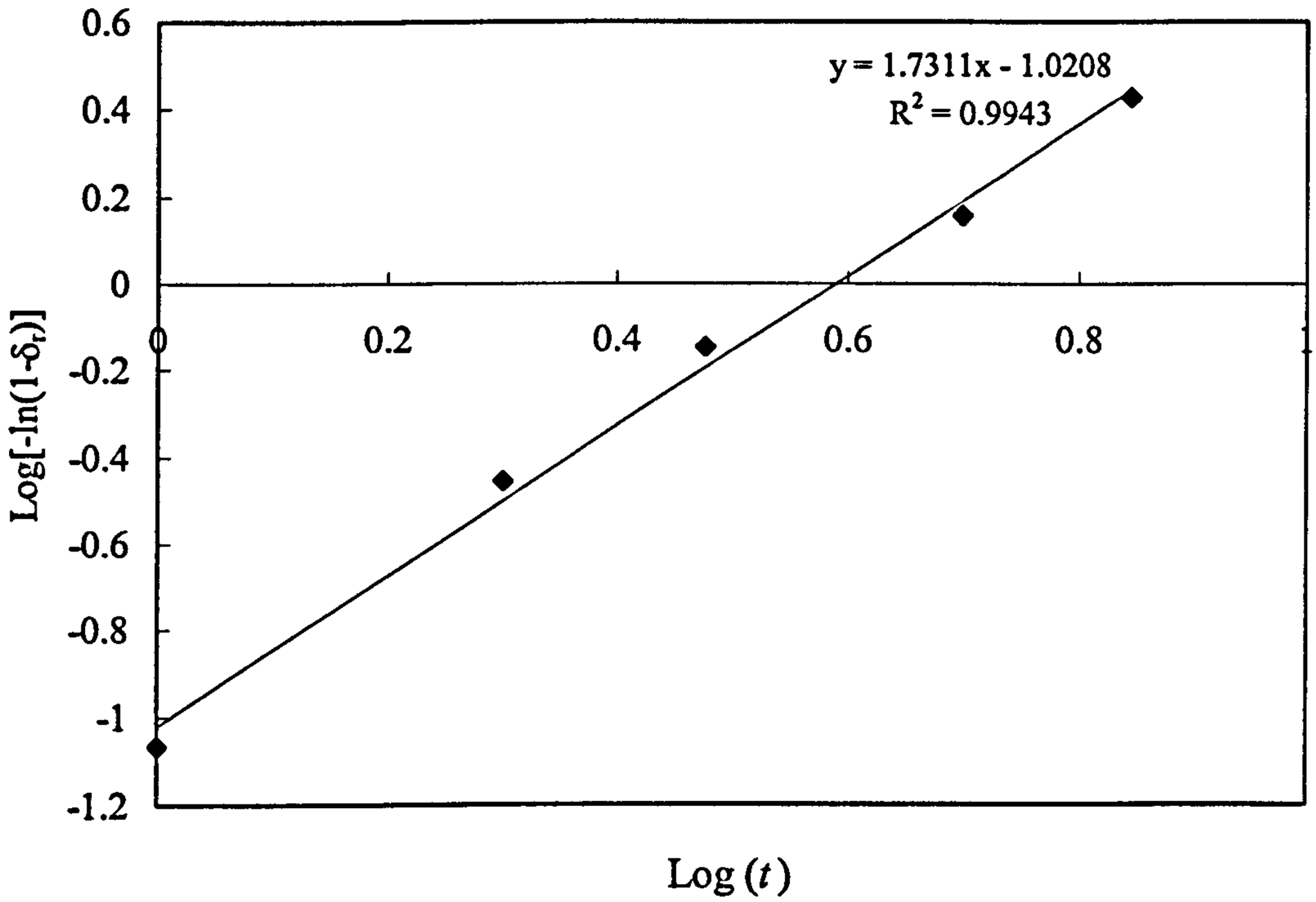

Figure A1 Plot of Log[-Ln(1-δ_t)] vs. Log(t) to obtain the Avrami parameters

From the plot, the equation of the linear trend line obtained is $y = 1.7311x - 1.0208$, from which the Avrami exponent, n, is 1.7311 and the logarithmic kinetic coefficient, Log K, is -1.0208 ($K = 0.0953$). The deposition half-time ($t_{1/2}$) is defined as the time at which the degree of deposition (δ) is 50% of the maximum achievable deposition, and can be calculated from the measured kinetics parameters using equation (3.7), *i.e.*

$$t_{1/2} = \left(\frac{\ln 2}{K}\right)^{1/n} = \left(\frac{\ln 2}{0.0953}\right)^{1/1.311} = 3.15 \text{ min.}$$

References

Al-Marzouqi, A. H., Zekri, A.Y., Jobe, B. and Dowaidar, A. (2007). Supercritical Fluid Extraction for the Determination of Optimum Oil Recovery Conditions. *Journal of Petroleum Science and Engineering*. **55**. 37-47.

Avrami, M. (1939). Kinetics of Phase Change I. General Theory. *Journal of Chemical Physics*. **7**. 1103-1112.

Avrami, M. (1940). Kinetics of Phase Change II. Transformation-Time Relations for Random Distribution of Nuclei. *Journal of Chemical Physics*. **8**. 212-224.

Baird, M.H.I. and Garstang, J.H. (1972). Gas Absorption in a Pulsed Bubble Column, *Chem Eng Sci*. **27**. 823–833.

Baird, M.H.I. and Rama Rao, N.V.R. (2002). Gas–Liquid Mass Transfer in a 15 cm Diameter Reciprocating Plate Column. Presented at United Engineering Foundation Conference on Process Innovation and Process Intensification, Edinburgh, Scotland, 8–13 September.

Baird, M.H.I., Rama Rao, N.V.R. and Latto, B. (1992). Liquid–Liquid Extraction Using Vortex Rings in a Batch Cell. *Trans IChemE, Part A, Chem Eng Res Des*. **70**(A4). 323–332.

Bellhouse, B.J., Bellhouse, F.H., Curl, C.M., MacMillan, T.I., Gunning, A.J., Spratt, E.H., MacMurray, S.B. and Nelems, J.M. (1973). A High Efficiency Membrane Oxygenator and Pulsatile Pumping System, and Its Application to Animal Trials. *Trans Am Soc Artif Intern Organs*. **19**. 72–79.

Bennett, D.C. (2001). *Inverse Phase Polymerisation of Acrylamide in a Batch Oscillatory Baffled Reactor*. Ph.D. Thesis, Strathclyde University, UK.

Bhattacharyya, A.R., Sreekumar, T.V., Liu, T., Kumar, S., Ericson. L.M., Hauge, R. H. and Smalley, R.E. (2003). Crystallisation and Orientation Studies in Polypropylene/Single Wall Carbon Nanotube Composite. *Polymer*. **44**. 2373-2377.

Bjorndalen, N. and M.R. Islam. (2004). The Effect of Microwave and Ultrasonic Irradiation on Crude Oil During Production with a Horizontal Well. *J Pet Sci Eng*. **43**. 139–150.

Bott, T.R. and Gudmundsson, J.S. (1977a). Deposition of Paraffin Wax from Flowing System. *Institute of Petroleum, Technical Report*. IP-77-007.

Bott, T.R. and Gudmundsson, J.S. (1977b). Deposition of Paraffin Wax from Kerosene in Cooled Heat Exchanger Tubes. *Can J Chem Eng*. **55**(4). 381-385.

Brunold, C. R., Hunns, J. C. B., Mackley, M. R. and Thompson, J. W. (1989). Experimental Observations on Flow Patterns and Energy Losses for Oscillatory Flow in Ducts Containing Sharp Edges. *Chem Eng Sci*. **44**(5). 1227-1244.

Campos, R.J., Litwinenko, J.W. and Marangoni, A.G. (2003). Fractionation of Milk Fat by Short-Path Distillation. *J Dairy Sci*. **86**. 735-745.

Carnahan, N.F. (1989). Paraffin Deposition in Petroleum Production. *J Pet Technol*. **41**(10). 1024-1025.

Caze, C., Devaux, E., Crespy, A., Cavrot, J.P. (1997). A New Method to Determine the Avrami Exponent by D.S.C. Studies of Non-Isothermal Crystallisation from the Molten State. *Polymer*. **38**(3). 497-502.

Changani, S. D., Belmar-Beiny, M. T. and Fryer, P. J. (1997), Engineering and Chemical Factors Associated with Fouling and Cleaning in Milk Processing. *Experimental Thermal and Fluid Science*. **14** (4). 392-406.

Chen, D.Z., He, P.S. and Pan, L.J. (2003). Cure Kinetics of Epoxy-based Nanocomposites Analysed by Avrami Theory of Phase Change. *Polymer Testing*. **22**. 689-697.

Cheng, X., Xue, Y. and Xie, C. (2003). Tribological Investigation of PTFE Composite Filled with Lead and Rare Earths-Modified Glass Fiber. *Material Letters*. **57**. 2553–2557.

Cole, R.J. and Jessen, F.W. (1960). Paraffin Deposition. *Oil Gas J*. **58**. 87-99.

Coleman, D.A. and Mitchell, W.S. (1991). Enhanced Mass Transfer for Membrane Processes. Trans IChemE, Part C. *Food Bioprod Proc*. **69**. 91–96.

Connor, M.T., Gutierrez, M.C.G., Rueda, D.R. and Calleja, F.J.B. (1997). Cold Crystallisation Studies on PET/PEN Blends as Revealed by Microhardness. *J. Mater. Sc*. **32**. 5615-5620.

Cordoba, A.J. and Schall, C.A. (2001a). Application of Heat Transfer Method to Determine Wax Deposition in a Hydrocarbon Binary Mixture. *Fuel*. **80**. 1285-1291.

Cordoba, A.J. and Shall, C.A. (2001b). Solvent Migration in a Paraffin Deposit. *Fuel.* 80. 1279-1284.

Creek, J.L., Lund, H.J., Brill, J.P. and Volk, M. (1999). Wax Deposition in Single Phase Flow. *Fluid Phase Equilibria.* **158**(1). 801-811.

de Boer, R.B., Leerlooyer, K., Eigner, M.R.P. and van Bergen, A.R.D. (1995). Screening of Crude Oils for Asphalt Precipitation: Theory, Practice, and the Selection of Inhibitors. *SPE Prod Facil.* 24987. **10**(1). 55-61.

Dickens, A. W., Mackley, M. R. and Williams, H. R. (1989). Experimental Residence Time Distribution Measurements for Unsteady Flow in Baffled Tubes. *Chem Eng Sci.* **44**. 1471-1479.

dos Santos, J.S.T., Fernandes, A.C. and Giulietti, Marco. (2004). Study of the Paraffin Deposit Formation Using the Cold Finger Methodology for Brazilian Crude Oils. *J Pet Sci Eng.* **45**. 47-60.

Evans, U.R. (1945). The Laws of Expanding Circles and Spheres in Relation to Lateral Growth of Surface Films and the Grain Size of Metals. *Trans. Faraday Soc.* **41**. 365-374.

Fabiyi, M.E. and Skelton, R.L. (1999). The Application of Oscillatory Flow Mixing to Photocatalytic Wet Oxidation. *J Photochem Photobiol A: Chem.* **129**. 17–24.

Fabiyi, M.E. and Skelton, R.L. (2000). Photocatalytic Mineralisation of Methylene Blue Using Buoyant TiO_2–Coated Polystyrene Beads. *J Photochem Photobiol A: Chem.* **132**. 121–128.

Fernandez-Lozano, J.A. and Rodriguez, Y.M. (1984). Rheological and Conductometric Properties of Two Different Crude Oils and Their Fractions. *Ind. Eng. Chem. Process Des. Dev.* **23**(1). 115-121.

Fernandez-Torres, M.J., A. M. Fitzgerald, W. R. Paterson and D. I. Wilson. (2001). A Theoretical Study of Freezing Fouling: Limiting Behaviour Based on a Heat and Mass Transfer Analysis. *Chemical Engineering and Processing*. **40**. 335-344.

Finnegan, S.M. and Howell, J.A., 1989, The Effect of Pulsatile Flow on Ultrafiltration Fluxes in a Baffled Tubular Membrane System. Trans IChemE, Part A. *Chem Eng Res Des*. **67**. 278–280.

Fitch, A. W., Ni, X. and Stewart, J. (2001) Characterisation of Flexible Baffles in an Oscillatory Baffled Column. *J Chem Technol Biotechnol*. **76**. 1074-1079.

Gaidhani, H.K., McNeil, B and Ni, X. (2003). Production of Pullulan Using an Oscillatory Baffled Bioreactor. *J Chem Technol Biotechnol*. **78**. 260-264.

Gao, S., Ni, X., Cumming, R.H., Greated, C.A. and Norman, P.I. (1998). Experimental Investigation of Particle Flocculation in a Batch Oscillatory Baffled Reactor. *Sep Sci Technol*. **33**(14). 2143–2157.

Godfrey, J.C. and Slater, M.J. (1994). Liquid–Liquid Extraction Equipment (John Wiley, New York, USA).

Gruse, W.A. and Stevens, D.R.: *Chemical Technology of Petroleum*, McGraw-Hill Book Publishers Inc., New York City (1960) Chap. XIV.

Hao, R., Ku, A. and Zeng, Y. (2004). Effect on Crude Oil by Thermophilic Bacterium. *J. Pet. Eng.* **43**. 247-258.

Hartley, R. and Bin Jadid, M. (1989). Use of Laboratory and Field Testing to Identify Potential Production Problems in the Troll Field. *SPE Prod Eng.* 4(1). 34-40.

Harvey, A.P. and Stonestreet, P. (2001). A Case Study of the Process Intensification of a Batch Saponification Plant. *Proceedings of the 6th World Congress of Chemical Engineers*, Melbourne, Australia, 24–29 September.

Harvey, A.P. and Stonestreet, P. (2002). A Mixing-Based Design Methodology for Continuous Oscillatory Flow Reactors. *Trans IChemE, Part A, Chem Eng Res Des.* **80**. 31–44.

Harvey, A.P., Mackley, M.R. and Stonestreet, P. (2001). Operation and Optimization of an Oscillatory Flow Continuous Reactor. *Ind Eng Chem Res.* **40**. 5371–5377.

Hay, J.N. (1971). Application of the Modified Avrami Equations to Polymer Crystallisation Kinetics. *Br. Polym. J.* 3(2). 74-82.

Hennesy, A.J., Neville, A. and Roberts, K.J. (1999). An Examination of Additive-Mediated Wax Nucleation in Oil Pipeline Environments. *J. Crystal Growth.* **198**(199). 830-837.

Hewgill, M. R., Mackley, M. R., Pandit, A. B. and Pannu, S. S. (1993). Enhancement of Gas-Liquid Mass Transfer Using Oscillatory Flow in a Baffled Tube. *Chem Eng Sci.* 48(4). 799-809.

Holder, G.A. and Winkler, J. (1965). Wax Crystallisation from Distillate Fuels, Part 2. *J. Inst. Pet.* **51**. 236-243.

Howes, T. and Mackley, M. R. (1990). Experimental Axial Dispersion for Oscillatory Flow through a Baffled Tube. *Chemical Engineering Science*. **45**(5). 1349-1358.

Howes, T., Mackley, M.R. and Roberts, E.P.L. (1991). The Simulation of Chaotic Mixing and Dispersion for Periodic Flows in Baffled Channels. *Chemical Engineering Science*. **46**(7). 1669-1677.

Howes, T. (1988). On the Dispersion of Unsteady Flow in Baffled Tubes. PhD thesis. Department of Chemical Engineering. Cambridge University. Cambridge.

Huang, X., Terech, P., Raghavan, S.R., Weiss, R.G. (2005). Kinetics of 5a-cholestan-3β-yl N-(2-naphthyl)carbamate/n-alkane Organogel Formation and Its Influence on the Fibrillar Networks. *Journal of the American Chemical Society*. **127**(12). 4336-4344.

Hutter J.L., Hudson S., Smith C., Tetervak, A and Zhang, J. (2004). Banded Crystallisation of Tricosane in the Presence of Kinetic Inhibitors During Directional Solidification. *Journal of Crystal Growth*. **273**. 292-302.

Imai, T., Nakamura, K. and Shibata, M. (2001). Relationship between the Hardness of an oil-wax gel and the Surface Structure of the Wax Crystals. *Colloids and Surfaces A*. **194**. 233-237.

Ismail, L., Westacott, R.E. and Ni, X-W. (2006). On the Characterisation of Wax Deposition in an Oscillatory Baffled Device. *J Chem Technol Biotechnol*. **81**(12). 1905-1914.

Ismail, L., Westacott, R.E., Ni, X. (2007). On the Effect of Wax Content on Paraffin Wax Deposition in a Batch Oscillatory Baffled Tube Apparatus. *Chem Eng J.* (2007). doi:10.1016/j.cej.2007.04.018.

Jennings, D.W. and Weispfennig, K. (2005). Experimental Solubility Data of Various *n*-Alkane Waxes: Effects of Alkane Chain Length, Alkane Odd Versus Even Carbon Number Structures, and Solvent Chemistry on Solubility. *Fluid Phase Equilibria*. **227**. 27–35.

Jessen, F.W. and Howell, J.N. (1958). Effect of Flow Rate on Paraffin Accumulation in Plastic, Steel and Coated Pipes. *Trans. AIME*. **213**. 80-84.

Jorda, R.M. (1966). Paraffin Deposition and Prevention in Oil Wells. *J Pet Technol.* **18**(10). 1605–1612.

Kane, M., Djabourova, M., Volleb, J.L., Lechairec, J.P. and Frebourg, G. (2003). Morphology Of Paraffin Crystals in Waxy Crude Oils Cooled in Quiescent Conditions and Under Flow. *Fuel*. **82**. 127-135.

Karr, A.E. (1959) Performance of a Reciprocate-Plate Extraction Column. *AIChE J.* **5**(4). 446–452.

Khedkar, J., Negulescu, I. and Meletis, E.I. (2002). Sliding Wear Behaviour of PTFE Composites. *Wear*. **252**. 361–369.

Knox, J., Waters, A.B. and Arnold, B.B. (1962). Checking Paraffin Deposition by Crystal Growth Inhibition. *SPE*. 443.

Knox, J.A., Arnold, B.B. and Waters A.B. (1966). Paraffin Control Method. *US Patent*: 3276519.

Latto, B. (1992). Vortex Ring Mixers for Slurries and Controlled Addition of Gases and Liquids. In Proceedings of 17th International Conference on Coal Utilization and Slurry Technologies, Pittsburgh, PA.

Lee, C.T., Mackley, M.R., Stonestreet, P. and Middelberg, A.P.J. (2001). Protein Refolding in an Oscillatory Flow Reactor. *Biotechnol Lett.* **23**(22). 1899–1901.

Leontaritis, K.J. and Mansoori, G.A. (1988). Asphaltene deposition: a survey of field experiences and research approaches. *J Pet Sc Eng*. **1**. 229-239.

Li, M., Su, J., Wu, Z., Yang, Y. and Ji, S. (1997). Study of the Mechanisms of Wax Prevention in a Pipeline with Glass Inner Layer. *Colloids and Surfaces A: Physicochem Eng Aspects*. **123-124**. 635-649.

Li, W., Kong, X., Zhou, E. and Ma, D. (2005). Isothermal Crystallisation Kinetics of Poly(ethylene Terephthalate)-Poly(ethylene Oxide) Segmented Copolymer with Two Crystallising Blocks. *Polymer*. **46**. 11655-11663.

Litwinenko, J.W., Singh, A.P. and Marangoni, A.J. (2004). Effects of Glycerol and Tween 60 on the Crystallisation Behaviour, Mechanical Properties, and Microstructure of Plastic Fat. *Crystal Growth and Design*. 4(1). 161-168.

Lo, T.C., Baird, M.H.I. and Hanson, C., 1983, Handbook of Solvent Extraction (Wiley-InterScience, New York, USA).

Long, J.T., 1967, Engineering for Nuclear Fuel Processing (Gordon and Breach, Reading, MA, USA).

Lu, M.G., Shim, M.J. and Kim, S.W. (1998). Curing Behaviour of Unsaturated Polyester System Analysed by Avrami Equation. *Thermochimica Acta*. **323**. 37-42.

Luo, H, Sietsma, J. and van der Zwaag, S. (2004). Effect of Inhomogeneous Deformation on the Re-crystallisation Kinetics of deformed Metals. *ISIJ International*. **44** (11). 1931-1936.

Mackay, M. E., Mackley, M, R, and Wang, Y. (1991). Oscillatory Flow within Tubes Containing Wall or Central Baffles. *Trans IChemE*. **69**. 506-513.

Mackley, M. R. and Ni, X. (1991). Mixing and Dispersion in a Baffled Tube for Steady Laminar and Pulsatile Flow. *Chem Eng Sci*. **46**. 3139–3151.

Mackley, M.R. and Ni, X. (1993). Experimental Fluid Dispersion Measurements in Periodic Baffled Tube Arrays. *Chem Eng Sci*. **48**, 3293–3305.

Mackley, M.R. and Sherman, N.E. (1992). Cross-Flow Cake Filtration Mechanisms and Kinetics. *Chem Eng Sci*. **47**(12). 3067–3084.

Mackley, M.R. and Sherman, N.E. (1993). Cake Filtration Mechanisms in Steady and Unsteady Flows. *J Membr Sci*. **77**. 113–121.

Mackley, M. R. and Stonestreet, P. (1995). Heat Transfer and Associated Energy Dissipation for Oscillatory Flow in Baffled Tubes. *Chem Eng Sci*. **50**. 2211-2224.

Mackley, M.R., Tweedle, G.M. and Wyatt, I.D. (1990). Experimental Heat Transfer Measurements for Pulsatile Flow in Baffled Tubes. *Chem Eng Sci.* **45**. 1237–1242.

Mackley, M. R., Smith, K. B. and Wise, N. P. (1993). The Mixing and Separation of Particle Suspensions Using Oscillatory Flow in Baffled Tubes.*Trans IChemE, Part A, Chem Eng Res Des.* **71**(A6). 649–656.

Madsen, H.E.L. and Boistelle, R. (1976). Solubility of Long Chain n-Paraffins in Pentane and Heptane. *J. Chem. Soc. Faraday Trans.* **1**(72). 1078-1081.

Mak, A.N.S., Koning, C.A.J., Hamersma, P.J. and Fortuin, J.M.H. (1991). Axial Dispersion in Single Phase Flow in a Pulsed Packed Column Containing Structured Packing. *Chem Eng Sci.* **46**. 819–826.

Masngut, A., Takriff, M.S., Mohammad, A.W., Kalil, M.S. and Kadhum, A.A.H. (2006). Performance of Oscillatory Flow Reactor and Stir Tank Reactor in Solvent Fermentation from Palm Oil Mill Effluent. *Proceedings of the 1st International Conference on Natural Resources Engineering and Technology 2006 24th – 25th July 2006; Putrajaya, Malaysia.* 691-699.

Matzain, A., Apte, M.S., Zhang, H.Q., Volk, M., Brill, J.P., and Creek, J.L. (2001). Investigation of Paraffin Deposition During Multiphase Flow in Pipelines and Wellbores – Part 2: Modeling. *Journal of Energy Resources Technology.* **123**. 150-157.

Matzain, A., Apte, M.S., Zhang, H.Q., Volk, M., Brill, J.P., and Creek, J.L. (2002). Investigation of Paraffin Deposition during Multiphase Flow in Pipelines and Wellbores – Part 1: Experiments. *Journal of Energy Resources Technology*. **124**. 180-186.

Maurício, M. H. P., Teixeira, A. M., Azevedo, L. F. A. and Paciornik, S. (2003). In-situ Microscopy of Wax Crystallisation. *Acta Microscopica*. **12**. 287-288.

Meares, P. (1965). *Polymers: Structure and Bulk Properties*. Van Norstrand, London.

Misra, S., Baruah, S. and Singh, K. (1995). Paraffin Problems in Crude Oil Production and Transportation. *SPE*. **10**(1). 50-54.

Monger-McClure, T.G., Tackett, J.E. and Merrill, L.S. (1999). Comparisons of Cloud Point Measurement and Paraffin Prediction Methods. *SPE Prod Facil*. 54519. **14**(1). 4-16.

Nelson, G. (2001) A Scale-Up Study in Suspension Polymerisation of Methylmethacrylate in a Pilot Oscillatory Baffled Reactor. Ph.D. Thesis, Heriot–Watt University, UK.

Nguyen, D.A., Fogler, H.S. and Chavadej, S. (2001). Fused Chemical Reactions. 2. Encapsulation: Application to Remediation of Paraffin Plugged Pipelines. *Ind Eng Chem Res*. **40**. 5058-5065.

Ni, X. and Gao, S. (1996a). Mass Transfer Characteristic of a Pilot Pulsed Baffled Reactor. *J Chem Technol Biotechnol*. **65**. 65-71.

Ni, X. and Gao, S. (1996b). Scale-up Correlation for Mass Transfer Coefficient in Pulsed Baffled Reactors. *Chem Eng J.* **63**. 157-166.

Ni, X. and Mackley, M.R. (1993). Chemical Reaction in a Batch Pulsatile Flow and Stirred Tank Reactors. *Chem Eng J Biochem Eng.* **52**(3). 107–114.

Ni, X., Zhang, Y. and Mustafa, I. (1998). An Investigation of Droplet Size and Size Distribution in Methylmethacrylate Suspensions in a Batch Oscillatory Baffled Reactor. *Chem Eng Sci.* **53**(16). 2903–2919.

Ni, X. and Pereira, N. (2000). Parameters Affecting Fluid Dispersion in a Continuous Oscillatory Baffled Tube. *AIChE J.* **46**(1). 37–45.

Ni, X. and Stevenson, C.C. (1999). On the Effect of Gap Size between Baffle Outer Diameter and Tube Inner Diameter on the Mixing Characteristics in an Oscillatory Baffled Column. *J Chem Technol Biotechnol.* **74**. 587-593.

Ni, X., Gao, S., Cumming, R, H. and Pritchard, D. W. (1995a). A Comparative Study of Mass Transfer in Yeast for a Batch Pulsed Baffled Bioreactor and a Stirred Tank Fermenter. *Chem Eng Sci.* **50**(13). 2127-2136.

Ni, X., Gao, S. Cumming, R, H and Pritchard, D. W. (1995b). A Study of Mass Transfer in Yeast in a Pulsed Baffled Bioreactor. *J Biotechnol Bioeng.* **45(2)**. 165-175.

Ni, X., Liu, S., Joyce, M. J., Grewal, P. S. and Greated, C. A. (1995c). A Study of Velocity Vector Profile and Strain Rate Distribution for Laminar and Oscillatory Flows in a Baffled Tube Using Particle Image Velocimetry. *J Flow Visual Image Proc.* **2**(2). 135–147.

Ni, X., and Gao, S. and Santangeli, L. (1997). On The Effect of Surfactant on Mass Transfer to Water-Glycerol Solutions in a Pulsed Baffled Reactor. *J Chem Technol Biotechnol.* **69**(2). 247–253.

Ni, X., Brogan, G., Struthers, A., Benett D.C., and Wilson S.F. (1998). A Systematic Study of the Effect of Geometrical Parameters on Mixing Time in Oscillatory Baffled Columns. *Trans. IChemE.* **76**. 635-642.

Ni, X., Zhang, Y., and Mustafa, I. (1999). Correlation of Polymer Particle Size with Droplet Size in Suspension Polymerisation of Methylmethacrylate in a Batch Oscillatory Baffled Reactor. *Chem Eng Sci.* **54**. 841–850.

Ni, X., Bennet, D.C., Symes, K.C. and Grey, B.D. (2000a). Inverse Phase Suspension Polymerisation of Acrylamide in a Batch Oscillatory Baffled Reactor. *J Appl Polym Sci.* **76**(11). 1669–1676.

Ni, X., Cosgrove, J.A., Arnott, A.D., Greated, C.A. and Cumming, R.H. (2000b). On the Measurement Of Strain Rate in an Oscillatory Baffled Column Using Particle Image Velocimetry. *Chem Eng Sci.* **55**(16). 3195–3208.

Ni X., Nelson, G. and Mustafa, I. (2000c). Flow Patterns and Oil-Water Dispersion in a 0.38m Diameter Oscillatory Baffled Column. *Can J Chem Eng.* **78**(1). 211–220.

Ni, X., Cosgrove, J.A., Cumming, R.H., Greated, C.A., Murray, K.R. and Norman, P. (2001a). Experimental Study of Flocculation of Bentonite and Alcaligenes Eutrophus in a Batch Oscillatory Baffled Flocculator. *Chem Eng Res Des.* **79**(A1). 33–40.

Ni, X., Johnstone, J.C., Symes, K.C., Grey, B.D. and Bennett, D.C. (2001b). Suspension Polymerisation Acrylamide in an Oscillatory Baffled Reactor: From Drops to Particles. *AIChE J.* **47**(8). 1746–1757.

Ni, X., Sommer de Gélicourt, Y., Baird, M.H.I. and Rama Rao, N.V. (2001c). Scale-Up of Single Phase Axial Dispersion in Batch and Continuous Oscillatory Baffled Tubes. *Can J Chem Eng.* **79**(3). 444–448.

Ni, X., Mignard, D., Saye, B., Johnstone, J.C. and Pereira, N. (2002). On the Evaluation of Droplet Breakage and Coalescence Rates in an Oscillatory Baffled Reactor. *Chem Eng Sci.* **57**(11). 2101–2114.

Ni, X., Mackley, M.R., Harvey, A.P., Stonestreet, P., Baird, M.H.I. and Rama Rao, N.V. (2003). Mixing Through Oscillation and Pulsations - A Guide to Achieving Process Enhancements in the Chemicals and Process Industries. *Trans IChemE.* **81**. 373-383.

Ni, X., Valentine, A., Liao A., Sermage, S.B.C., Thomson, G.B. and Roberts, K.J. (2004). On the Crystal Polymorphic Forms of L-Glutamic Acid Following Temperature Programmed Crystallization in a Batch Oscillatory Baffled Crystalliser. *Crystal Growth and Design.* **4**(6). 1129 -1135.

Nishimura, T., Bian, Y.N. and Kunitsugu, K. (2004). Mass-Transfer Enhancement in a Wavy-Walled Tube by Imposed Fluid Oscillation. *AIChE J.* **50**(4). 762 – 770.

Oliveira, M.S.N.F. (2003). *Characterisation of a Gas-Liquid Oscillatory Baffled Column.* Ph.D. Thesis, Heriot–Watt University, UK.

Oliveira, M.S.N. and Ni, X. (2001). Gas Holdup and Bubble Diameters in a Gassed Oscillatory Baffled Column. *Chem Eng Sci.* **56**(21). 6143–6148.

Pal, S. and Nandi, A. K. (2005). Cocrystallisation Mechanism of Poly(3-alkyl thiophenes) with Different Alkyl Chain Length. *Polymer.* **46**. 8321-8330.

Parks, C.F. (1960). Chemical Inhibitors Combat Paraffin Deposition. *Oil Gas J.* **58**(14). 97-99.

Patton, C.C. and Cassad, B.M. (1970). Paraffin Deposition from Refined Wax-Solvent System. *SPE 2503.* **10**. 17-24.

Pauly, J., Daridon, J.L. and Dauphin, C. (2004). Solid Deposition as a Function of Temperature in the nC_{10} + (nC_{24}–nC_{25}–nC_{26}) System. *Fluid Phase Equilibria.* **224**(2). 237-244.

Pedersen, K.S. (1995). Prediction of Cloud Point Temperatures and Amount of Wax Precipitation. *SPE Prod Facil.* 27629. **10**(1). 46-49.

Pereira, R.P. and Rocco, A.M. (2005). Nanostructure and Crystallisation Kinetics of Poly(ethylene oxide)/poly(4 - vinylphenol -co- 2 - hydroxyethyl methacrylate) Blends. *Polymer.* **46**. 12493–12502.

Pereira, N. (2002). Characterisation of a Continuous Oscillatory Baffled Tubular Reactor. Ph.D. Thesis, Heriot–Watt University, UK.

Ribeiro, F. S., Mendes, P. R.S. and Braga, S. L. (1997). Obstruction of Pipelines Due to Paraffin Deposition during the Flow of Crude Oils. *Int. J. Heat Transfer.* **40**(18). 4319-4328.

Roberts, E.P.L and Mackley, M.R. (1995). The Simulation of Stretch Rates for the Quantitative Prediction and Mapping of Mixing within a Channel Flow. *Chem Eng Sci.* **50**(23). 3727-3746.

Roberts, E.P.L. and Mackley, M.R. (1996). The Development of Assymetry and Period Doubling for Oscillatory Flow in Baffled Channels. *Journal of Fluid Mechanics.* **328**. 19-48.

Schneider, S., Drujon, X., Wittmann, J.C. and Lotz, B. (2001). Impact of Nucleating Agents of PVDF on the Crystallisation of PVDF/PMMA Blends. *Polymer.* **42**. 8799-8806.

Sharples, A. (1966). Overall kinetics of crystallisation Pages 44-59 in Introduction to Polymer Crystallisation. A. Sharples, ed. Edward Arnold Ltd. London.

Shock, D.A., Sudbury, J.D. and Crockett, J.J. (1955). Studies of the Mechanism of Paraffin Deposition and Its Control. *J Pet Technol.* **7**(9). 23-30.

Singh, P., Venkatesan R. and Fogler, H.S. (2000). Formation and Aging of Incipient Thin Film Wax-Oil Gels. *AIChE J.* **46**(5). 1059-1074.

Singh, P., Venkatesan, R. Fogler, H.S. and Nagarajan, N.R. (2001). Morphological Evolution of Thick Wax Deposits during Aging. *AIChE J.* **47**(1). 6-18.

Siripurapu S., Gay Y.J., Royer J.R., DeSimone J.M., Spontak R.J., Khan S.A. (2002). Generation of Microcellular Foams of PVDF and its Blends using Supercritical Carbon Dioxide in a Continuous Process. Polymer. **43**(20). 5511-5520.

Smith, K.B. (2000). The Scale-Up of Oscillatory Flow Mixing. Ph.D. Thesis, Cambridge University, UK.

Sobey, I.J. (1980). On Flow Through Furrowed Channels. Part 1. Calculated Flow Patterns. *Journal of Fluid Mechanics*. **96**. 1-26.

Sperling, L.H. (1986). Kinetics of Crystallisations Pages 177-191 in Introduction to Physical Polymer Science. L.H. Sperling, ed. John Wiley and Sons. New York.

Srivastava, S.P., Handoo,J., Agrawal, K.M. and Joshi G.C. (1992). Crystallisation Behaviour of n-Paraffins in Bombay High Middle Distillate Wax/Gel. *Fuel*. **71**(5). 533-537

Stevens, G.G., 1996, Suspension Polymerisation in Oscillatory Flow. Ph.D. Thesis, Cambridge University, UK.

Stonestreet, P. and van der Veeken, P.M.J. (1999). The Effects of Oscillatory Flow and Bulk Flow Components on the Residence Time Distribution in Baffled Tube Reactors. *Trans IChemE, Part A, Chem Eng Res Des*. **77**. 671–684.

Thanh, N.X., Hsieh, M. and Philp, R.P. (1999). Waxes and Asphaltenes in Crude Oils. *Organic Geochemistry*. **30**. 119-132.

Towler, B. F. and Rebbapragada, S. (2004). Mitigation of Paraffin Wax Deposition Cretaceous Crude Oils of Wyoming. *J Pet Sci Eng*. **45**. 11-19.

van Dijck, W.J.D. (1935). Tower with Internal Perforated Plate Suitable for Extracting Liquids by Treatment with Other Liquids and for Similar Concurrent Processes. U.S. Patent 2011186.

Venkatesan, R., Nagarajan, N.R., Paso, K., Yi, Y.B., Sastry, A.M. and Fogler H.S. (2005). The Strength of Paraffin Gels Formed Under Static and Flow Conditions. *Chem Eng Sci.* 60(13). 3587-3598.

Vinogradov, A.M., Schmidt, V.H., Tuthill, G.F. and Bohannan, G.W. (2004). *Mechanics of Materials.* 36. 1007-1016.

Wang, X and Vlassak, J. J. (2006). Crystallization Kinetics of Amorphous NiTi Shape Memory Alloy Thin Films. *Scripta Materialia.* 54(5). 925-930.

Wardbaugh, L.T. and Boger, D.V. (1991). Flow Characteristics of Waxy Crude Oils: Application to Pipeline Design. *AIChE J.* 37(6). 871-885.

Weingarten, J.S. and Euchner, J.A. (1988). Methods for Predicting Wax Precipitation and Deposition. *SPE Prod Engng* 15654. 121-126.

Wilson, B., Ni, X. and Sherrington, D.C. (2001a). A Study of a Phase Transfer Catalytic Reaction between N-Butyl Bromide and Sodium Phenolate in an Oscillatory Baffled Reactor in *Studies in Surface Science and Catalysis*. 481.

Wilson, B., Ni, X. and Sherrington, D.C. (2001b). On the Investigation of a Phase Catalysis Reaction in an Oscillatory Baffled Reactor. *Industrial and Engineering Chemistry Research.* 40. 5300-5304.

Woo, G.T., Garbis, S.J. and Gray, T.C. (1984). Long-Term Control of Paraffin Deposition. *SPE.* 13126. 59-67.

Zhang, Y., Ni, X. and Mustafa, I. (1996). A Study of Oil-Water Dispersion in a Pulsed Baffled Reactor. *J Chem Technol Biotechnol.* 66(3). 305-311.

Zhang, Y. (1998). *A Study of Suspension Polymerisation of Methylmethacrylate and Styrene in a Batch Oscillatory Baffled Reactor*. Ph.D. Thesis Strathclyde University, UK.

Zhao, Q. and Liu, Y. (2004). Investigation of Graded Ni–Cu–P–PTFE Composite Coatings with Antiscaling Properties. *Applied Surface Science*. **229**. 56–62.

Zisman, W.A. (1963). Influence of Constitution on Adhesion. *Ind Eng Chem*. **55**(10). 18-38.